MARTIN MARIETTA ENERGY SYSTEMS LIBRARIES
3 4456 0250849 0

CENTRAL RESEARCH LIBRARY
DOCUMENT COLLECTION

ORNL-3085
UC-34 – Physics

PHYSICS DIVISION

ANNUAL PROGRESS REPORT

FOR PERIOD ENDING FEBRUARY 10, 1961

CENTRAL RESEARCH LIBRARY
DOCUMENT COLLECTION
LIBRARY LOAN COPY
DO NOT TRANSFER TO ANOTHER PERSON
If you wish someone else to see this document, send in name with document and the library will arrange a loan.

OAK RIDGE NATIONAL LABORATORY
operated by
UNION CARBIDE CORPORATION
for the
U.S. ATOMIC ENERGY COMMISSION

Printed in USA. Price $2.50. Available from the
Office of Technical Services
Department of Commerce
Washington 25, D.C.

LEGAL NOTICE

This report was prepared as an account of Government sponsored work. Neither the United States, nor the Commission, nor any person acting on behalf of the Commission:

A. Makes any warranty or representation, expressed or implied, with respect to the accuracy, completeness, or usefulness of the information contained in this report, or that the use of any information, apparatus, method, or process disclosed in this report may not infringe privately owned rights; or

B. Assumes any liabilities with respect to the use of, or for damages resulting from the use of any information, apparatus, method, or process disclosed in this report.

As used in the above, "person acting on behalf of the Commission" includes any employee or contractor of the Commission, or employee of such contractor, to the extent that such employee or contractor of the Commission, or employee of such contractor prepares, disseminates, or provides access to, any information pursuant to his employment or contract with the Commission, or his employment with such contractor.

ORNL-3085
UC-34 – Physics
TID-4500 (16th ed.)

Contract No. W-7405-eng-26

PHYSICS DIVISION

ANNUAL PROGRESS REPORT

for Period Ending February 10, 1961

J. L. Fowler, Director
E. O. Wollan, Associate Director

DATE ISSUED

MAR 28 1961

OAK RIDGE NATIONAL LABORATORY
Oak Ridge, Tennessee
operated by
UNION CARBIDE CORPORATION
for the
U. S. ATOMIC ENERGY COMMISSION

MARTIN MARIETTA ENERGY SYSTEMS LIBRARIES

3 4456 0250849 0

FOREWORD

This is the third Physics Division progress report made on an annual basis. As in previous years, the report contains the abstracts for papers which have been published or which have been prepared for publication. In such cases, reprints or preprints of the articles will be available. Preliminary results of work in progress are reported, as previously, in some detail. Since this work is of a preliminary nature, the authors should be contacted with regard to the inclusion of any of these results in other publications.

TABLE OF CONTENTS AND SUMMARY

GAMMA-RAY DIFFRACTION BY RESONANT NUCLEI

G. T. Trammell 1

Abstract of paper to be published in *Proceedings of International Conference on Chemical Effects of Nuclear Transformations, Prague*, October 1960.

ELASTIC SCATTERING BY BOUND NUCLEI

G. T. Trammell 1

The familiar zero-point motion form factor which appears in the expression for the elastic scattering from bound scatterers is correct only for "fast" collisions. A quite different expression may result in resonance scattering. A general formula for the bound scattering amplitude in terms of the free scattering amplitudes for slow neutrons is given.

FLUCTUATION-DISSIPATION RELATIONS FOR NEUTRON DIFFRACTION

Richard L. Becker 4

Abstract of paper to be submitted to *Physics of Fluids*.

BOUND PAIRS AND REACTION MATRIX SINGULARITIES

Richard L. Becker 5

Abstract of paper to be submitted to *Annals of Physics*.

CENTER-OF-MASS ENERGY IN OVERHAUSER'S SELF-CONSISTENT FIELD WITH GIANT DENSITY FLUCTUATIONS

Richard L. Becker 5

For a large but finite system the energy of Overhauser's solution contains a contribution attributable to the motion of the center of mass, analogous to that in the shell model. It is shown that this contribution vanishes as $1/N$, thus removing an objection to the solution.

NUMERICAL STUDY OF THE DISTORTED-WAVE THEORY OF DIRECT NUCLEAR REACTIONS

R. H. Bassel, R. M. Drisko, and G. R. Satchler 10

A computer program has been written and is being used to study the distorted-wave theory of direct nuclear reactions. Some preliminary results are given.

POLARIZATION PHENOMENA IN DEUTERON STRIPPING REACTIONS

L. C. Biedenharn and G. R. Satchler 12

Abstract of invited paper, *International Conference on Polarization Phenomena, Basel, July 1960*; to be published in *Helvetica Physica Acta*, 1961.

COLLECTIVE EFFECTS IN INELASTIC SCATTERING

W. T. Pinkston and G. R. Satchler 13

Abstract of paper published in *Proceedings of International Conference on Nuclear Structure, Kingston, Ontario*, 1960.

DETECTION OF DEUTERON ALIGNMENT WITH s-WAVE REACTIONS

H. B. Willard 13

Abstract of paper to be published in *Helvetica Physica Acta*.

AN EFFICIENT EXCITATION METHOD FOR AN OPTICAL MASER
T. A. Welton 13

A discussion is given of some of the principles involved in the design of an efficient optical maser. It is shown that if the problem of mode isolation can be solved, coherent light can be produced at an arbitrary power level with an efficiency that would be of practical interest.

RECOIL ENERGY SPECTRUM FOR THE BETA DECAY OF He^6
C. H. Johnson, Frances Pleasonton, and T. A. Carlson 18

Measurements have been made of the recoil energy spectrum of singly charged Li^6 ions from the beta decay of He^6. The spectrum, which was obtained with very good counting statistics, shows good agreement with predictions for the axial-vector interaction. An evaluation of experimental uncertainties is in progress; a preliminary analysis gives a correlation coefficient of $\lambda = -0.324 \pm 0.010$ (axial-vector theory, $\lambda = -\frac{1}{3}$).

AN ABSOLUTE DETERMINATION OF THE He^6 BETA-DECAY ENERGY
Frances Pleasonton, C. H. Johnson, and T. A. Carlson 22

Measurements of the end point of the recoil energy spectrum of Li^6 ions yielded an absolute determination of the He^6 beta-decay energy. The value assigned is 3.507 ± 0.005 Mev.

ELECTRON SHAKEOFF FOLLOWING $He^6 \xrightarrow{\beta^-} Li^6$
T. A. Carlson, Frances Pleasanton, and C. H. Johnson 24

The relative intensities of singly, doubly, and triply charged lithium ions formed following the β^- decay of He^6 have been measured as a function of recoil energy, and the results are compared with theory.

LEVEL STRUCTURE OF N^{14}
J. K. Bair, H. O. Cohn, and H. B. Willard 28

Abstract of published paper: *Phys. Rev.* **119**, 2026 (1960).

LEVELS IN N^{14} AT 11.74 AND 11.82 Mev
J. K. Bair 29

Abstract of paper submitted to the *Physical Review*.

NEUTRONS FROM THE He^3 BOMBARDMENT OF SOME LIGHT NUCLEI
J. L. Duggan, P. D. Miller, and R. F. Gabbard 29

Techniques have been developed for pulsing the ORNL 3-Mv Van de Graaff accelerator, using He^3 singly charged ions to peak currents of 500 μa with a pulse duration of about 2 nanoseconds. A large-volume plastic detector has been used with this beam to give an over-all system resolution of about 4 nanoseconds. With these tools the $Li^7(He^3,n)B^9$, $Be^9(He^3,n)C^{11}$, and $C^{13}(He^3,n)O^{15}$ reactions have been investigated.

THE $Be^9(\alpha,n)C^{12}$ REACTION AND THE PARAMETERS OF THE 7.66-Mev STATE OF C^{12}
F. Ajzenberg-Selave and P. H. Stelson 33

Abstract of published paper: *Phys. Rev.* **120**, 500 (1960).

THE $Al^{27}(n,\alpha)Na^{24}$ CROSS SECTION AS A FUNCTION OF NEUTRON ENERGY
H. W. Schmitt and J. Halperin 33

Abstract of published paper: *Phys. Rev.* **121**, 827 (1961).

TOTAL CROSS SECTION OF Pb^{208}
E. C. Campbell and J. L. Fowler 33

The total cross section of Pb^{208} has been determined with ~3 kev resolution from 1.0 to 1.9 Mev, with ~10 kev resolution from 1.9 to 2.7 Mev, and with ~20 kev resolution up to 4.3 Mev.

CARBON-13 NEUTRON TOTAL CROSS SECTION
H. O. Cohn, J. K. Bair, and H. B. Willard 37

Abstract of paper submitted to the *Physical Review.*

NEUTRON TOTAL CROSS SECTIONS IN THE kev ENERGY RANGE
H. Muenzer, K. Nishimura, and W. M. Good 37

The neutron total cross sections of the isotopes Se^{76}, Se^{77}, Se^{78}, Se^{80}, and Se^{82} have been measured in the energy range 4 to 50 kev. Resonances were observed in Se^{76}, Se^{78}, Se^{80}, and Se^{82} with mean spacings of 1.4, 3.7, 4.4, and 7.0 kev respectively.

STATISTICAL PARAMETERS OF MEDIUM-WEIGHT NUCLEI FROM kev NEUTRON TOTAL AND CAPTURE CROSS SECTIONS
P. D. Miller, J. H. Gibbons, J. H. Neiler, W. M. Good, and R. L. Macklin 39

Millimicrosecond time-of-flight techniques, used for studying total cross sections of separated isotopes from 3 to 50 kev for nuclei $A = 45$ to 88, have resulted in the determination of s-wave level densities and strength functions. Average radiative capture cross sections for $A = 79$ to 196 and energies 7 to 170 kev provided p-wave strength functions and estimates of s-wave level densities.

TOTAL NEUTRON CROSS SECTION OF B^{10} IN THE THERMAL-NEUTRON ENERGY RANGE
H. W. Schmitt, R. C. Block, and R. L. Bailey 42

Abstract of published paper: *Nuclear Phys.* **17**, 109 (1960).

HIGH-RESOLUTION TOTAL CROSS SECTION MEASUREMENTS ON Np^{237} AND Am^{241}
G. G. Slaughter, J. A. Harvey, and R. C. Block 42

Measurements have been made of the total neutron cross sections of Np^{237} (from 4 to 100 ev) and Am^{241} (from 5.4 to 43 ev). Resonance parameters, strength functions, and average level spacings were derived from the data.

ANALYSIS OF BREIT-WIGNER RESONANCES USING AN IBM 704 COMPUTER
J. A. Harvey and S. E. Atta 44

A shape-fitting program and an area-analysis program have been written for the IBM 704 computer in order to obtain parameters of Breit-Wigner resonances from transmission data.

ENERGY SPECTRA OF CORRELATED FRAGMENT PAIRS FROM THE SPONTANEOUS FISSION OF Cf^{252}
W. T. Joyner, H. W. Schmitt, J. H. Neiler, and R. J. Silva 48

Abstract of published paper: *IRE Trans. on Nuclear Sci.* **NS-8**, 54 (1961).

NEUTRON RADIATIVE CAPTURE MEASUREMENTS
R. C. Block, F. C. VonderLage, and L. W. Weston 48

Additional radiative capture measurements have been carried out with the 28-in.-diam spherical liquid scintillator detector installed at the 11.5-m flight station of the ORNL fast chopper. The radiative capture cross sections of intermediate and heavy weight elements have been measured in the 200- to 6000-ev energy range.

GAMMA-RAY SPECTRA FROM 30-kev NEUTRON CAPTURE
F. W. K. Firk and J. H. Gibbons 54

Preliminary results have been obtained in attempts to measure gamma rays from 30-kev neutron radiative capture. Neutrons are obtained from the $Li^7(p,n)Be^7$ reaction near threshold, using the proton beam from the 3-Mv pulsed Van de Graaff. The detector is a large NaI crystal. Spectra have been observed from Fe, Ni, Cu, Ag, Ta, and Au.

COULOMB EXCITATION OF THE SECOND 2^+ STATES IN W, Os, AND Pt NUCLEI
F. K. McGowan and P. H. Stelson 57

Abstract of paper to be published in the *Physical Review*.

COULOMB EXCITATION OF SECOND 2^+ STATES IN EVEN-EVEN MEDIUM-WEIGHT NUCLEI
P. H. Stelson and F. K. McGowan 58

Abstract of published paper: *Phys. Rev.* **121**, 209 (1961).

COULOMB EXCITATION OF Li^7, F^{19}, AND Na^{23} BY Ne^{20} IONS
P. H. Stelson and F. K. McGowan 58

Abstract of published paper: *Nuclear Phys.* **16**, 92 (1960).

COULOMB EXCITATION OF STATES IN Th^{232} AND U^{238}
F. K. McGowan and P. H. Stelson 59

Abstract af published paper: *Phys. Rev.* **120**, 1803 (1960).

VIBRATIONS IN SPHERICAL AND NEARLY SPHERICAL NUCLEI
P. H. Stelson 59

Abstract of published paper: pp 787–800 in *Proceedings of the International Conference on Nuclear Structure*, ed. by D. A. Bromley and E. W. Vogt, University of Toronto Press, Toronto, Canada, 1960.

COULOMB EXCITATION WITH Ne^{20} IONS
P. H. Stelson and F. K. McGowan 60

Abstract of published paper: pp 47–56 in *Reactions Between Complex Nuclei*, ed. by A. Zucker, F. T. Howard, and E. C. Halbert, Wiley, New York, 1960.

CONTROL OF GAMMA RADIATION IN HEAVILY SHIELDED TARGET ROOMS
H. E. Banta and G. W. Leddicotte 60

Abstract of paper presented at a meeting of the Southeastern Section of the American Physical Society, Gatlinburg, Tennessee, April 7–9, 1960.

GAMMA-GAMMA ANGULAR CORRELATIONS IN Xe^{132}
R. L. Robinson, E. Eichler, and N. R. Johnson 61

Angular correlations of three gamma-ray cascades in Xe^{132} have been measured. Spins of levels at 1.30 and 1.99 Mev are both established as 2.

DECAY OF I^{132}
R. L. Robinson, E. Eichler, and N. R. Johnson 62

Abstract of paper submitted to the *Physical Review*.

COULOMB EXCITATION OF LEVELS IN Se^{77}
R. L. Robinson, F. K. McGowan, and P. H. Stelson 63

Information on transitions from Coulomb-excited levels in Se^{77} at 242, 440, and 515 kev is reported.

MÖSSBAUER EFFECT WITH Ni^{61}
F. E. Obenshain and H. H. F. Wegener 68

Abstract of paper to be published in the *Physical Review*.

MÖSSBAUER EFFECT FOR Ni^{61} WITH APPLIED MAGNETIC FIELDS
H. H. F. Wegener and F. E. Obenshain 69

Abstract of paper to be submitted to *Zeitschrift für Physik*.

A STUDY BY THE MÖSSBAUER METHOD OF THE HFS SPLITTING OF Au^{197} ALLOYED IN Fe, Co, AND Ni
L. D. Roberts and J. O. Thomson 69

The lifetime of the 77-kev level of Au^{197} has been measured as 2 ± 0.2 mμsec. The magnetic field at the Au nucleus in Au-Fe, Au-Co, and Au-Ni alloys has been measured as 280,000 gauss, 220,000 gauss, and unmeasurably small respectively.

MAGNETIC STRUCTURE PROPERTIES OF RARE-EARTH METALS
W. C. Koehler, E. O. Wollan, M. K. Wilkinson, and J. W. Cable 72

Abstract of paper presented at Rare Earth Seminar (proceedings to be published by McGraw-Hill, New York, April 1961).

NEUTRON DIFFRACTION INVESTIGATION OF MAGNETIC ORDERING IN DYSPROSIUM
M. K. Wilkinson, W. C. Koehler, E. O. Wollan, and J. W. Cable 72

Abstract of paper to be published in the *Journal of Applied Physics* (suppl).

NEUTRON DIFFRACTION STUDY OF METALLIC ERBIUM
J. W. Cable, E. O. Wollan, W. C. Koehler, and M. K. Wilkinson 73

Abstract of paper to be published in the *Journal of Applied Physics* (suppl).

MAGNETIC ORDERING IN RARE-EARTH INTERMETALLIC COMPOUNDS
H. R. Child, M. K. Wilkinson, J. W. Cable, E. O. Wollan, and W. C. Koehler 73

Neutron diffraction investigations have given the paramagnetic moments, magnetic ordering temperatures, ordered magnetic moments, and ordered moment orientation for a group of rare-earth intermetallic compounds with the NaCl-type structure.

NEUTRON DIFFRACTION BY HELICAL SPIN STRUCTURES
W. C. Koehler 76

Abstract of paper to be published in the *Journal of Applied Physics*.

NEUTRON DIFFRACTION INVESTIGATIONS OF METALLIC CERIUM AT LOW TEMPERATURES
M. K. Wilkinson, H. R. Child, C. J. McHargue, W. C. Koehler, and E. O. Wollan 76

Abstract of paper submitted to the *Physical Review*.

A NEUTRON DIFFRACTION INVESTIGATION OF THE MAGNETIC ORDER IN MnI_2
J. W. Cable, M. K. Wilkinson, E. O. Wollan, and W. C. Koehler 76

Abstract of paper to be published in the *Physical Review*.

VIBRATIONAL SPECTRUM OF THE $NCSe^-$ ION
H. W. Morgan 77

The infrared and Raman spectra of KNCSe have been studied and the observed frequencies assigned to the fundamental modes of the $NCSe^-$ ion.

APPLICATIONS OF SOLID SOLUTION INFRARED SPECTRA: THE FREQUENCY CALIBRATION OF PRISM SPECTROMETERS AND THE MEASUREMENT OF SPECTRAL SLIT WIDTH
P. A. Staats and H. W. Morgan 77

Sixteen narrow absorption bands, spaced through the region 2200 to 700 cm^{-1}, provide calibration points for spectrometers equipped with NaCl prisms. These bands are observed in solid solutions, produced by cooling a molten alkali halide containing six added compounds.

APPLICATIONS OF SOLID SOLUTION INFRARED SPECTRA: THE DETERMINATION OF TRACE AMOUNTS OF POLYATOMIC INORGANIC IONS
J. R. Lawson, R. L. Barnett, Jr., and H. W. Morgan 79

Abstract of paper to be published in *Analytical Chemistry*.

VAPOR-PHASE INFRARED ABSORPTION SPECTRA OF TiF_4, ZrF_4, AND HfF_4
M. Blander and H. W. Morgan 79

Vapor-phase infrared spectra of TiF_4, ZrF_4, and HfF_4 have been studied in a heated cell. The observed absorptions have been assigned to the stretching motions of these molecules.

AN IMPROVED Li^6-LOADED GLASS SCINTILLATOR FOR NEUTRON DETECTION
F. W. K. Firk, G. G. Slaughter, and R. J. Ginther 80

Abstract of paper to be submitted to *Nuclear Instruments & Methods*.

DEVELOPMENT OF A POLARIZED-ION SOURCE
J. E. Sherwood, S. J. Ovenshine, and R. F. King 81

Polarized deuteron currents of the order of 10^{-8} amp have been obtained. Polarization has been confirmed by observing anisotropy in the neutron yield of the $T(d,n)He^4$ reaction.

LARGE-AREA GERMANIUM SURFACE-BARRIER COUNTERS
F. J. Walter, J. W. T. Dabbs, and L. D. Roberts 84

Abstract of published paper: *Rev. Sci. Instr.* **31**, 756 (1960).

PULSE CHARACTERISTICS OF SOME FAST PHOTOTUBES
C. W. Williams, R. P. Cumby, and J. H. Neiler 84

A system for testing phototubes by means of light pulsing has been constructed, and a group of phototubes were tested to determine their pulse characteristics under fast pulse conditions.

PROPERTIES OF SEMICONDUCTOR DETECTORS
J. W. T. Dabbs, F. J. Walter, and L. D. Roberts 86

Resolution, stability, and noise in silicon detectors have been studied at 77 and 300°K. Detailed considerations regarding pulse shapes and rise times at the amplifier are presented.

RESPONSE OF SILICON DETECTORS TO FISSION FRAGMENTS
H. W. Schmitt, J. H. Neiler, F. J. Walter, and R. J. Silva 91

The response of silicon surface-barrier detectors to fission fragments has been found not to be strictly proportional to fragment energy. Pulse-height defects range from 6 to 26 Mev, depending on silicon resistivity and detector bias.

PUBLICATIONS 95

PAPERS PRESENTED AT SCIENTIFIC AND TECHNICAL MEETINGS 98

ANNOUNCEMENTS 102

ADVISORY COMMITTEE 103

ACTIVITIES RELATED TO EDUCATIONAL INSTITUTIONS 103

PHYSICS SEMINARS 108

PHYSICS DIVISION ANNUAL PROGRESS REPORT

GAMMA-RAY DIFFRACTION BY RESONANT NUCLEI[1]

G. T. Trammell

A theory of the interaction of waves with a crystal of resonators is developed. The dispersion relation for the waves in the crystal and the reflection coefficient near Bragg angles are obtained. It is stressed that for systems excited (and reradiating) coherently, the partial radiation width appearing in the resonance denominators differs from that of an isolated resonator.

[1]Abstract of paper to be published in *Proceedings of International Conference on Chemical Effects of Nuclear Transformations, Prague, October 1960.*

ELASTIC SCATTERING BY BOUND NUCLEI

G. T. Trammell

In the expression giving the amplitude of the elastically scattered waves (of slow neutrons, of x rays, etc.) from atoms bound in crystals, the effect of the zero point and temperature motion of the scattering atom is contained in a factor (multiplying the fixed-scatterer amplitude),

$$\left\langle e^{-i(\vec{k}_f-\vec{k}_0)\cdot\vec{r}} \right\rangle, \tag{1}$$

where $\vec{k}_f$ and $\vec{k}_0$ are the wave vectors of the scattered and incident radiations, respectively, $\vec{r}$ is position of the nucleus of the scattering atom, and the brackets indicate the expected value for the crystalline state involved. This factor comes immediately from the Born approximation in the case of Thomson scattering or magnetic scattering of neutrons, and, by making use of the Fermi pseudo potential, in the case of nuclear potential scattering of neutrons as well.

On the other hand, the corresponding factor in the expression for the elastically scattered resonance radiation in a Mössbauer-type experiment may be obtained from a formula of Lamb[1] and is

$$\left\langle e^{-i\vec{k}_f\cdot\vec{r}} \right\rangle \left\langle e^{i\vec{k}_0\cdot\vec{r}} \right\rangle. \tag{2}$$

As one immediately guesses, (1) and (2) are the correct expressions in the extreme cases that the collision time is very short or very long, respectively, compared to the time for the atom in the crystal to move a distance comparable to a wavelength.

[1]W. E. Lamb, *Phys. Rev.* 55, 190 (1939).

The displacement of an atom from its equilibrium position in a crystal is due to many independent oscillations (normal modes). Therefore[2] (1) and (2) are given by

$$e^{-i(\vec{k}_f-\vec{k}_0)^2\langle r^2\rangle/2} = e^{-2k_0^2\sin^2(\theta/2)\langle r^2\rangle} \tag{1'}$$

and

$$e^{-k_0^2\langle r^2\rangle}, \tag{2'}$$

where $k_0 = |\vec{k}_0| = |\vec{k}_f|$ and $\theta = \measuredangle(\vec{k}_f, \vec{k}_0)$. The elastic wave from very fast collisions falls off from a maximum of 1 at $\theta = 0$ to $e^{-2k_0^2\langle r^2\rangle}$ at $\theta = 180°$, whereas for the very slow collision the amplitude is independent of angle. (1′) and (2′) are seen to cross at $\theta = 90°$.

The elastically scattered wave is the contributor to the scattering at the Bragg angles. Off resonance, the "potential" scattering contributes to the Bragg peaks. Its amplitude will be governed by (1′). On resonance, the angular dependence of the Bragg peak amplitudes will be intermediate between (1′) and (2′).

According to a formula of Lamb,[1] the amplitude of the elastically scattered wave in the resonance case is given by

$$\sum_n \frac{\left\langle \chi_{n0}\left|e^{-i\vec{k}_f\cdot\vec{r}}\right|\chi_n\right\rangle\left\langle \chi_n\left|e^{i\vec{k}_0\cdot\vec{r}}\right|\chi_{n0}\right\rangle}{E_{k0}-E_R-(\epsilon_n-\epsilon_{n0})+i\Gamma}\cdot\frac{\Gamma_i}{k_0} \tag{3}$$

times a factor depending on polarizations, multipolarity, etc. In (3) the χ's are crystal wave functions, the ϵ's are their energy eigenvalues, $E_R - i\Gamma$ is the resonance "energy," and Γ_i is the partial width for the incident particle. (3) may also be written,

$$\frac{\Gamma_i}{ik_0}\int_0^\infty e^{i(E_{k0}-E_R)t}e^{-\Gamma t}\left\langle \chi_{n0}\left|e^{-i\vec{k}_f\cdot\vec{r}(t)}e^{i\vec{k}_0\cdot\vec{r}(0)}\right|\chi_{n0}\right\rangle, \tag{3'}$$

where $\vec{r}(t)$ is nuclear c.m. position operator in the Heisenberg representation.

Expressions (1) or (2) result from (3′) if in $\vec{r}(t)$ we put $t = 0$ or $t = \infty$, respectively [we make use of $\left\langle e^{-i\vec{k}_f\cdot\vec{r}(\infty)}e^{i\vec{k}_0\cdot\vec{r}(0)}\right\rangle = \left\langle e^{-i\vec{k}_f\cdot\vec{r}}\right\rangle\left\langle e^{i\vec{k}_0\cdot\vec{r}}\right\rangle$].[3]

To estimate the regions of validity of (1) and (2) we assume for simplicity that the temperature of the crystal is much less than the Debye temperature, Θ, so that χ_{n0} may be taken as the crystal ground state. Making the constant sound velocity approximation for the crystal lattice we have $\Theta = \omega_{max}$ $(K = \hbar = 1)$, and $\langle r^2\rangle \doteq (2M\Theta)^{-1}$, where ω_{max} is the angular frequency of the

---

[2] F. Bloch, *Z. Physik* **74**, 295 (1932).

[3] L. Van Hove, *Phys. Rev.* **95**, 249 (1954).

shortest sound wave and M is the atomic mass. Now taking account of the fact that

$$\sum_n (\epsilon_n - \epsilon_{n0}) \left| \left\langle \chi_n \right| e^{i\vec{k}_0 \cdot \vec{r}} \left| \chi_{n0} \right\rangle \right|^2 = k_0^2/2M ,$$

the recoil energy,[4] we estimate that the contributions to (3) involving intermediate energy transfers greater than the order of Max $(k_0^2/2M, \Theta)$ are negligible. (This crude approximation can be much improved by explicitly considering the contributions of intermediate excitation of various numbers of phonons.[5]) Then, if $|E_{k0} - E_R + i\Gamma| \gg$ Max $(k_0^2/2M, \Theta)$, closure may be applied in (3), yielding

$$\frac{1}{E_{k0} - E_R + i\Gamma} \exp\left[-\frac{k_0^2 \sin^2(\theta/2)}{M\Theta} \right] . \tag{4}$$

If $|E_{k0} - E_R + i\Gamma| \ll$ Max $(k^2/2M, \Theta)$ the term $n = n_0$ may be separated off in (3), yielding approximately

$$\frac{e^{-k_0^2/2M\Theta}}{E_{k0} - E_R - i\Gamma} + \frac{\left(1 - e^{-k_0^2/2M\Theta}\right)}{\text{Max}\,(k^2/2M, \Theta)} . \tag{4'}$$

The second, nonresonant, term in (4′) is negligible if

$$e^{-k_0^2/2M\Theta} \gg |E_{k0} - E_R + i\Gamma| \div \text{Max}\,(k_0^2/2M, \Theta) .$$

The validity of (3) for gamma-ray resonances may be verified by a rather straighforward application of the Wigner-Weisskopf[6] procedure.

For slow-neutron resonances, its validity is not so immediately clear. For slow-neutron nuclear scattering (resonant or not), one can derive the formula for the scattering amplitude,

$$f = \frac{M+m}{M} \sum_n a(k_n') \left\langle \chi_{n0} \right| e^{-i\vec{k}_f \cdot \vec{r}} \left| \phi_n \right\rangle \left\langle \phi_n \right| e^{i\vec{k}_0 \cdot \vec{r}} \left| \chi_{n0} \right\rangle , \tag{5}$$

where ϕ_n is a crystal wave function with the mass of the compound nucleus $(M + m)$ substituted for the mass of the struck nucleus, and $a(k_n')$ is the free-particle scattering length for c.m. energy $(k_0^2/2m) - (\epsilon_n' - \epsilon_{n0})$.

---

[4] H. J. Lipkin, *Ann. Phys.* (N.Y.) **9**, 332 (1960).

[5] Ref 1 and R. Weinstock, *Phys. Rev.* **65**, 1 (1944).

[6] V. Weisskopf and E. Wigner, *Z. Physik* **63**, 54 (1930).

Near a resonance we obtain

$$f = \frac{M+m}{M} R \left\langle \chi_{n0} \middle| e^{-i(\vec{k}_f - \vec{k}_0)\cdot\vec{r}} \middle| \chi_{n0} \right\rangle$$

$$+ \frac{M+m}{M} \gamma^2 \sum_n \frac{\left\langle \chi_{n0} \middle| e^{ik_f \cdot r} \middle| \phi_n \right\rangle \left\langle \phi_n \middle| e^{ik_0 \cdot r} \middle| \chi_{n0} \right\rangle}{E_{k0} - E_R - (\epsilon_n' - \epsilon_{n0}) + i\Gamma_n}, \tag{6}$$

where R represents the constant part of the scattering length (potential scattering), and

$$\Gamma_n = \gamma^2 [2\mu(E_{k0} - \epsilon_n' + \epsilon_{n0})]^{1/2} + \Gamma_\gamma \ .$$

The resonant term in (6) is of the form of (3) if $m/M << 1$ and if the neutron width is small relative to the gamma-ray width.

The first term of (6) is the usual Fermi pseudo potential result, and for n-p scattering it is known[7] that its validity depends on the smallness of a (= R in this case) $\div$ L, where L measures the amplitude of the nuclear swing in the crystal. At resonance $a \sim \lambda\!\!\!^{-} \sim L$, but the validity of (6) (single-collision approximation) can be shown to depend on the smallness of

$$\left(\frac{m}{M+m}\right)^3 \cdot \frac{a}{L},$$

which will be small for slow neutrons even at resonance.

[7]G. Breit, *Phys. Rev.* 71, 218 (1947).

FLUCTUATION-DISSIPATION RELATIONS FOR NEUTRON DIFFRACTION[1]

Richard L. Becker

Fluctuation-dissipation (FD) relations are relations between responses of driven systems and their equilibrium fluctuations. Usually the system is considered in interaction with an external field (signal generator). Using perturbation theory, one may generalize to situations in which the reaction on the driving system must be included. The scattering of a neutron wave packet by a fluid initially in equilibrium is treated, using the Fermi pseudo potential and the Van Hove statistical space-time correlation function $G(\vec{r}, t)$. The relevant response functions, for example, $d^2\sigma/d\Omega\, dE$ and the time-dependent local particle density in the fluid, are expressed most directly in terms of both Re G and $\hbar^{-1}$(Im G). We regard such expressions as primitive FD relations. A systematic presentation is given of integral representations of Re G in terms of $\hbar^{-1}$(Im G) and of

[1]Abstract of paper to be submitted to *Physics of Fluids*.

their converses. These statistical relations are valid for any system in equilibrium and are independent of considerations of driving the system. Although Im G equals zero in the classical limit, $\hbar^{-1}$(Im G) does not. On eliminating $\hbar^{-1}$(Im G) in favor of Re G by means of one of the statistical relations, the responses may be expressed in terms of Re G alone, which corresponds to the usual form of FD relations.

BOUND PAIRS AND REACTION MATRIX SINGULARITIES[1]

Richard L. Becker[2]

Two contributions to the foundations of the Brueckner theory are made. By approaching the infinite medium as the limit of a sequence of finite systems of the same average particle density and increasing volume, it is shown that the integrals over reaction matrix elements occurring in the expression for the energy should be principal-value integrals, thus removing the difficulties in the usual formulation caused by reaction matrix singularities. It is also shown how the negative-energy bound-state solutions of the wave equation for an interacting pair in the presence of a medium may be incorporated into the lowest order of the theory. Their existence is a "non-adiabatic" effect corresponding to the formation of "diatomic molecules," and their use requires a modification going outside the bounds of perturbation theory. For attractive interactions sufficiently strong that "molecular" states exist, it is essential to include their contribution to the binding energy even in an infinite medium, for, unlike the continuum states, their energy shift does not vanish inversely with the volume.

---

[1]Abstract of paper to be submitted to *Annals of Physics*.

[2]Part of this work was performed while the author was a visiting Fellow at Princeton University, Princeton, N.J.

CENTER-OF-MASS ENERGY IN OVERHAUSER'S SELF-CONSISTENT FIELD WITH GIANT DENSITY FLUCTUATIONS

Richard L. Becker

The usual solution of the Hartree self-consistent field approximation to the problem of an infinite medium of fermions (e.g., nucleons) interacting pairwise involves single-particle states which are momentum eigenfunctions, and a single-particle potential which is independent of position. It is gratifying that the Hartree potential is translation invariant, because the original Schroedinger many-body Hamiltonian is translation invariant. The solution implies a constant

particle density, which is therefore independent of the location of the origin of the coordinate frame. By filling up momentum space symmetrically about the origin, one obtains a Hartree state (product of single-particle states) of an N-particle system for which the expectation value of the center-of-mass momentum

$$\frac{P^2}{2mN} = \frac{1}{2mN} \sum_{i,j=1}^{N} \vec{p}_i \cdot \vec{p}_j$$

is zero. The energy of this state is therefore an approximation to the intrinsic (internal) energy of the system. By filling up states asymmetrically one obtains a Hartree state corresponding to a translating system. The intrinsic energy of this state of the system is the Hartree energy minus the center-of-mass energy.

In the nuclear shell model a single-particle potential is employed which is centered on a definite point of space, which is taken to be the origin. As the single-particle wave functions are not momentum eigenfunctions, the Hartree product state is not an eigenfunction of the total linear momentum. The energy of any shell-model state therefore contains vibrational energy of the center of mass as well as intrinsic energy. A considerable literature on this subject has appeared.[1] Lipkin[1] has given a clear discussion of this situation and of related ones. Since $P^2/2Nm$ commutes with the original Hamiltonian H, the exact wave function is also an eigenfunction of the "intrinsic" Hamiltonian $H' = H - (P^2/2Nm)$, and the eigenvalue of H' is the intrinsic energy. If H_s is the shell-model Hamiltonian, $H_s' = H_s - (P^2/2Nm)$ is regarded as the shell-model approximation to the intrinsic Hamiltonian H'.

Returning to the case of a large system, with the aim of finally taking the limit $N \to \infty$ while keeping the average density $\rho_0 = N/\Omega$ constant, we consider Overhauser's[2] Hartree solution in which the single-particle states are not plane waves but are distorted plane waves of the form (in one dimension)

$$\phi_k(x) = \cos\theta\, e^{ikx} + \sin\theta\, e^{i(1-q/|k|)kx} . \tag{1a}$$

The single-particle potential is of the form

$$U(x) = A + B\cos qz . \tag{1b}$$

For a given two-particle interaction $v(x_i - x_j)$, it has been shown by Overhauser that an approximately self-consistent solution of the above form[3] exists. The slight approximation consists in neglecting Fourier components of the wave function with $|k| > 2k_F$, where k_F is the Fermi wave number. (In the ideal degenerate Fermi gas, the Fermi sea consists of those states with $|k| \leqq k_F$.) The self-consistency requirement, for a given assumed value of q, provides a relation between θ

---

[1] *Cf.* H. J. Lipkin, *Ann. Phys.* (*N.Y.*) **9**, 169 (1960) and references to the earlier literature given therein.

[2] A. W. Overhauser, *Phys. Rev. Letters* **4**, 415 (1960).

[3] The departure from constancy of both the Hartree potential and the particle density in Overhauser's solution is the simplest possible, in the sense that the fluctuation involves only one Fourier component.

and the single-particle potential. For given q one then obtains an eigenvalue of the Hartree Hamiltonian, say $E[q, \theta(q)]$. Overhauser's class of functions θ_k includes the plane-wave basis $\{e^{ikx}\}$ as a special case ($\theta = 0$ or $q = 0$). For a large class of two-particle potentials, self-consistent Overhauser solutions with $\theta \neq 0$ exist for a range of values of $q \lesssim 2k_F$. When such a solution exists it has been shown to have an eigenvalue of the Hartree Hamiltonian which is less than that of the corresponding Hartree Hamiltonian for the plane-wave case. As both the plane-wave solution and the distorted-wave solution are stationary solutions of the Rayleigh-Ritz variational problem, it would be interesting to investigate the θ dependence of the Rayleigh-Ritz energy for fixed q. It must be qualitatively as in one of the two parts of Fig. 1, where no significance is to

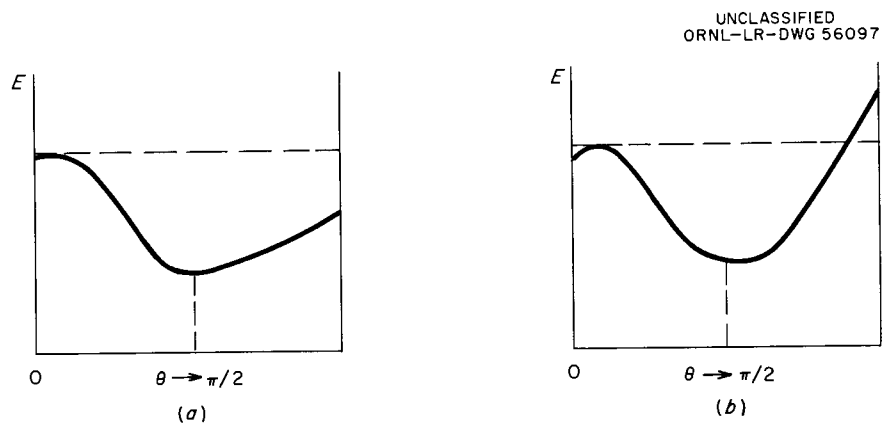

Fig. 1. Energy vs Theta.

be attached to the numerical value of θ for which the curves, as drawn, have a minimum. In either case, the energy of the plane-wave state ($\theta = 0$) is a relative maximum as a function of θ. Furthermore, one may vary q. The minimum energy as a function of q is found[2] to occur for $q \approx 2k_F$, for rather clear physical reasons.[2]

Objections to the use of a non-translation-invariant Hartree Hamiltonian for an infinite medium have been voiced. The point of view to be taken here is that the difficulty is the same as in the case of the nuclear shell model and may be overcome in the same way. For a large but finite system, the eigenvalue of the Hartree Hamiltonian in Overhauser's solution consists of an energy of center-of-mass motion as well as an intrinsic energy. We have evaluated the center-of-mass kinetic energy, obtaining

$$E_{CM} = \frac{q^2}{4m} \cdot \frac{1}{N} \sum_{i=1}^{N/2} \sin^2 (2\theta_i) \, . \tag{2}$$

This energy is independent of N for a large system and thus becomes negligible as $N \to \infty$ in comparison with the eigenvalue of the Hartree Hamiltonian, which is proportional to N. For an infinite medium the Overhauser energy is an approximation to the intrinsic energy, whereas for a finite system the intrinsic energy is lower than the Overhauser eigenvalue by a small amount. Details of the evaluation of E_{CM} follow.

For a state of zero linear momentum, $\vec{P}$ states must be occupied symmetrically in k space. We first note that

$$\phi_k(x_1)\,\phi_{-k}(x_2) = e^{ikx_{12}}\left[\cos^2\theta + e^{-iqx_{12}}(\sin^2\theta - \sin 2\theta \cos qX_{12})\right]$$

$$\equiv e^{ikx_{12}}[12]\,, \tag{3}$$

where

$$x_{12} = x_1 - x_2\,, \qquad X_{12} = \frac{x_1 + x_2}{2}. \tag{3a}$$

The pair state has a normalization integral

$$\left\langle \phi_k \phi_{-k} \,|\, \phi_k \phi_{-k} \right\rangle = \int_0^L dX_{12} \int_{-L}^L dx_{12}\,|[12]|^2 = 2L^2\,. \tag{4}$$

Also,

$$\left\langle \phi_k \phi_{-k} \left| -\frac{\partial^2}{\partial X_{12}^2} \right| \phi_k \phi_{-k} \right\rangle = -q^2 \sin 2\theta \int_0^L dX_{12} \cos qX_{12} \int_{-L}^L dx_{12}\,[12]^* e^{-iqx_{12}}$$

$$= 2Lq^2 \sin 2\theta \int_0^L dX_{12} \cos qX_{12}[\sin^2\theta - \sin 2\theta \cos qX_{12}]$$

$$= L^2 q^2 \sin^2(2\theta)\,. \tag{5}$$

For a two-particle system one sees immediately that

$$E_{CM} = \frac{\left\langle \phi_k \phi_{-k} \left| -\frac{1}{4m}\frac{\partial^2}{\partial X^2} \right| \phi_k \phi_{-k} \right\rangle}{\left\langle \phi_k \phi_{-k} \,|\, \phi_k \phi_{-k} \right\rangle} = \frac{q^2}{4m}\cdot\frac{1}{2}\sin^2(2\theta)\,. \tag{6}$$

For a system of N particles (N is assumed to be even),

$$\Phi^{(N)} = \prod_{i=1}^{N/2} \phi_{k_i}(x_{2i})\,\phi_{-k_i}(x_{2i+1})\,, \tag{7}$$

and the normalization integral is

$$\left\langle \Phi^{(N)} \,|\, \Phi^{(N)} \right\rangle = \prod_{i=1}^{N/2} \int_0^L dX_{2i,2i+1} \int_{-L}^L dx_{2i,2i+1}\,|[2i, 2i+1]|^2$$

$$= (2L^2)^{N/2}\,. \tag{8}$$

One may, through successive coordinate transformations, as schematically indicated in Fig. 2, obtain

$$X_{2i,2i+1} = X + f(\text{relative coordinates}) \,, \tag{9}$$

where X is the center-of-mass coordinate of the entire system,

$$X = \frac{1}{N} \sum_{j=1}^{N} x_j \,. \tag{10}$$

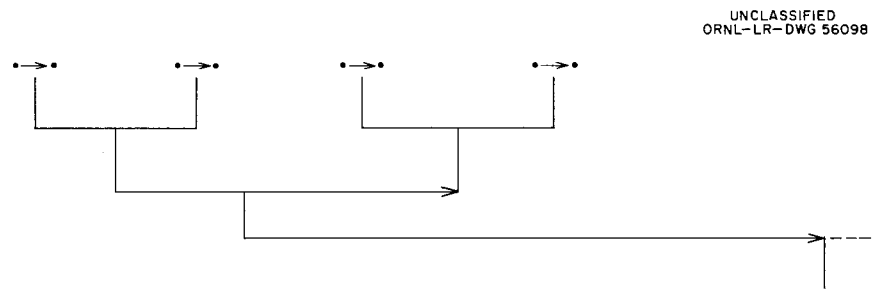

Fig. 2. Structure of the Coordinate Transformations.

In the first step, one replaces the individual-particle coordinates by relative coordinates of pairs together with the center-of-mass coordinates of pairs. One repeats the same procedure with pairs of pairs, etc. It is not necessary that N be a number which may be written as $N = 2^M$. (Some "seeded" particles may advance in this "tournament" through "byes.") Then

$$-\frac{\partial^2}{\partial X^2}\Phi^{(N)} = -q^2 \left\{ \sum_{i=1}^{N/2} \sin(2\theta_i) e^{-iqx_{2i,2i+1}} \cos qX_{2i,2i+1} \times \prod_{j\neq 1} [2j, 2j+1] \right\} e^{i\sum_l k_l x_{2l,2l+1}} \,, \tag{11}$$

and, hence, from (4) and (5)

$$\frac{1}{2mN} \left\langle \Phi^{(N)} \middle| -\frac{\partial^2}{\partial X^2} \middle| \Phi^{(N)} \right\rangle = \frac{q^2}{2mN} (2L^2)^{(N-2)/2} \left[-\frac{2L^2}{2} \sum_{i=1}^{N/2} \sin^2(2\theta_i) \right] . \tag{12}$$

Dividing (12) by (8) gives (2).

The analysis of the center-of-mass energy may be extended to three dimensions and to the Hartree-Fock method, with the same conclusion.

NUMERICAL STUDY OF THE DISTORTED-WAVE THEORY OF DIRECT NUCLEAR REACTIONS

R. H. Bassel[1] R. M. Drisko[1] G. R. Satchler

A program has been written, for use on the IBM 704 or 7090 computer, to calculate the predictions of the distorted-wave Born approximation theory of direct nuclear reactions. The theory is based upon a transition amplitude of the form

$$T = \int \phi_2(\vec{k}_2, \vec{r})^* \, (B \mid V \mid A) \, \phi_1(\vec{k}_1, \vec{r}) \, d\vec{r} \, ,$$

where the $\phi(k,r)$ are distorted waves describing the motion of the incident and outgoing particles. The distortion arises from scattering both by the Coulomb field and the nuclear optical potential; without it the ϕ would be plane waves. The $(B \mid V \mid A)$ is the matrix element of the interaction between the initial and final nuclear internal states; it plays the role of a form factor. By having a choice of form factors available in the program we are able to calculate stripping or knock-on reactions (in the usual zero-range force approximation) or inelastic scattering, with a variety of nuclear models. The optical potentials presently available have a Saxon real part, and choice of Saxon or surface Gaussian imaginary part. We may compute differential cross sections, polarizations, and gamma-ray angular correlation coefficients. In addition we may study the radial distribution of the integrands of the amplitudes T and so discover if the reactions are localized in any particular region.

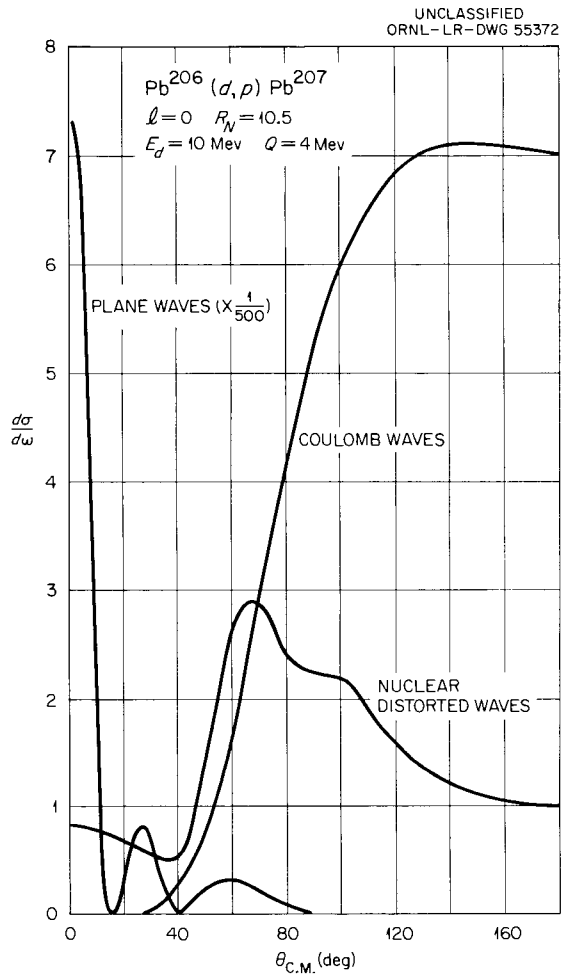

Fig. 1. Effect of Nuclear Distortion when the Deuteron Energy Is Below the Coulomb Barrier.

Some preliminary studies have been made with this program at energies ranging from 3 to 300 Mev.[2] Protons of 150 and 300 Mev exciting the 4.43-Mev level in C^{12} were considered and distortion effects found to be considerable. Inelastic scattering at lower energies is also being studied, with particular attention to the angular correlation

[1] Electronuclear Research Division.

[2] R. M. Drisko, R. H. Bassel, and G. R. Satchler, *Bull. Am. Phys. Soc.* **6**, 56 (1961); G. R. Satchler, R. M. Drisko, and R. H. Bassel, *Bull. Am. Phys. Soc.* **6**, 66 (1961); R. H. Bassel, R. M. Drisko, and G. R. Satchler, *Bull. Am. Phys. Soc.* 6, 67 (1961).

of subsequent gamma rays with the inelastic particles. A survey of distortion effects in deuteron stripping reactions was also initiated. As an example, the results for the reaction $Pb^{206}(d,p)Pb^{207}$ are illustrated. For purposes of comparison, a hypothetical Q value of 4 Mev is used for all the curves shown. Figure 1 illustrates the importance of the nuclear distortion even when the deuteron energy is below the Coulomb barrier. Figures 2 through 4 compare the differential cross sections for angular momentum transfer $l = 0$ to 4 for deuteron energies of 10, 15, and 20 Mev. For contrast, two calculations for $B^{11}(d,n)C^{12}$ are shown in Fig. 5. The weaker deuteron potential gives a "best fit" to the elastic deuteron scattering from B^{11} at 3 Mev. Both cases show the type of backward peaking which, if observed experimentally, is usually ascribed to the "heavy-particle stripping" process.

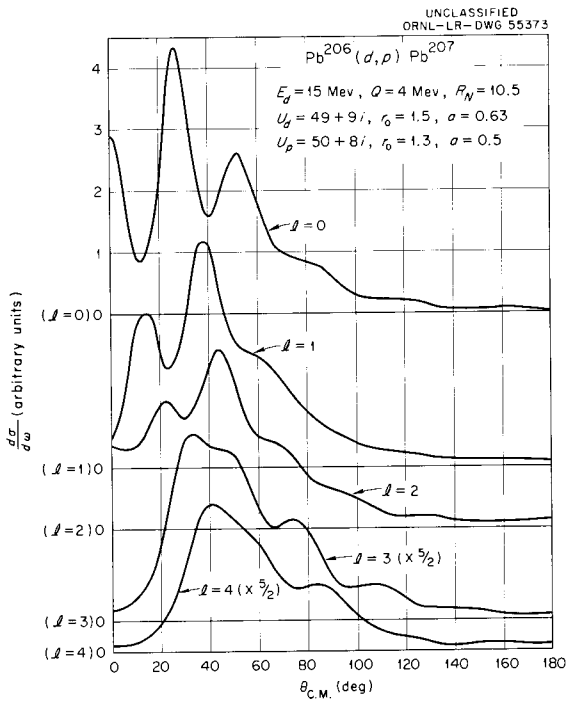

Fig. 3. Differential Cross Section for Angular Momentum Transfer ($L = 0$ to 4) for Deuteron Energy of 15 Mev.

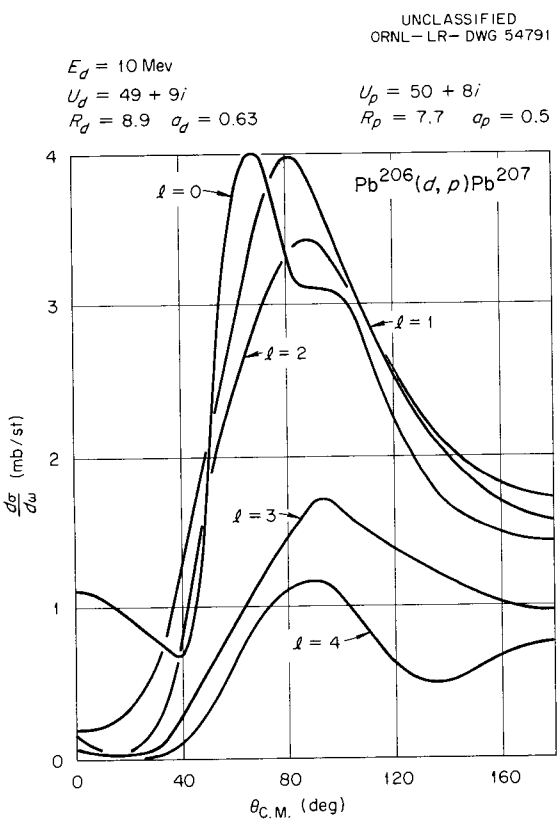

Fig. 2. Differential Cross Section for Angular Momentum Transfer ($L = 0$ to 4) for Deuteron Energy of 10 Mev.

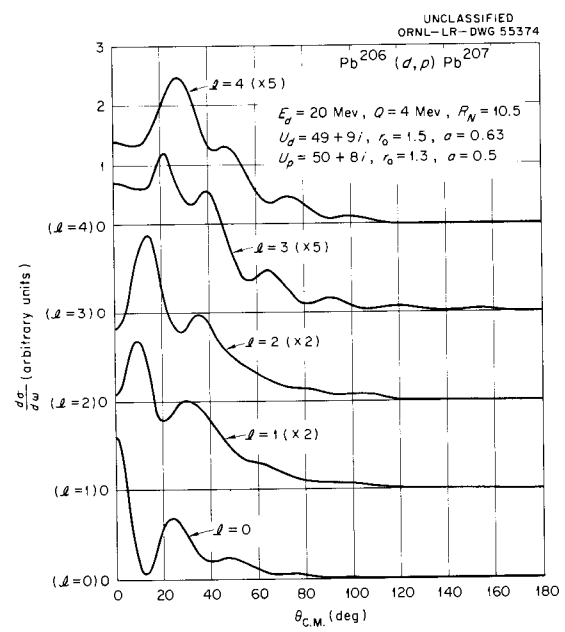

Fig. 4. Differential Cross Section for Angular Momentum Transfer ($L = 0$ to 4) for Deuteron Energy of 20 Mev.

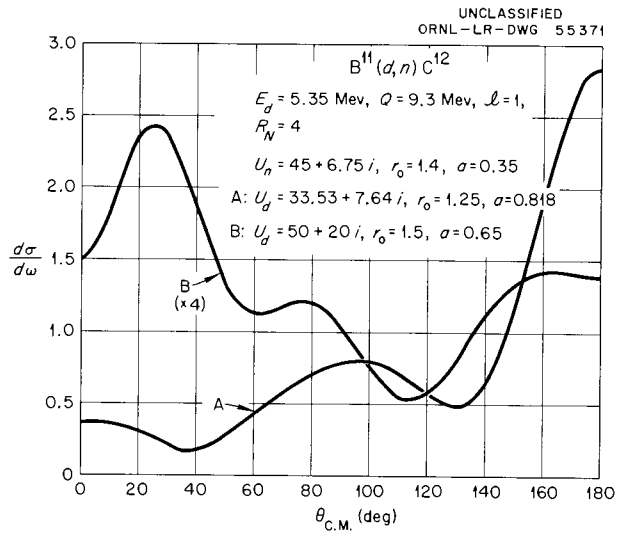

Fig. 5. Two Calculations for the Reaction $B^{11}(d,n)C^{12}$.

POLARIZATION PHENOMENA IN DEUTERON STRIPPING REACTIONS[1]

L. C. Biedenharn[2] G. R. Satchler

Polarization phenomena in the usual theory of (d,p) reactions (i.e., the distorted-wave theory without explicit spin-orbit coupling) are shown to have a common origin, which is in effect simply a measurement of neutron-transfer angular-momentum direction (multiplied by quantum geometrical factors). The limitations implied by this result are discussed.

The effect of explicit spin-orbit couplings is discussed in detail for the important case where the transfer angular momentum is zero. It is shown that for this case the proton polarization is approximately given by the *derivative* of the (unpolarized) angular distribution. (Conditions are given under which this approximation is useful.)

Symmetry considerations in the distorted-wave theory are also discussed, and illustrated by application to Coulomb effects. Various numerical examples illustrate the qualitative predictions of the present discussion.

---

[1]Abstract of invited paper, *International Conference on Polarization Phenomena, Basel, July 1960;* to be published in *Helvetica Physica Acta,* 1961.

[2]Consultant, from Rice University, Houston, Tex.

COLLECTIVE EFFECTS IN INELASTIC SCATTERING[1]

W. T. Pinkston[2] G. R. Satchler

Inelastic scattering is closely analogous to an electric multipole radiative transition and will show similar collective enhancement. Spin-flip transitions are little affected, the enhancement being found in the spin-independent amplitudes. The enhancement varies with scattering angle and modifies the conclusions drawn from polarization and gamma-correlation measurements about the angular momentum coupling in the target nucleus, especially in the p shell, since these depend upon the ratio of spin-flip to spin-independent amplitudes.

---

[1]Abstract of paper published in *Proceedings of International Conference on Nuclear Structure, Kingston, Ontario, 1960.*

[2]Summer participant from Vanderbilt University, Nashville, Tenn.

DETECTION OF DEUTERON ALIGNMENT WITH s-WAVE REACTIONS[1]

H. B. Willard

A brief review is made of some properties possessed by oriented deuteron beams with tensor moments up to rank 2. In particular, it is pointed out that angular distributions may result from aligned deuteron beams, even though the reaction may be initiated by s waves and/or proceed through the contribution from a single element of the reaction matrix. Specific calculations are carried out for the 107-kev resonance in the $T(d,n)He^4$ reaction, the 430-kev resonance in the $He^3(d,p)He^4$ reaction, and the 940-kev resonance in the $C^{12}(d,p)C^{13}$ reaction. Several suggestions are made for these reactions as analyzers of deuteron alignment.

---

[1]Abstract of paper to be published in *Helvetica Physica Acta.*

AN EFFICIENT EXCITATION METHOD FOR AN OPTICAL MASER

T. A. Welton

The optical maser originally described by Schawlow and Townes[1] offers a new method for handling energy, through its ability to produce coherent light. Coherent light can be made to have an extremely narrow line width, and can be propagated in a beam with a spreading angle

---

[1]A. L. Schawlow and C. A. Townes, *Phys. Rev.* 112, 1940 (1958).

determined only by diffraction. The realization of these potentialities for practical applications must await the development of an efficient method for generating the inverted population of atomic states required for maser operation. Although the use of optically excited fluorescence in transparent crystals (ruby) allowed the first successful demonstration of maser action at optical frequencies, such a device is grossly inadequate when large quantities of electrical energy are to be transformed to coherent radiation. The electrically excited gas maser (helium-neon), recently demonstrated by Javan, Bennett, and Herriott[2] at Bell Laboratories, is a device of much greater inherent promise for practical applications although still subject to very serious limitations in its present form. The gas maser has been independently studied (theoretically, that is!) at this Laboratory, and a device has been originated which is seriously proposed for construction. A description of one essential feature of this device (the method for supplying excited atoms) follows.

We require a light path of length L and cross-sectional area A^2 (A will denote *linear* aperture), in which light travels a mean distance $\bar{L}$ (extinction distance) before its intensity has dropped by a factor of $1/e$. We assume that the desired mode isolation has been achieved by some method, not here described. Thus far, the extinction arises only from absorption associated with the repeated reflections which confine the light within the specified light path. If now a gas at low pressure is introduced in the light path (resonator), no appreciable additional extinction will be produced unless the light frequency is close to the frequency of one of the optical transitions joining the normal gas atoms to the various excited states. If such an approximate resonance exists, then the additional extinction is easily calculated by use of the optical dispersion formula, the relevant parameters being the gas pressure, the oscillator strength for the transition, the collision broadening of the line, the broadening by quenching collisions, and the temperature, which determines the Doppler broadening.

Suppose we designate the upper state of the absorbing transition by 1 (thus far assumed to be the ground state) and the lower state by 2. If some of the atoms are in the excited state, the total cross section for interaction with the light remains essentially unchanged, but a new process enters the picture, namely induced emission. A photon colliding with an atom in state 2 has a large cross section for producing an atom in state 1, with a coincident rise of the quantum number for the radiation oscillator by one. Thus, we say that a second photon *coherent* with the first has been produced. In general, an excited gas atom yields a cross section for induced emission which is proportional to the number of coherent photons incident on the atom. Similarly the normal atoms will have a closely related cross section (Einstein's relation between the two B coefficients) for removing one photon from the beam. The net result is that the intensity of a beam of light traveling along the light path obeys the simple approximate equation

$$\frac{1}{I}\frac{dI}{dx} = -\frac{1}{\bar{L}} + \frac{1}{\sqrt{128\pi^3}}\sqrt{\frac{Mc^2}{kT}}\left(n_1 - \frac{g_1}{g_2}n_2\right)\frac{1}{\nu^3 c\tau A^2 L}, \tag{1}$$

[2]A. Javan, W. R. Bennett, Jr., and D. R. Herriott, *Phys. Rev. Letters* **6**, 106 (1961).

where

I = intensity at distance x along the path,

M = mass of the atom,

n_1 = total number of excited atoms,

n_2 = total number of normal atoms,

g_1, g_2 = statistical weights of the two states,

$\nu = 1/\lambda$, where λ = the wavelength of the light,

τ = the mean life for the spontaneous transition from 1 to 2.

We have assumed that the Doppler broadening dominates the line shape around the maximum of the cross sections and that the discrete extinctions at each reflection can be adequately replaced by an equivalent continuous extinction coefficient, $1/\bar{L}$. If n_1 and n_2 are adjusted to make $(1/I)/(dI/dx) > 0$, we will have achieved criticality, and the isolated mode (or modes) can build up in intensity so long as excited atoms are supplied to maintain this condition. The criticality condition is

$$n_1 - \frac{g_1}{g_2} n_2 > \sqrt{128\pi^3} \sqrt{\frac{kT}{Mc^2}} \frac{L}{\bar{L}} A^2 \nu^3 c\tau , \tag{2}$$

or

$$n_1 - \frac{g_1}{g_2} n_2 > \sqrt{\frac{2kT}{\pi Mc^2}} \frac{L}{\bar{L}} \frac{g_1}{g_2} \frac{A^2 \nu}{f r_0} , \tag{3}$$

where f is the oscillator strength for the transition and r_0 is the classical electron radius, 2.8×10^{-13} cm.

From (3), it is simple to see some of the conditions to be sought for a useful excitation method. Primarily, it is extremely advantageous to keep n_2 as low as possible so that n_1 can be somewhere near the lower limit imposed by (3). This has the effect of keeping the energy lost by spontaneous emission, which is proportional to n_1, as low as possible. The power that can be delivered by the system is seen to be also proportional to A^2, since the reflectors with area A^2 can handle only a certain maximum power per unit area. More precisely, denoting the spontaneous power by P_s, we have

$$P_s = \frac{8\pi^2 hc^2}{\lambda^4} \frac{g_1}{g_2} \sqrt{\frac{2kT}{\pi Mc^2}} \frac{L}{\bar{L}} A^2 \frac{n_1}{n_{10}} , \tag{4}$$

where n_{10} is the minimum critical value of n_1, obtained by setting $n_2 = 0$ and replacing the inequality by an equality in (3). We further let P_b be the power dissipated in heating the reflectors. The simplest resonator (Fabry-Perot) requires two reflections for a pulse of light to return to its starting condition, but more complicated resonators offer considerable advantage for practical application, six reflections being a useful choice. Again, in a simple resonator with two reflections, L and $\bar{L}$ are related by

$$\bar{L} = \frac{L}{1 - \alpha} , \tag{5}$$

where α is the reflection coefficient for the reflecting surfaces. Under suitable conditions, $1 - \alpha$ can be made as small as 0.01, but practical application will probably not allow $1 - \alpha$ to be much smaller than 0.05. Also, under practical conditions we must use $(1 - \alpha + \eta + \zeta)$ rather than $1 - \alpha$, where η is a number, probably about 0.05, to allow for imperfections in the reflectors, and ζ represents the energy removal for external use. We thus write

$$\bar{L} = \frac{2L}{r(1 - \alpha + \eta + \zeta)} , \tag{6}$$

where r is the reflection number (2 or 6, for example).

It appears that suitable cooling provision will allow removal of about 1 kw of heat per square centimeter of reflector, 10 kw/cm^2 being extremely marginal, and 0.1 kw/cm^2 being trivial. We therefore write

$$P_b = rQA^2 , \tag{7}$$

where Q is the permitted heat removal per unit area, in absolute units ($Q = 10^{10}$ ergs cm^{-2} sec^{-1} for 1 kw/cm^2). Last, we denote by P_o the output power in the form of coherent radiation. From some rough calculations, it appears that an optimum system will have a large enough fraction of the resonating energy extracted to approximately match the losses due to reflector heating and reflector imperfections. Thus ζ will be roughly 0.1, and we obtain

$$P_o = \frac{r\zeta}{1 - \alpha} QA^2 . \tag{8}$$

We can now estimate the efficiency of conversion from excited atoms to output coherent radiation. Combining (4) and (6), we obtain

$$P_s = \frac{8\pi^2 hc^2 n_1}{\lambda^4 n_{10}} \frac{g_1}{g_2} \sqrt{\frac{2kT}{\pi Mc^2}}\, r(1 - \alpha + \eta + \zeta)\, A^2 . \tag{9}$$

The λ^4 imposes a heavy penalty on the use of short wavelengths, as noted by Schawlow and Townes. In addition $1 - \alpha$, η, and the related ζ all increase rapidly in going from the near infrared, red, and yellow to blue, violet, and ultraviolet, maser action being already probably impossible and certainly useless in the near ultraviolet. For example, we will evaluate (7), (8), and (9) for the sodium resonance radiation ($\lambda \cong 0.6 \times 10^{-4}$ cm). We take $T = 800°$K and M = the atomic mass of sodium. The ratio g_1/g_2 will be taken as unity, although it is actually 2 for one of the D lines. We obtain

$$\begin{aligned} P_s &= 10^7 \frac{n_1}{n_{10}} rA^2 , \\ P_b &= 10^{10}\, rA^2 , \\ P_o &= 2 \times 10^{10}\, rA^2 , \end{aligned} \tag{10}$$

assuming $Q = 10^{10}$ ergs cm^{-2} sec^{-1}, $1 - \alpha = 0.05$, $\eta = 0.05$, $\zeta = 0.10$. Actually, an extra amount of energy, here equal to P_b, is wasted by errors (since $\eta = 1 - \alpha$), so we obtain for the efficiency

$$\epsilon = \frac{P_o}{P_o + P_s + 2P_b} = \frac{1}{2 + 0.5 \times 10^{-3}(n_1/n_{10})} . \tag{11}$$

We therefore see that spontaneous emission will make serious inroads on the efficiency if n_1/n_{10} goes above a few thousand. It is of interest to calculate the partial pressure of sodium corresponding to $n_1 = n_{10}$. From (3), we obtain ($f \cong 1$ for the D lines)

$$\frac{n_{10}}{LA^2} \cong \frac{10^{11}}{L} \text{ atoms/cm}^3 , \tag{12}$$

while the factor of 10^3, allowed before spontaneous emission becomes a serious problem, will bring us only to $10^{14}/L$ atoms/cm^3. It is interesting to note that a sodium pressure of 1 μ (a reasonable lower limit for efficient electrical excitation) corresponds to 0.35×10^{14} atoms/cm^3. It is therefore clear that a fairly sophisticated excitation scheme is demanded, since L might easily be as large as 10^3 cm.

Javan[3] has suggested a most ingenious method, recently embodied in the highly successful helium-neon gas maser.[2] Two (or possibly more) gases are used, of which one is present at relatively high pressure so that it can carry an electrical discharge, while a second, which is present at lower pressure, is actually responsible for the maser action and receives its excitation by collision (quenching) with excited atoms of the first type. In order to achieve suitable level populations with a large disproportion between the pressures of the two gases, the cross section for the quenching collisions must be as high as possible. This in turn requires a close coincidence between some excited state of the first species of atom and an excited state of the other species. This cross section will also be much enhanced if the two transitions involved are both optically allowed. If high efficiency is desired, several other conditions must be satisfied. First, the excited state of the first species must be easily produced by an electrical discharge. Thus, the transition in the first species might be a resonance transition with nearly unit oscillator strength, or the excited state might be metastable, although this would tend to reduce the quenching cross section. Second, it is most advantageous if all the subsequent downward transitions in the second species can be utilized for simultaneous maser operation. This is in fact essential if high power levels are to be reached, since if population inversion must be maintained by spontaneous emission from the lower level of a maser transition, the coherent output is approximately limited to the spontaneous power. There exist a number of possible combinations of atoms which appear to satisfy these conditions, and a study is being made of several of the more promising cases.

---

[3]A. Javan, *Phys. Rev. Letters* 3, 518 (1959).

RECOIL ENERGY SPECTRUM FOR THE BETA DECAY OF He^6

C. H. Johnson Frances Pleasonton T. A. Carlson

The beta decay process is a three-body breakup with the emission of two leptons and a residual nucleus. The angular correlation between the leptons can be found indirectly by observing the recoiling nucleus. An He^6 recoil experiment is subject to a straightforward theoretical analysis because He^6 decays through a pure allowed Gamow-Teller transition to one final state. For this case the asymmetry parameter for the correlation between the electron and antineutrino is

$$\lambda = -\frac{1}{3}\frac{(|C_A|^2 + |C_{A'}|^2) - (|C_T|^2 + |C_{T'}|^2)}{(|C_A|^2 + |C_{A'}|^2) + (|C_T|^2 + |C_{T'}|^2)},$$

where the C's are the usual tensor and axial-vector coupling constants. One can determine λ from the shape of the recoil energy spectrum[1,2] and thus find the relative strengths of the tensor and axial-vector interactions.

Measurements on He^6 began at this Laboratory in 1958, using the recoil spectrometer which Snell and Pleasonton[3] had used for an earlier investigation of Ar^{37}. Preliminary results[4,5] were readily obtained which showed the interaction to be predominantly axial vector, in agreement with recoil measurements by Herrmannsfeldt *et al.*[6,7] and with an abundance of other theoretical and experimental evidence. It was at once apparent that our equipment was capable of excellent statistical accuracy over a wide region of the energy spectrum, and a program was begun to reduce and to evaluate uncertainties other than those from counting statistics. This program has been terminated and the results, with a partial analysis, are presented here.

The experimental apparatus was described previously.[4] Briefly, He^6 created by the $Be^9(n,\alpha)He^6$ reaction in the fast flux of the Oak Ridge Research Reactor is swept to our laboratory and admitted, after purification, into a large conical source volume. The activity of the source is monitored by a proportional counter, and Li^6 ions recoiling from the decay of He^6 are observed with the spectrometer, which subtends a small solid angle at the tip of the source. The spectrometer utilizes both magnetic and electrostatic analysis in tandem, so that independent spectra can be obtained for singly and doubly charged Li^6 ions. Ions accepted by the analyzers are detected by an electron multiplier. Backgrounds, which are minimized by three stages of differential pumping, are generally determined by applying a negative voltage bias to the source.

---

[1] O. Kofoed-Hansen, *Phys. Rev.* 74, 1785 (1948).

[2] M. E. Rose, *The Beta-Decay Interaction and the Analysis of Recoil Experiments*, ORNL-1593 (Sept. 15, 1953).

[3] A. H. Snell and F. Pleasonton, *Phys. Rev.* 100, 1396 (1955).

[4] F. Pleasonton, C. H. Johnson, and A. H. Snell, *Bull. Am. Phys. Soc.* 4, 78 (1959).

[5] C. H. Johnson, F. Pleasonton, and A. H. Snell, *Phys. Div. Ann. Progr. Rept. Mar. 10, 1959*, ORNL-2718, p 5.

[6] W. B. Herrmannsfeldt *et al.*, *Phys. Rev. Letters* 1, 61 (1958).

[7] J. S. Allen *et al.*, *Phys. Rev.* 116, 134 (1959).

The first step toward greater precision was to increase the source activity by removal of restrictions in the flow system. Radioactive contaminants, mostly N^{16}, were more effectively removed by passing the He^6 over hot titanium chips and past a cold trap containing nitrogen "slush." The flow rate was stabilized so that any contaminants that do enter the source have an activity proportional to the true He^6 activity; hence, the monitor, which does not discriminate against all contaminants, responds in proportion to the He^6 activity.

The improved trapping in the flow system reduced the operating pressures to less than 2×10^{-6} mm Hg in the source and to less than 1×10^{-6} mm Hg in the analyzers. At these pressures, scattering of the ions in the residual gas gives rise to negligible distortion of the spectrum. The validity of this statement was checked by observing that the spectrum was not distorted when the pressure was increased by a factor of 5 to 8 in the source, the magnet chamber, or the electrostatic deflector. In order to minimize scattering from the various walls, an extensive set of thin baffles were installed in the source, in the magnet chamber, and in all collimators. Tests for possible scattering from the electrostatic deflector plates and from the walls of the magnet chamber were made by detuning the analyzers relative to each other; no spurious counts were observed.

Repeated runs over the spectrum were made in order to study reproducibility, and, as a result, several improvements were made. For example, it was found that the magnet must operate on a given hysteresis loop in order for the fluxmeter to give a reproducible measurement of the average field. Although a high degree of stability was finally achieved, there remained some random fluctuations outside of the excellent counting statistics. For this reason the statistical uncertainty in the final analysis will be based on the reproducibility of several runs rather than on the usual counting statistics.

A rather general test of the equipment was made by observing both "accelerated" and "nonaccelerated" spectra. "Nonaccelerated" refers to measurements with the source and analyzers both at ground potential, whereas "accelerated" refers to measurements where source voltages are applied to shift each nonaccelerated point to twice its energy. The fact that the accelerated and nonaccelerated spectra are found to be in good agreement serves to check several possible errors. A discrepancy between these spectra could have revealed an error in background measurements since the background becomes relatively unimportant for the accelerated run. Stray magnetic fields could be evidenced by relative distortion of the nonaccelerated spectrum. A difference in the spectra could indicate edge effects in the analyzers since the accelerated beam is focused and, hence, collimated relative to the normal beam. The focusing process in itself does not distort the accelerated spectrum since all points receive the same energy magnification.

As a further precaution against stray magnetic fields, shielding was placed around the electrostatic deflector and around the collimators. To check for stray fields in the source volume, the spectrum was observed with the source shortened to one-third its normal length; the spectrum obtained was the same as that from the long source, indicating that stray fields have a negligible effect even for low-energy ions starting at the far end of the source.

Throughout the program the ion detector's efficiency remained the major source of uncertainty. The detector is an electron multiplier with an Ag-Mg cathode followed by ten stages of electron

multiplication. Measurements were begun with a multiplier following Allen's design,[8] but final measurements were made with a box-and-grid multiplier. In either case the energy-analyzed ions were accelerated to several kev at the multiplier's entrance in order to achieve nearly 100% efficiency for secondary electron emission. The necessity of increasing the energy of the ions created the basic problem of separating the dependence of efficiency on ion energy from the dependence on focusing effects which may vary the number of ions hitting the cathode. Ideally, these effects should be determined with a calibrated Li^6 ion source, but the inherent difficulties of a precise calibration are formidable. An alternative procedure was followed, namely, to design the multiplier's cathode geometry to minimize focus effects and to test the design with the recoil ion beam itself.

Figure 1 shows horizontal and vertical sections of the cathode geometry, which was designed in conjunction with a box-and-grid dynode structure. In this figure, ions are incident from above,

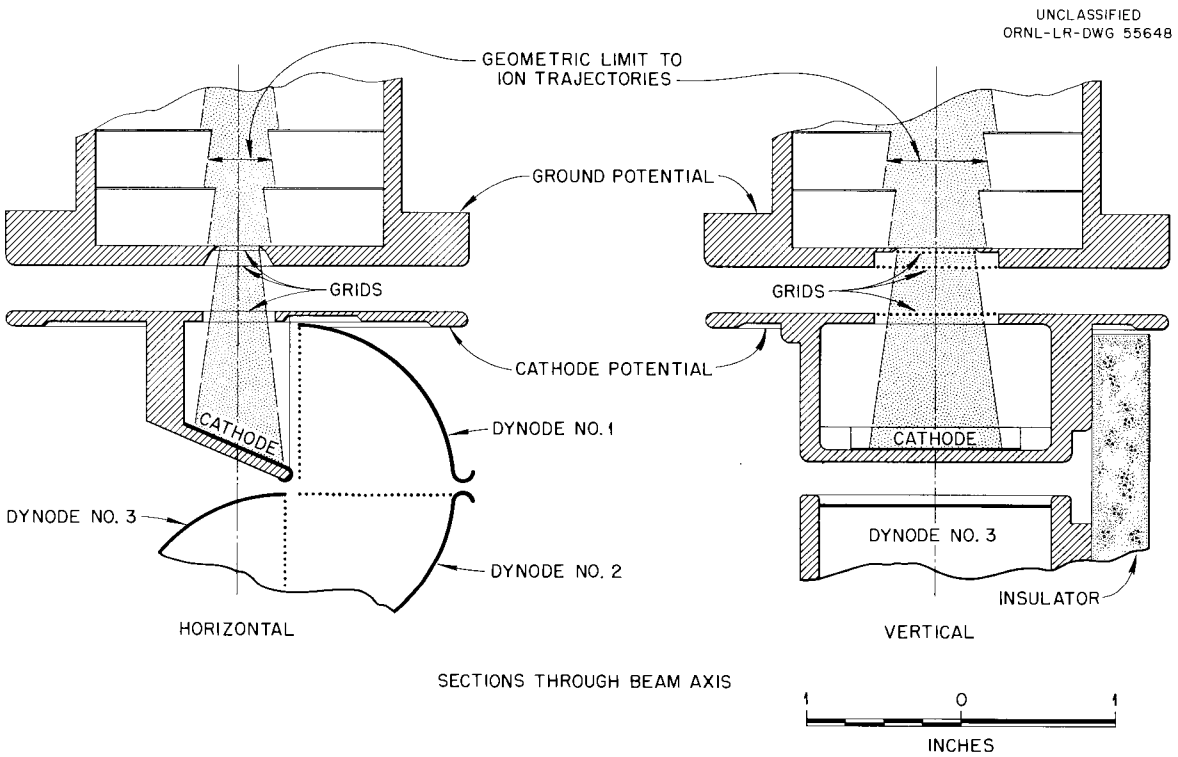

Fig. 1. Horizontal and Vertical Sections of the Cathode Geometry for the Box-and-Grid Electron Multiplier.

and the geometric limits imposed by the collimator on the ion trajectories are indicated. The ions are accelerated by the field between two plates containing grids of 0.001-in. wires on 0.031-in. centers. The beam-defining aperture is in field-free space preceding the first grid. A third grid is shown between the aperture and the ground-plane grid. This grid, which tests with the recoil ions

[8] J. S. Allen, *Rev. Sci. Instr.* 18, 739 (1947).

showed to be necessary, apparently shields the aperture from minute fields which penetrate the ground-plane grid. Two stabilized 5-kev supplies are associated with the multiplier; one supply, isolated from ground, provides the operating voltage for the multiplier, and the other, which is frequently cascaded with the first, provides the ground-to-cathode accelerating voltage.

The cathode geometry was designed with the aid of a rubber dam model to ensure that all the ions accelerated through the grids strike the cathode and that all secondary electrons, except those hitting the dynode grid, are collected to the first dynode. After installation in the spectrometer the electron collection efficiency was studied by observing the counting rate as a function of the cathode-to-dynode voltage. The counting rate reached a plateau starting at 250 v, and subsequent operation was in the plateau region. As an added precaution against failure to detect secondary electrons, the over-all gain of the multiplier and its amplifier was increased until the counting rates were essentially independent of the amplifier's discriminator level.

Further tests of the cathode geometry were made by observing the counting rate as a function of accelerating voltage for various analyzed ion energies. If the probability for secondary electron formation and collection is independent of position on the cathode, the detection efficiency is

$$\epsilon = e(E_c)\, f(E_c/E_0)\,,$$

where the energy effect e is a function of the ion energy E_c at the cathode, and the focus effect f is a function of the energy multiplication imposed by the accelerating voltage. The validity of this equation was established by a family of counting rate curves for various analyzed energies, E_0. Unfortunately, these curves give only partial information on the functions e and f. For example, a necessary but not sufficient condition for independence from focus effects is that all the curves have the same shape, that is to say, the same E_c dependence. The third grid between the aperture and ground plane was installed because the multiplier had failed to satisfy this condition. The geometry shown in the figure was successful, however, to better than 1%, so that the efficiency is interpreted to be nearly independent of focus effects. Other interpretations of the focus dependence may not be as reasonable but certainly are possible and must be given some weight in the final assignment of uncertainties.

Assuming that the efficiency of the detector has no focus dependence, one can observe the true recoil spectrum by maintaining a constant energy E_c at the cathode. Figure 2 is such a

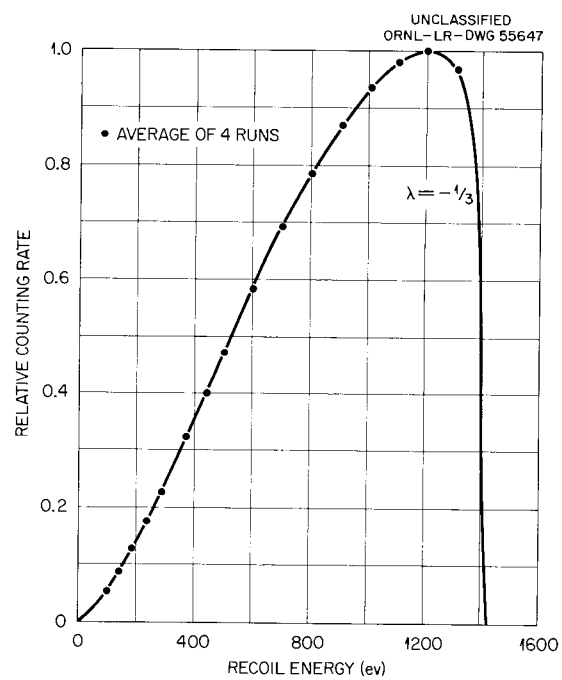

Fig. 2. Recoil Energy Spectrum for Singly Charged Li^6 Ions from the Beta Decay of He^6. The solid curve is calculated for the pure axial-vector interaction.

spectrum for singly charged Li^6 recoil ions obtained for $E_c = 4400$ ev. Uncertainties from counting statistics are less than the dimensions of the points. This particular set of data constitutes an "accelerated" run with elevated source potentials. The counting rates have been corrected for background and are relative to the counts from the source monitor; the energy scale is discussed in the immediately following paper. The solid curve was calculated for the axial-vector interaction, $\lambda = -\frac{1}{3}$.

Obviously the axial-vector interaction gives a good fit to the data. A least-squares analysis[9] of the several runs is in progress. For this analysis one requires the decay energy and the relative abundances of singly and doubly charged recoil ions; these are given in the two immediately following papers. At the present stage of analysis, involving only the four runs shown in Fig. 2, we find $\lambda = -0.324 \pm 0.010$. It is possible that, in the final analysis, the quoted error will be increased in accordance with our uncertainty of the true focus effect.

---

[9]We are indebted to Arline Culkowski of the Mathematics Panel for coding the least-squares analysis for the Oracle.

AN ABSOLUTE DETERMINATION OF THE He^6 BETA-DECAY ENERGY

Frances Pleasonton C. H. Johnson T. A. Carlson

The preceding section discusses the recoil spectrum of Li^6 ions following the radioactive decay of He^6. Measurements of the end point of the recoil energy spectrum yielded, as a bonus, an absolute determination of the He^6 beta-decay energy. This method is limited in application relative to the conventional measurements of beta-particle spectra, but it has inherent advantages. First, the recoil spectrum drops abruptly to zero rather than asymptotically as does the beta-particle spectrum; second, recoil energies are low so that the spectrometer calibration depends only on simple voltage measurements which can be made with a high degree of accuracy; and third, since the decay energy varies approximately (for energetic decays) as the square root of the end-point energy, the uncertainty in the decay energy is half the uncertainty in the end point.

Briefly, the measurement was to observe the spectrum first with the He^6 source at the same potential as the spectrometer and then with the source raised to a potential sufficient to shift the end point to twice its original energy. The source potential was then just equal to the end-point energy. The following details are pertinent to the precision of the measurement.

In Fig. 1 the solid circles show the relative counting rates near the end point for "nonaccelerated" recoil ions, that is, ions observed with the source and spectrometer at the same potential. The abscissa is proportional to energy but its absolute value is not known at this stage of the discussion. The open circles represent "accelerated" data which are plotted at half their energy and normalized on the average to the "nonaccelerated" data. Each of these datum points was obtained by setting the spectrometer to accept ions having twice the energy of the corresponding nonaccelerated point and adjusting the source

potential proportionately so that the end point appeared at just twice its original energy. (As is discussed below, allowance was made for effects of finite resolution near the end point.) At this stage of the discussion the absolute energy scale is established: it is just equal to the source potentials for the double-energy run. Voltages were measured with a precision resistance divider, potentiometer, and standard cell.

In order to find the decay energy, these data are compared to the predicted spectral shape.[1] Two solid curves are shown in the figure. One is the spectrum for the axial-vector ($\lambda = -\frac{1}{3}$) interaction – certainly a good approximation for this purpose. The experimental curve falls off less abruptly than the theoretical one because of the energy spread in the spectrometer. It would be logical to unfold the resolution function from the data; however, this presupposes a measurement of the function with a source having the same geometric divergence as the He^6 source itself. A satisfactory alternative is to fold various resolution functions into the theoretical curve until one is found to fit the data. The second curve in the figure shows the resulting fit, which was obtained with a resolution function consistent with measurements by an $(He^4)^+$ ion source. The resulting decay energy is 3.505 Mev.

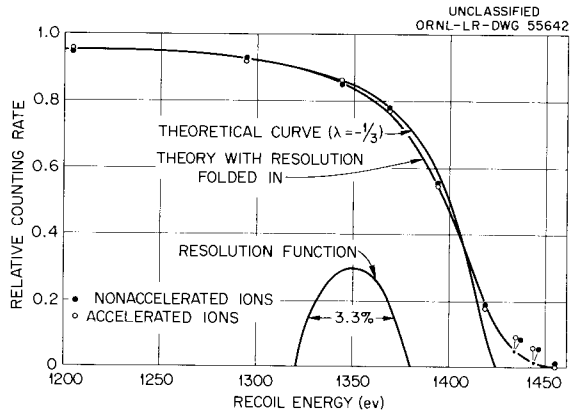

Fig. 1. End Point for the Recoil Energy Spectrum of $(Li^6)^+$ Ions from the Beta Decay of He^6. The size of circles is greater than the uncertainties from counting statistics.

It must be emphasized that the choice of the resolution function is not a critical step in the analysis, since any reasonable function leaves the theoretical curve unchanged in its flat maximum region and merely pivots the approach to zero with varying degrees of inflection through a point at about 40% of the maximum (1400 ev; see Fig. 1). Thus one could simply match these two points of the theory to the experiment; however, the more detailed fitting shown in the figure reduces the error and also establishes an essentially correct resolution function.

It was stated parenthetically that allowances were made for finite resolution in the double-energy run. To be precise, a double-energy point was measured by doubling the energy setting for the spectrometer and by applying a source potential which doubled the *average* energy transmitted by the spectrometer. This distinction is important only near the end point, where the average energy is less than the actual spectrometer setting. In order to make this slight adjustment it was necessary to know the position of the end point and the resolution function; for this reason the above detailed comparison with theory was actually made for the nonaccelerated data before proceeding with the accelerated measurements.

---

[1] M. E. Rose, *The Beta-Decay Interaction and the Analysis of Recoil Experiments*, ORNL-1593 (Sept. 15, 1953).

Known sources of uncertainties in the above decay energy arise from the measurement of the source potential and the matching of the various curves at the end point. We assign a standard deviation of 0.4% in the end point. Thus the decay energy with its uncertainty is 3.505 ± 0.007 Mev.

A second measurement of the end point was made in a more conventional manner simply by calibrating the spectrometer with an $(He^4)^+$ ion source. Details will not be given here. The observed decay energy is 3.509 ± 0.004 Mev. The quoted error is based on known uncertainties in calibration; however, it is probable that a systematic uncertainty arises because the radioactive He^6 source and the $(He^4)^+$ ion source have different geometric divergences. For this reason the uncertainty is increased to ±0.006 Mev.

Uncertainties in the voltage measurements which are common to both results are negligible relative to the quoted uncertainties. The weighted average for the decay energy of He^6 from these two measurements is 3.507 ± 0.005 Mev. This is in good agreement with a beta-spectrum end point of 3.50 ± 0.02 reported by Schwartzschild, Rustad, and Wu,[2] and with an energy difference of 3.55 ± 0.03 Mev derived from nuclear-reaction Q values.[3] The weighted average, 3.515 ± 0.017 Mev, of these two earlier measurements was used for the most recent tabulation of masses.[4] The present measurement, therefore, will give a slightly lower value for the tabulated mass of He^6 as well as a reduced uncertainty.

---

[2]A. Z. Schwartzschild, B. M. Rustad, and C. S. Wu, *Bull. Am. Phys. Soc.* 1, 336 (1956).

[3]K. W. Allen *et al.*, *Phys. Rev.* 96, 684 (1954).

[4]F. Everling, L. A. König, J. H. E. Mattauch, and A. H. Wapstra, *Nuclear Phys.* 15, 342 (1960).

ELECTRON SHAKEOFF FOLLOWING $He^6 \xrightarrow{\beta^-} Li^6$

T. A. Carlson Frances Pleasonton C. H. Johnson

Following the beta decay of He^6, the resulting singly charged Li^6 may be sufficiently excited to lose one or both of its two orbital electrons. Furthermore, if both electrons are put into excited but bound states, they may decay by an Auger process, or autoionization, in which one electron goes back to the ground state while the other is completely removed. Atomic excitation as a result of beta decay can arise in any one of three ways. In the first way, which is by far the most important, excitation is caused by the sudden nonadiabatic change in nuclear charge. In the second, excitation may result in cases where the neutrino and beta particle impart a high recoil energy to the atom. Third, as the beta ray, having emerged from the nucleus, passes through the cloud of orbital electrons surrounding that nucleus, it may interact with one of those electrons.

To shed light on the different modes of excitation, investigations have been carried out in which He^6 was allowed to decay in a specially designed mass spectrometer which analyzed the Li^6 ions by means of a tandem arrangement of magnetic and electrostatic deflectors. With this arrangement,

measurements were made on both the charge distribution and the recoil energy spectra of the lithium ions resulting from the β^- decay of He^6. The spectrometer is identical to that discussed in a companion paper on the measurement of the recoil spectrum of the singly charged lithium ion. In the companion paper and in an earlier report,[1] a more extensive discussion of the spectrometer and its performance may be found. However, a few points should be mentioned here. In order to guard against any possible drifts in the over-all performance of the He^6 flow system, data on $(Li^6)^{2+}$ and $(Li^6)^{3+}$ were taken concurrently with measurements on $(Li^6)^+$ ions, and the analyzer settings for the doubly and triply charged ions were made by dividing the settings established for the singly charged ions by the charge of the ion being investigated. Finally, data taken on $(Li^6)^{2+}$ and $(Li^6)^{3+}$, at gas pressures greater than five times those used under normal operating conditions, were found to be unaltered, in accordance with previous measurements on $(Li^6)^+$.

The object of the experiment was to measure the relative amounts of the differently charged lithium ions as a function of recoil energy. The principal problem involved in this measurement is the lack of knowledge of the relative efficiency of detection for these ions. However, the counting rates as a function of the energy of the ions striking the multiplier cathode tend to level off at higher energies for both $(Li^6)^+$ and $(Li^6)^{2+}$. At sufficiently high total energy, therefore, any difference in multiplier efficiency should be minimized. The ratio of $(Li^6)^{2+}/[(Li^6)^+ + (Li^6)^{2+}]$ for ions of 1200 ev recoil energy has been measured six times (using two separate activations of multiplier plates) at energies high enough so that the data are taken in the flat portion of the energy efficiency curve. The results range from 0.105 to 0.108. We give as the best value 0.106 ± 0.003, which includes the uncertainty of the relative efficiencies.

Before evaluating the ratio [total number of $(Li^6)^{2+}$]/[total number of $(Li^6)^+ + (Li^6)^{2+}$], we must first ascertain the shapes of the recoil energy spectra for the different ions. The spectrum for $(Li^6)^{2+}$ is presented in Fig. 1 and is substantially the same as that for $(Li^6)^+$, although there is a slight suggestion that there may be a greater proportion of higher energy ions in the case of $(Li^6)^{2+}$. A more careful investigation of the relative intensities of charge-1 and charge-2 Li^6 ions as a function of recoil energy was made by accelerating the ions before analysis, which increased the counting rates and improved the signal to background ratio. This acceleration was carried out by raising the potential of the source volume relative to that of the analyzers. Care was taken in comparing the intensities of two differently charged ions to use identical

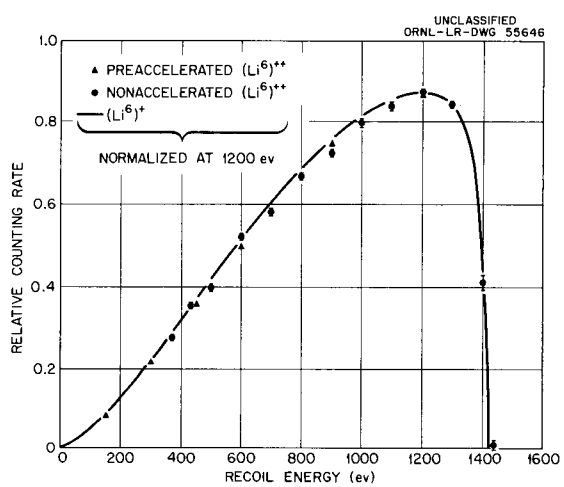

Fig. 1. Recoil Energy Spectrum of $(Li^6)^{2+}$.

[1] C. H. Johnson, F. Pleasonton, and A. H. Snell, *Phys. Div. Ann. Progr. Rept. Mar. 10, 1959*, ORNL-2718, p 4.

energy multiplication ratios in this "preacceleration." To help concentrate attention on the change in relative intensities with the change in recoil energy, and to eliminate any spurious errors, the 1200-ev point was included in each run and all the data normalized to that point. The results of these observations are shown in Fig. 2, together with a straight-line least-squares analysis. The intercept at zero energy gives the component of the ratio $(Li^6)^{2+}/(Li^6)^+$ which is independent of recoil energy. Using this ratio we can then evaluate from the rest of the data in Fig. 2 the relative number of $(Li^6)^{2+}$ ions which require recoil energy for their formation.

Possessing, now, knowledge of the spectral shapes for $(Li^6)^+$ and $(Li^6)^{2+}$, we calculate the percentage of doubly charged lithium ions to be 10.5 ± 0.3. Of this amount, $(0.4 \pm 0.1)\%$ are ions which require recoil energy for their formation.

A determination of the ratio of $(Li^6)^{3+}/(Li^6)^+$ was made in a manner similar to the investigation of $(Li^6)^{2+}/(Li^6)^+$, except that all the data were obtained from preaccelerated ions. Figure 3 shows the recoil spectrum of $(Li^6)^{3+}$ as compared with that of $(Li^6)^+$, while Fig. 4 gives the ratio of $(Li^6)^{3+}/(Li^6)^+$ as a function of recoil energy. Because of poor statistics and because the assignment of energy dependence is more complicated than that for the doubly charged ion, evaluation of the number of ions dependent on recoil energy for their formation is not possible. However, the data clearly show that recoil energy plays an important role in the formation of $(Li^6)^{3+}$. On the other hand, it also seems apparent that recoil energy alone cannot account for all the $(Li^6)^{3+}$ observed. The percentage of the total number of decays leading to $(Li^6)^{3+}$ is 0.050 ± 0.005, where the error includes the uncertainty about the relative spectral shapes of charges 1 and 3.

Discussion of Theoretical Calculations

Following the decay of He^6, the nucleus increases its charge by 1, and the beta particle leaves before the orbital electrons can adjust to their new environment. This nonadiabatic excitation can result in appreciable ionization. Winther[2] has calculated the probability of this process leading to

[2]A. Winther, *Kgl. Danske Videnskab. Selskab, Mat.-fys. Medd.* 27(2) (1952).

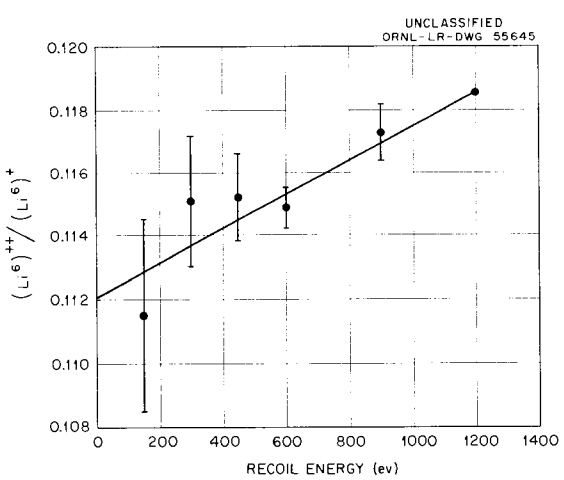

Fig. 2. Ratio of $(Li^6)^{2+}/(Li^6)^+$ as a Function of Recoil Energy (Normalized at E_r = 1200 ev).

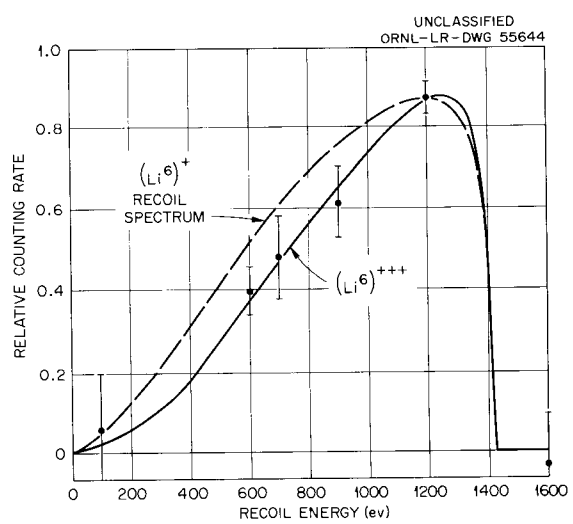

Fig. 3. Recoil Energy Spectrum of $(Li^6)^{3+}$.

ionization by evaluating the probabilities of transition to the final states of $(Li^6)^{2+}$ in which one electron is in the 1*s* state while the other is in some bound state. The sum of these transition probabilities subtracted from unity should give the probability of losing an electron, for transition to any other state will lead to ionization. This is so because if neither electron finds itself in the ground state, ionization will occur even though they both might still be bound, for in that case they will decay nearly completely by autoionization. In fact, most of the ionization of $(Li^6)^+$ proceeds by this method. Winther gives (10.5 ± 1.5)% as the calculated ratio of $(Li^6)^{2+}/[(Li^6)^+ + (Li^6)^{2+}]$, which agrees quite well with our experimental findings.

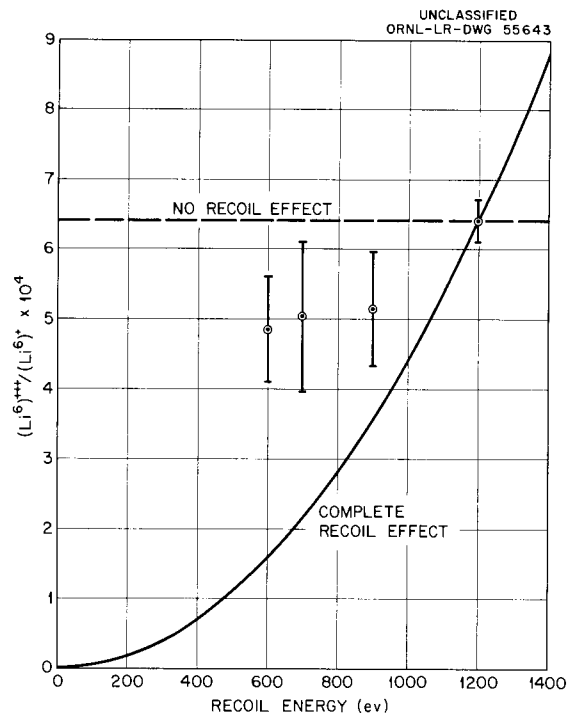

Fig. 4. Ratio of $(Li^6)^{3+}/(Li^6)^+$ as a Function of Recoil Energy.

Winther has also made an estimate of ionization which proceeds by means of a direct collision between the beta particle and an orbital electron. This probability, 10^{-4}, is too small to play an important part in the understanding of our experimental results.

To make an estimate of the effect that recoil energy plays in ionization, we have used the approximation that the probability of losing an electron by recoil energy is the order of $(v/v_0)^2$, where v_0 is the velocity of the orbital electron and v the velocity of the recoiling atom. Winther has confirmed the use of this approximation by a more exact calculation, using lithium wave functions corresponding to a moving atom. This approximation, which implies a first-order dependence on recoil energy, is the basis for the straight-line analysis shown in Fig. 2. In evaluating the role that recoil energy plays in the formation of $(Li^6)^{2+}$ we need only concern ourselves with the bound states in which at least one electron is in the ground state, for in the other cases ionization would take place whether there were recoil energy or not. By using the population distribution of the bound states following beta decay as given by Winther[2] and the binding energies of the orbital electrons concerned, we have estimated that about 0.4% of the total number of decays should result in those $(Li^6)^{2+}$ ions which require recoil energy for their formation. This agrees fortuitously well with the experimental results.

In the production of triply charged Li^6, recoil energy may play a role in removing zero, one, or two electrons, where the electrons may be in the ground state or in excited states. These modes of production would correspond approximately to a zero-, first-, or second-order dependence on recoil energy. The situation is too complicated for analysis, and the best that can be done is to set some

reasonable limits. Winther[2] calculated that the probability of shaking off both electrons by a sudden Coulombic change at the nucleus would be less than 0.001. By use of ground-state binding energies, a reasonable lower limit, about 10^{-5}, can be assigned for the probability of shaking off electrons by means of recoil energy.

A summary of the results on the charge spectra of Li^6 appears in Table 1.

Table 1. Charge Spectrum of Li^6 Following the Beta Decay of He^6

Percentage of the total number of decays

Charge	Experiment			Theory		
	Independent of Recoil Energy	Dependent on Recoil Energy	Total	Independent of Recoil Energy	Dependent on Recoil Energy	Total
1	89.4 ± 0.3		89.4 ± 0.3	89.1		89.1
2	10.1 ± 0.3	0.4 ± 0.1	10.5 ± 0.3	10.5 ± 1.5	~0.4	10.9
3	*	*	0.050 ± 0.005	<0.1	$>10^{-3}$	?

*These values have not been determined quantitatively, but each is a significant fraction of 0.050.

LEVEL STRUCTURE OF N^{14}[1]

J. K. Bair H. O. Cohn H. B. Willard

Yields and angular distributions of the gamma rays from the first and second levels in C^{13} following excitation by inelastic proton scattering have been measured. Levels are observed at bombarding proton energies 3.80 Mev (Γ = 100 kev), 4.1 Mev (Γ = 150 kev), 4.14 Mev, and 4.52 Mev (Γ = 150 kev). The first three levels result in excitation of the first excited state and the last in excitation mainly of the second excited state of C^{13}. Nitrogen-14 excitation energies corresponding to these levels are 11.07, 11.3_5, 11.39, and 11.74 Mev. Possible spin and parity assignments are made on the basis of the gamma-ray angular distribution of the 4.52-Mev level. The $C^{13}(p,n)N^{13}$ neutron yield has been rerun, yielding better values of the resonant energies. Neutron angular distributions are given for several bombarding proton energies.

[1]Abstract of published paper: *Phys. Rev.* **119**, 2026 (1960).

LEVELS IN N^{14} AT 11.74 AND 11.82 Mev[1]

J. K. Bair

The known angular distribution of the $C^{13}(p,p'\gamma)C^{13}$ 3.68-Mev gamma rays is not sufficient to uniquely determine the spin and parity of the 11.74-Mev N^{14} level for the case of arbitrary channel-spin mixing. To resolve this ambiguity the angular distribution of the inelastically scattered protons has been measured. Of the previous possibilities, $J^{\pi} = 1^+, 2^{\pm}$, and 3^-, the assignment 1^+ is selected. A new level is found at 11.82 Mev in N^{14} having a width of about 100 kev, and decaying through the 3.09-Mev level in C^{13}. An angular distribution of the inelastically scattered protons from this new level shows strong interference effects.

[1]Abstract of paper submitted to the *Physical Review.*

NEUTRONS FROM THE He^3 BOMBARDMENT OF SOME LIGHT NUCLEI

J. L. Duggan[1] P. D. Miller R. F. Gabbard[2]

The ion source for the Oak Ridge National Laboratory 3-Mv accelerator has been modified to provide a peak beam of about 500 μa of singly charged He^3 ions. This beam has been pulsed in the Van de Graaff terminal at a repetition rate of 2 Mc/sec to give pulses of about 20 nanoseconds duration. After acceleration and magnetic analysis, a 2- to 3-nanosecond pulse is separated from the 20-nanosecond burst by a newly installed pulser operated at 12 Mc/sec and synchronized with the terminal pulsing frequency. In order to detect the neutrons a large-volume plastic scintillator on a 4-in. photomultiplier was used. The over-all system resolution has been about 4 nanoseconds for neutrons. Other elements of the time-of-flight system have been described previously.[3]

Figure 1 shows a typical time spectrum from the $Be^9(He^3,n)C^{11}$ reaction. The ground-state neutrons appear in channel 228 and have an energy of about 9.5 Mev. The most intense group, in channel 125, consists of the unresolved fourth and fifth excited states. The highest excited state appearing, the 8.11-Mev state, produces neutrons with an energy of about 2 Mev.

The $Li^7(He^3,n)B^9$ reaction has been studied at bombarding energies ranging from about 1 to 2.8 Mev. The 0° excitation curve for the ground-state group is shown in Fig. 2. The angular distribution of these ground-state neutrons at a bombarding energy of about 2.0 Mev is shown in Fig. 3. This angular distribution shows approximate symmetry about 90°. Figure 4 shows the spectrum of neutrons from this reaction at 0° and a bombarding energy of about 2.0 Mev. The first and second excited states are not resolved. Neutrons from three-body breakup are observed between the

[1]ORINS Fellow from Louisiana State University.

[2]Summer research participant from University of Kentucky.

[3]W. M. Good, J. H. Neiler, and J. H. Gibbons, *Phys. Rev.* **109**, 926 (1958).

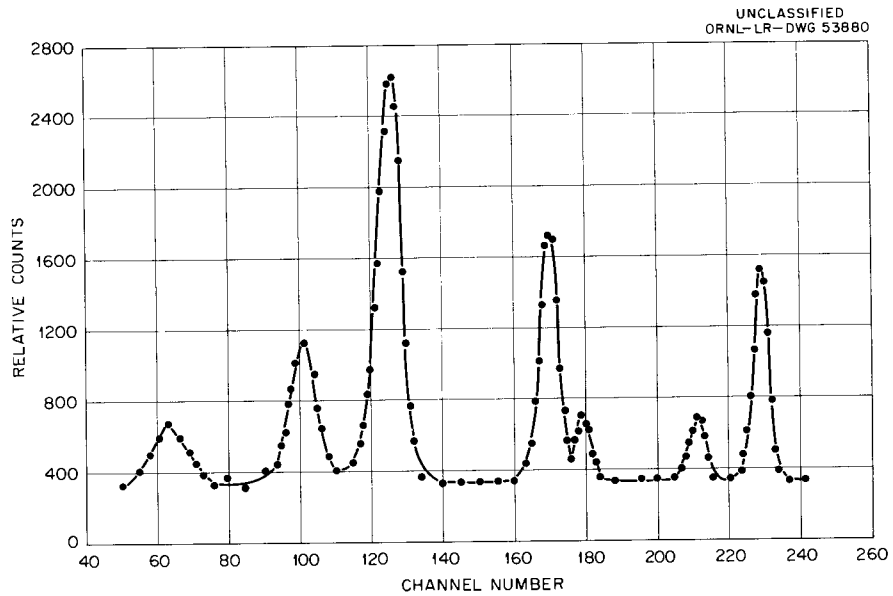

Fig. 1. Neutron Time Spectrum for the $Be^9(He^3,n)C^{11}$ Reaction for a Bombarding Energy of 2.5 Mev and $\theta = 0°$. Time increases to the left. The flight path was 6 m.

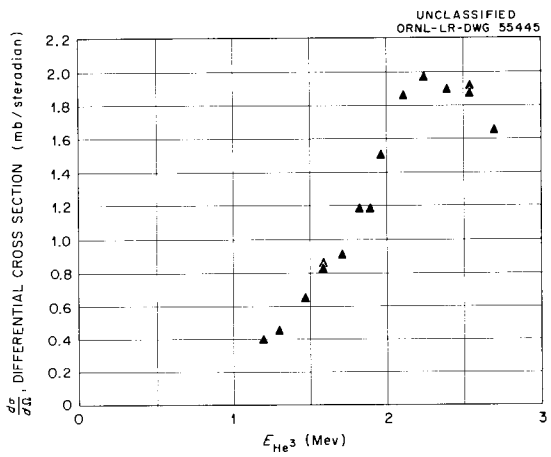

Fig. 2. Excitation Function for the $Li^7(He^3,n)B^9$ Reaction at 0° for the Ground-State Neutrons.

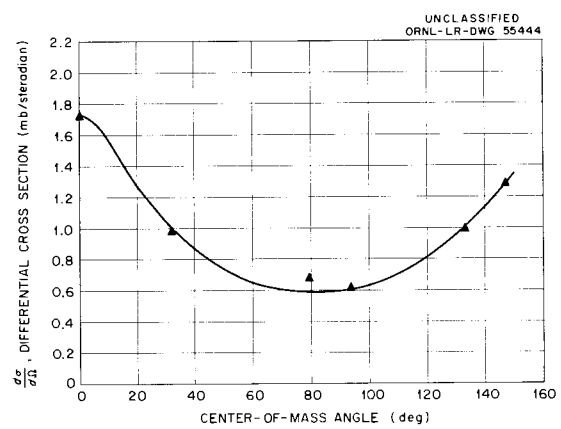

Fig. 3. Angular Distribution of the Ground-State Neutrons for the $Li^7(He^3,n)B^9$ Reaction at a Bombarding Energy of 2.0 Mev. The data are incomplete, but there appears to be approximate symmetry about 90°.

ground and first excited states. A broad three-body continuum is also observed for neutrons with energies less than those which populate the second excited state of B^9. The cross sections for all of the reactions studied are estimated to be accurate to about 50%.

The excitation curves for neutrons populating the various states of C^{11} are all very similar in shape. The excitation curves for the third excited state of C^{11} at 0° and at 81.5° are shown as being typical in Fig. 5. The angular distributions of the neutron groups from the $Be^9(He^3,n)C^{11}$ reaction have been compared to the angular distributions of protons from the $Be^9(He^3,p)B^{11}$ reaction[4] for the

[4]H. D. Holmgren, M. L. Bullock, and W. E. Kunz, *Phys. Rev.* 104, 1446 (1956).

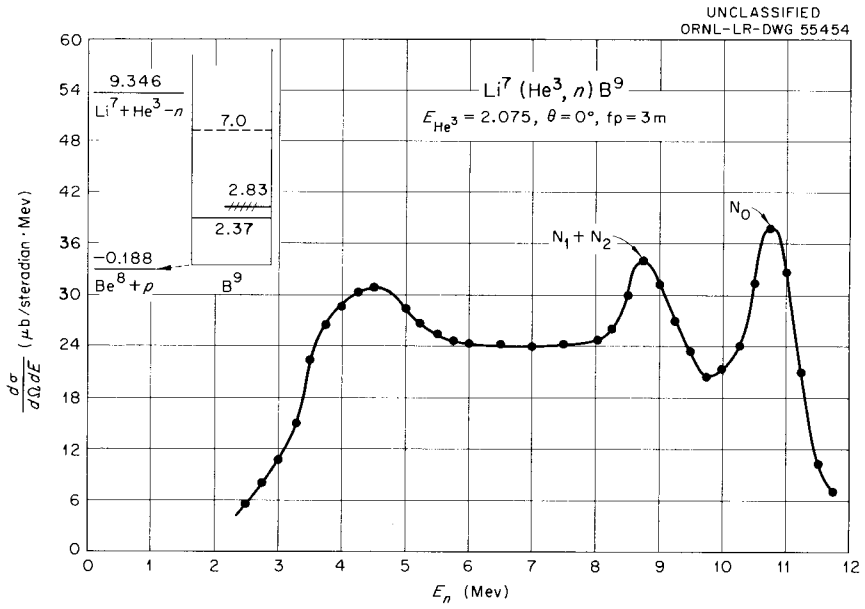

Fig. 4. Neutron Energy Spectrum for the Reaction $Li^7(He^3,n)B^9$ at a Bombarding Energy of 2.0 Mev and a Detector Angle of 0°.

corresponding mirror states of the two residual nuclei. Figure 6 shows an example where the angular distributions are very similar, and Fig. 7 shows an example where the angular distributions are strikingly different. It is suggested that in cases where the angular distributions are quite similar, the (He^3,p) reaction goes primarily by capture of a deuteron in its singlet state, and that in the cases where the angular distributions are quite different, the (He^3,p) reaction may take place with a significant amplitude for capturing a deuteron in its triplet state. It is of course forbidden to capture two neutrons into a single orbital with a channel spin 1.

The $C^{13}(He^3,n)O^{15}$ reaction has been investigated only at 0°. Figures 8 and 9 show the excitation curves for the only two resolved neutron groups from this reaction. The most striking feature of the reaction is the resonance at 1.55 Mev. This resonance corresponds to a new excited state in O^{16} with an excitation energy of 24.04 Mev, and a laboratory width of about 100 kev.

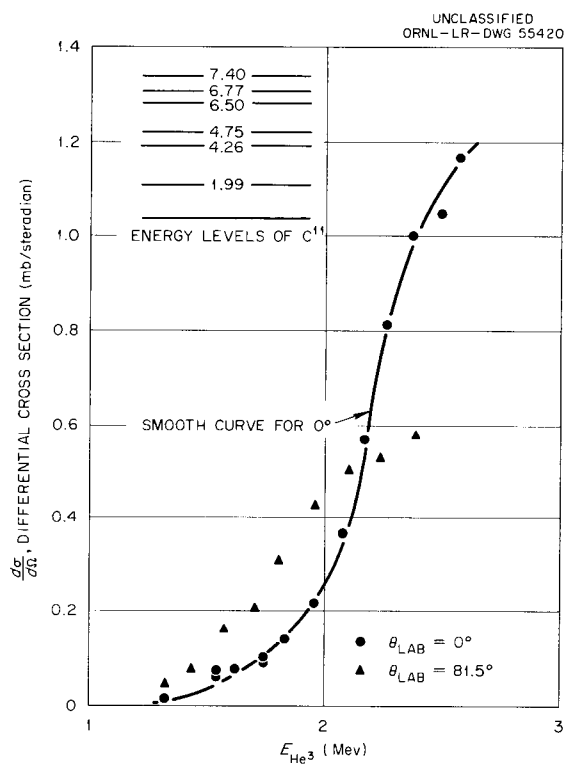

Fig. 5. Excitation Functions of Neutrons to the Third Excited State of C^{11} for the $Be^9(He^3,n)C^{11}$ Reaction at Two Angles.

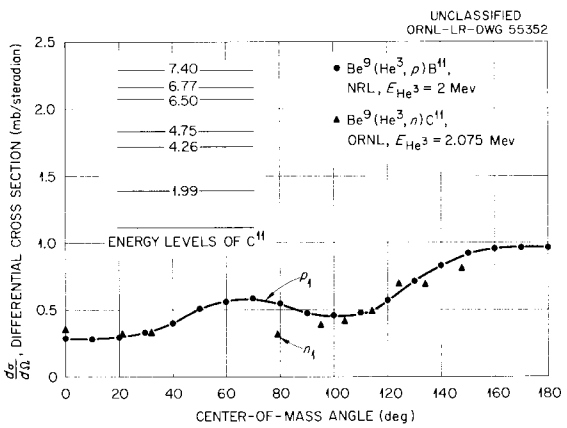

Fig. 6. Angular Distributions of Neutrons and Protons to the First Excited States of C^{11} and B^{11}, Respectively, from the Reactions $Be^9(He^3,n)C^{11}$ and $Be^9(He^3,p)B^{11}$, Both Observed at an He^3 Bombarding Energy of About 2 Mev. Note similarity in magnitude and shape.

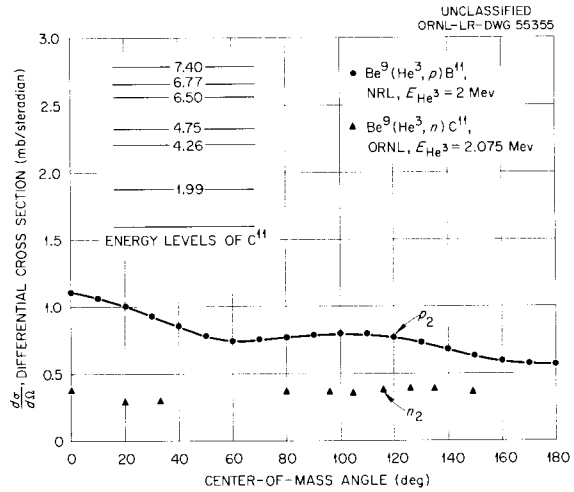

Fig. 7. Angular Distributions for the Second Excited States of the $Be^9(He^3,p)B^{11}$ and $Be^9(He^3,n)C^{11}$ Reactions, Showing Very Little Similarity in Shape or Magnitude.

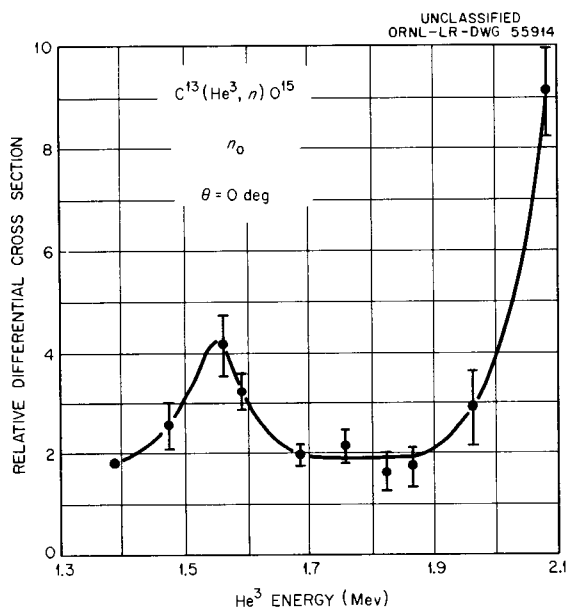

Fig. 8. Excitation Function for the Ground-State Neutrons from the $C^{13}(He^3,n)O^{15}$ Reaction at 0°.

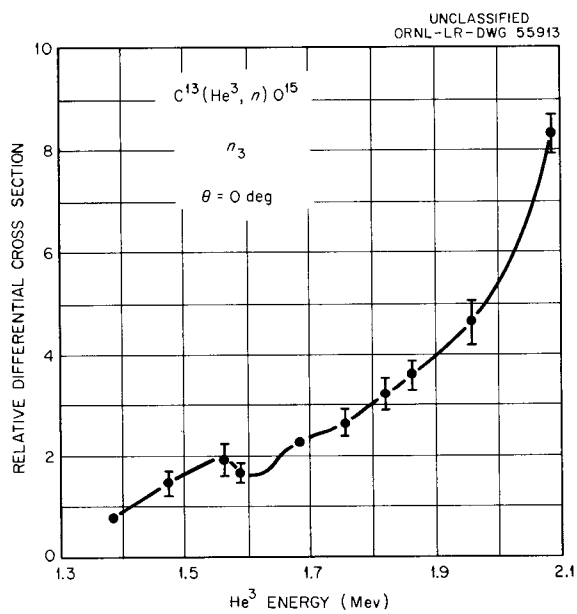

Fig. 9. Excitation Function for the Third-Excited-State Neutrons from the $C^{13}(He^3,n)O^{15}$ Reaction.

THE $Be^9(\alpha,n)C^{12}$ REACTION AND THE PARAMETERS OF THE 7.66-Mev STATE OF C^{12}[1]

F. Ajzenberg-Selove[2] P. H. Stelson

The $Be^9(\alpha,n)C^{12}$ reaction has been studied at $\bar{E}_\alpha = 5.6$ and 5.78 Mev. Neutron groups have been observed to the first three states of C^{12}. The ratio of the populations of the 4.43- and 7.66-Mev states has been determined to be 8.1 $\pm$ 1 at $\bar{E}_\alpha = 5.6$ Mev. This value, together with information from a number of other sources, demonstrates that the 7.66-Mev state has $J^\pi = 0^+$, that its width for alpha emission is approximately the Wigner limit ($\Gamma \sim 8$ ev), and that in $\sim 10^{-3}\%$ of the cases the state decays to the ground state of C^{12} by pair emission. It is also estimated that the 7.66-Mev state can decay by gamma emission via the 2^+, 4.43-Mev state with a probability of 1/5000. This information reinforces the proposal that the 7.66-Mev state has the necessary properties to participate in the buildup of the elements in red giant stars.

---

[1]Abstract of published paper: *Phys. Rev.* **120**, 500 (1960).
[2]Haverford College, Haverford, Pa.

THE $Al^{27}(n,\alpha)Na^{24}$ CROSS SECTION AS A FUNCTION OF NEUTRON ENERGY[1]

H. W. Schmitt J. Halperin[2]

The cross section for the $Al^{27}(n,\alpha)Na^{24}$ reaction has been measured as a function of neutron energy in the range $6.1 \leqq E_n \leqq 8.3$ Mev and at 14.8 Mev. Measurements were made relative to the fission cross section of U^{238}; activation techniques were used to determine the number of $Al^{27}(n,\alpha)$ events. While a number of peaks and valleys appear in the curve for cross section vs energy, there is a general increase in cross section with increasing energy consistent with the Coulomb penetrability of the alpha particle.

---

[1]Abstract of published paper: *Phys. Rev.* **121**, 827 (1961).
[2]Chemistry Division.

TOTAL CROSS SECTION OF Pb^{208}

E. C. Campbell J. L. Fowler

Since nuclei having doubly closed shells form relatively tightly bound cores, the interaction of nucleons with such nuclei should be describable by the independent-particle model. Neutron scattering from such nuclei, combined with bound-state information, allows one to construct phenomenological nuclear potentials which describe the essentially single-particle states of such nuclei as O^{17}

(refs 1, 2) or perhaps Pb^{209} (ref 3). In the latter case the neutron scattering phase shifts ($\delta_{s1/2}$, $\delta_{p1/2}$, and $\delta_{p3/2}$) have been deduced from the total cross section of Pb^{208} only up to 700 kev.[4] The identification of the bound levels of Pb^{209} is in an incomplete state.[3,5] It is of considerable importance, therefore, to acquire more detailed information on the bound and virtual levels of Pb^{209}. In particular, any high angular momentum states which occur in neutron scattering from Pb^{208} are of great interest.

A preliminary investigation of the total cross section of Pb^{208} with 10 kev resolution has revealed much unresolved structure in the 0.9 to 2.6 Mev range[1] (Fig. 1). The lead sample for these measurements was a naturally occurring lead in Tennessee shale which has the following composition: Pb^{208}, 71.3%; Pb^{206}, 26.7%; and Pb^{207}, 2.0%. The effect of the Pb^{206} was compensated for by use of a radiogenic lead (Pb^{208}, 3.0%; Pb^{206}, 88.3%; and Pb^{207}, 8.6%). Thus the effective sample for the data of Fig. 1 was equivalent to 99% Pb^{208}. The data indicated by open points were obtained with the $T(p,n)$ neutron source having an energy spread as indicated by the horizontal bars of Fig. 1. The solid points were obtained with a $Li^7(p,n)$ neutron source of somewhat lower energy spread ($\sim$10 kev). For both sets of data, the neutron detector was a biased propane recoil counter. Approximate inscattering corrections (max $\sim$8%) have been applied by use of differential cross section measurements on normal lead.[6,7] The $Li^7(p,n)$ data have also been corrected for the effect of the second group of neutrons. The indicated errors are due to statistics.

It is apparent from Fig. 1 that better energy resolution is necessary in order to unravel the resonance structure. Consequently, the total cross section from 1 to 1.9 Mev has been remeasured with $\sim$3 kev resolution. The $Li^7(p,n)$ reaction produced by protons from the 5.5-Mv Van de Graaff served as the neutron source. The sample, in the form of a $1\frac{1}{8}$-in.-diam cylinder, was a separated lead isotope, 99.75% Pb^{208} (ref 8). For the energy range 1.4 to 1.9 Mev, 116.18 g (17.86 g/cm^2) was used; for the 1.0 to 1.4 Mev range, the sample was reworked to give 20.07 g/cm^2. Neutrons were detected with a stilbene crystal from which pulses due to gamma rays were depressed by means of Brooks-Owen pulse shape discrimination.[9] With the bias settings used for the 1.4 to 1.9 Mev range, neutrons were counted with about 10% efficiency, which was 3000 times the efficiency for counting 1.3-Mev gamma rays. Different, but comparable, settings were used for the 1.0 to 1.4 Mev interval. As in the case of the 10 kev data of Fig. 1, inscattering corrections were calculated by use of published differential cross sections of normal lead.[6,7] The detector was further from the neutron source in the

---

[1] J. L. Fowler, E. G. Corman, and E. C. Campbell, p 474 in *Proceedings of the International Conference on Nuclear Structure* (ed. by D. A. Bromley and E. W. Vogt), University of Toronto Press, Toronto, Canada, 1960.

[2] Y. Akiyama, *Progr. Theoret. Phys.* (*Kyoto*) 23, 903 (1960).

[3] J. Blomqvist and S. Wahlbom, *Arkiv Fysik* 16, 545 (1960).

[4] R. M. Wilenzick, G. E. Mitchell, K. K. Seth, and H. W. Lewis, private communication, 1960.

[5] B. L. Cohen, R. E. Price, and S. Mayo, paper submitted to the *Physical Review* (1960).

[6] D. J. Hughes and R. C. Carter, *Neutron Cross Sections: Angular Distributions*, BNL-400 (1956).

[7] J. L. Fowler, *Bull. Am. Phys. Soc.* 5, 443 (1960).

[8] The enriched Pb^{208} isotope was obtained from the Isotopes Division of the Oak Ridge National Laboratory.

[9] F. D. Brooks, *Nuclear Instr. & Methods* 4, 151 (1959).

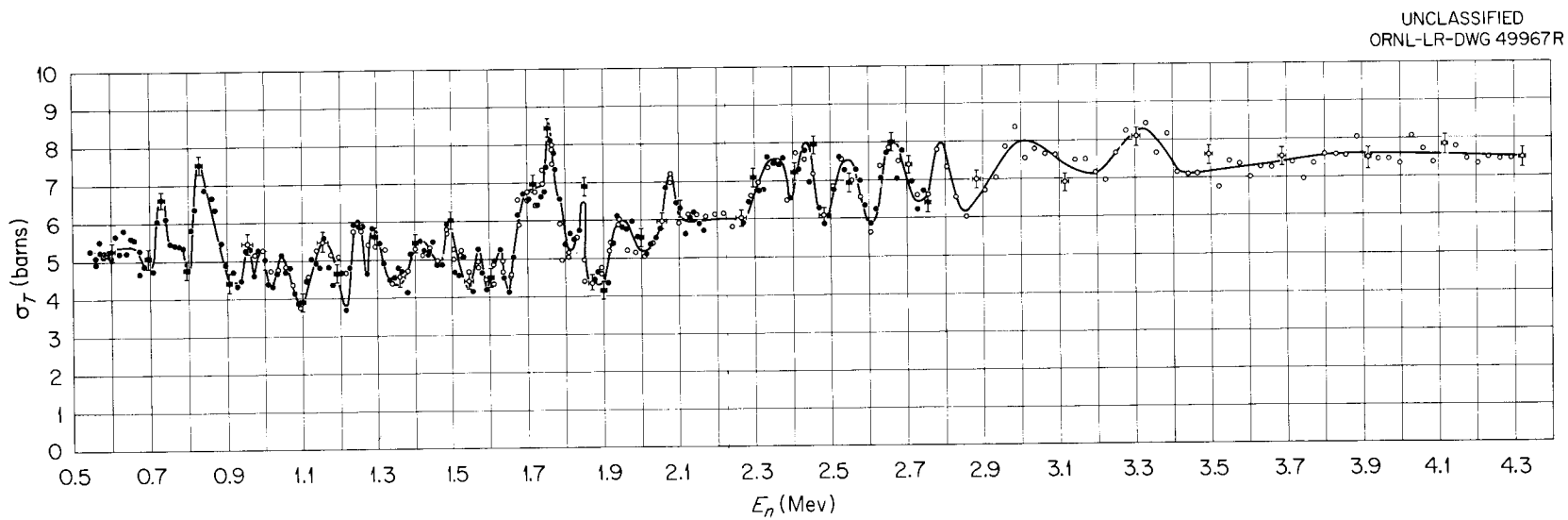

Fig. 1. Total Neutron Cross Section of Pb^{208}. Open circles for $T(p,n)$ neutrons, closed circles for $Li^7(p,n)$ neutrons. Energy resolution indicated by horizontal bars.

case of the 3 kev data, so that the inscattering correction was reduced to about half that of the data of Fig. 1.

Figure 2 gives the 3 kev total cross section measurements from 1.4 to 1.9 Mev. The correction for the second group of neutrons from the $Li^7(p,n)$ reaction was made by use of the data of Fig. 1. As soon as the 1.0 to 1.4 Mev data, which have been obtained very recently, are analyzed, the 1.4 to 1.9 Mev curves can be recorrected. In the energy range 1.0 to 1.9 Mev, at least 46 resonances were observed. In the interval represented by Fig. 2, the peak cross sections show resonances corresponding to J values in the range $\frac{1}{2}$ to $\frac{7}{2}$. Widths of the levels varied from less than 3 kev to $\sim$100 kev.

The resonance at 1.75 Mev is of particular interest. When the observed peak height is corrected ($\sim$10%) for the energy resolutions, one obtains a 6.0 $\pm$ 0.6 barn resonance of approximately 11 kev full width at half maximum. At 1.75 Mev, this corresponds to a $J = \frac{7}{2}$ resonance, which means either an f or a g level. If it is a g level (even parity), it has a rather large fraction of the single-particle width, so that one might suppose it is associated with the upper member of a doublet split by spin-orbit coupling, the lower member of which is the $g_{9/2}$ ground state of Pb^{209}. Angular distributions of scattered neutrons should serve to decide whether the 1.75-Mev state is an f or a g state. The high efficiency of the crystal detectors used with the Brooks-Owen technique for gamma-ray suppression makes it possible to consider angular distribution measurements with energy resolution sufficient to resolve this 11-kev resonance. A beam collimator and shield are being assembled to make these differential measurements.

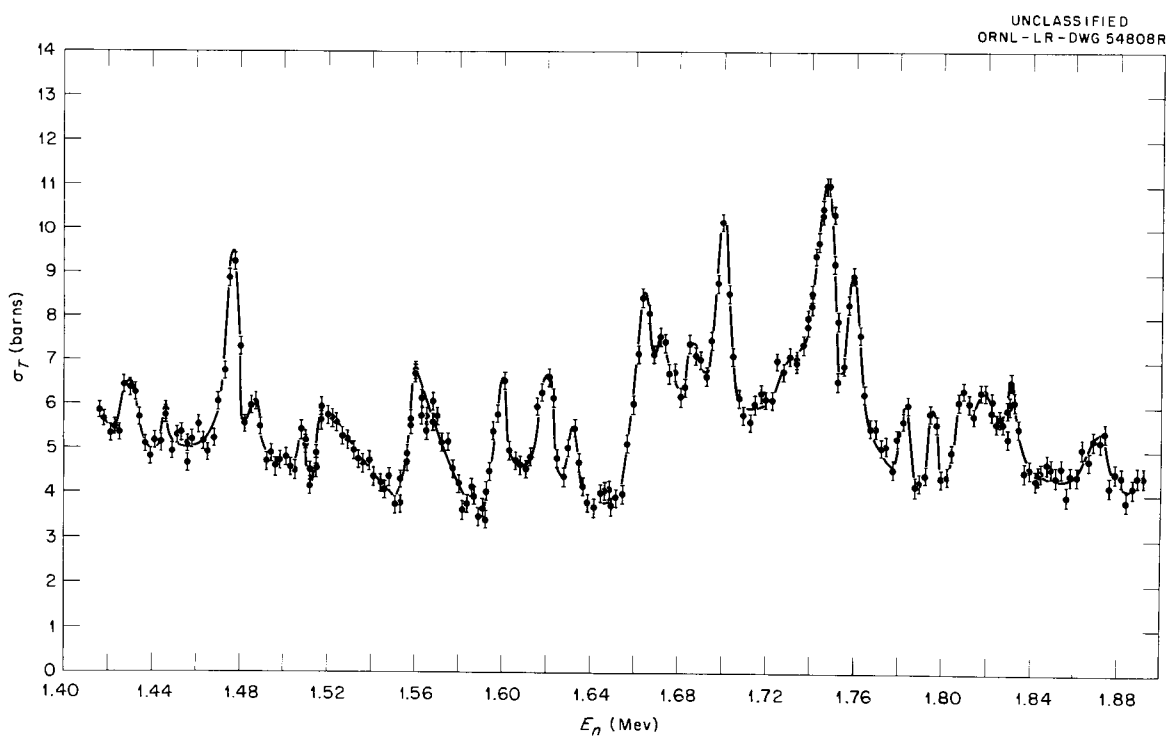

Fig. 2. Total Neutron Cross Section of Pb^{208}. $Li^7(p,n)$ neutron source, resolution $\sim$3 kev.

CARBON-13 NEUTRON TOTAL CROSS SECTION[1]

H. O. Cohn J. K. Bair H. B. Willard

The total neutron cross section of C^{13} was measured for neutron energies from 110 kev to 9 Mev and from 16 Mev to 23 Mev. Four narrow resonances were observed as well as broad resonance structure above 3 Mev. The most probable spin assignments based on the resonance heights and widths are as follows:

$E_R = 153 \pm 5$ kev	$\Gamma = 13$ kev	$J = 1^+$
$E_R = 1751 \pm 8$ kev	$\Gamma = 20$ kev	$J = 1$
$E_R = 2432 \pm 10$ kev	$\Gamma = 17$ kev	$J = 2$
$E_R = 2454 \pm 10$ kev	$\Gamma = 10$ kev	$J \geqq 1$

[1]Abstract of paper submitted to the *Physical Review*.

NEUTRON TOTAL CROSS SECTIONS IN THE kev ENERGY RANGE

H. Muenzer[1] K. Nishimura[2] W. M. Good

The isotopes Se^{76}, Se^{77}, Se^{78}, Se^{80}, and Se^{82} have recently been added to the list of isotopes for which neutron total cross sections have been determined in the energy range 4–50 kev. In order to achieve higher detection efficiency than employed in previous measurements, the thickness of the B^{10} neutron to gamma converter was increased to about 1.5 cm. The flight paths were chosen to keep the time resolution approximately 1% of the flight time.

Selenium-77 showed no structure, due in part to the narrowness of the resonances and in part to the fact that the obtainable sample was small. The average cross section was about 6 barns. Figure 1 shows the results obtained in the case of Se^{80}. The results for Se^{76}, Se^{78}, and Se^{82} are similar in appearance apart from the occurrence of prominent resonances such as those at 3.96 and 4.72 in Se^{80}. Table 1 gives a listing of the resonances in the even isotopes. Also given is mean spacing as determined from a histogram of the number of levels of energy greater than the minimum measured energy vs energy.

The spacings of levels in the isotopes of zinc and germanium have been previously reported.[3] In Fig. 2 the level spacings in zinc, germanium, and selenium are presented. Also shown in Fig. 2 are

[1]Visiting investigator from the Institut für Radiumforschung und Kernphysik, der Österreichischen Akademie der Wissenschaften, Vienna, Austria.

[2]Visiting investigator from Japan Atomic Energy Research Institute, Tokai.

[3]P. D. Miller *et al.*, "Statistical Parameters of Medium Weight Nuclei from kev Neutron Total and Capture Cross Sections," p 959 in *Proceedings of the International Conference on Nuclear Structure* (ed. by D. A. Bromley and E. W. Vogt), University of Toronto Press, Toronto, Canada, 1960.

the data of Newson and Gibbons[4] for odd target nuclei in the same region of neutron number. the spacings in the odd target nuclei have a correlation factor $(2I + 1)/\beta$, where I is the spin of the target nucleus and β is the Bethe-Hurwitz factor.

[4]H. W. Newson and J. H. Gibbons, chap. V. L., "Neutron Cross Sections in the kev Region," in *Fast Neutron Physics*, Part II, ed. by J. B. Marion and J. L. Fowler, Interscience, New York (in press).

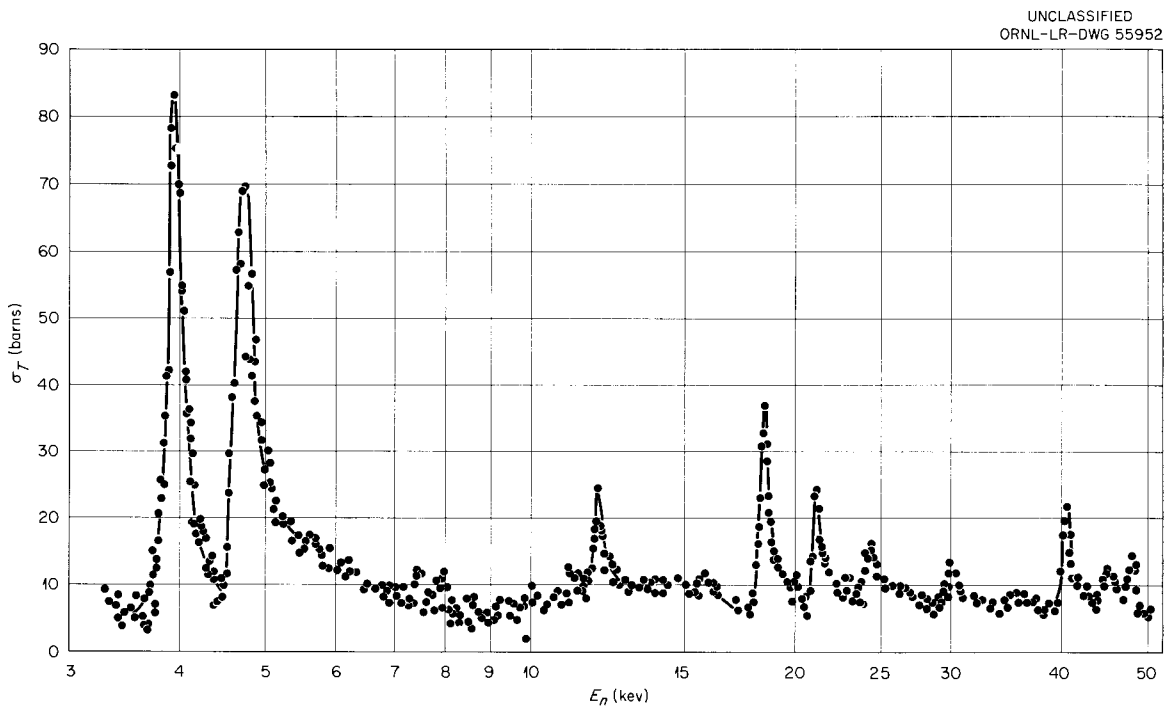

Fig. 1. Total Cross Section of Se^{80}.

Table 1. Tabulation of Neutron Resonances and Mean Level Spacings in the Isotopes of Selenium

	Se^{76}	Se^{78}	Se^{80}	Se^{82}
Energy	4.95	5.70	3.96	6.60
	5.95	8.50	4.84	13.8
	6.60	10.0	11.7	23.0
	7.80	17.0	18.3	26.5
	9.25	26.8	20.9	
	12.9	29.2	24.0	
	24.5	31.0	30.0	
	34.8	37.5	40.4	
		40.0	48.0	
		45.0		
$\bar{D}$	1.44	3.71	4.39	7.02

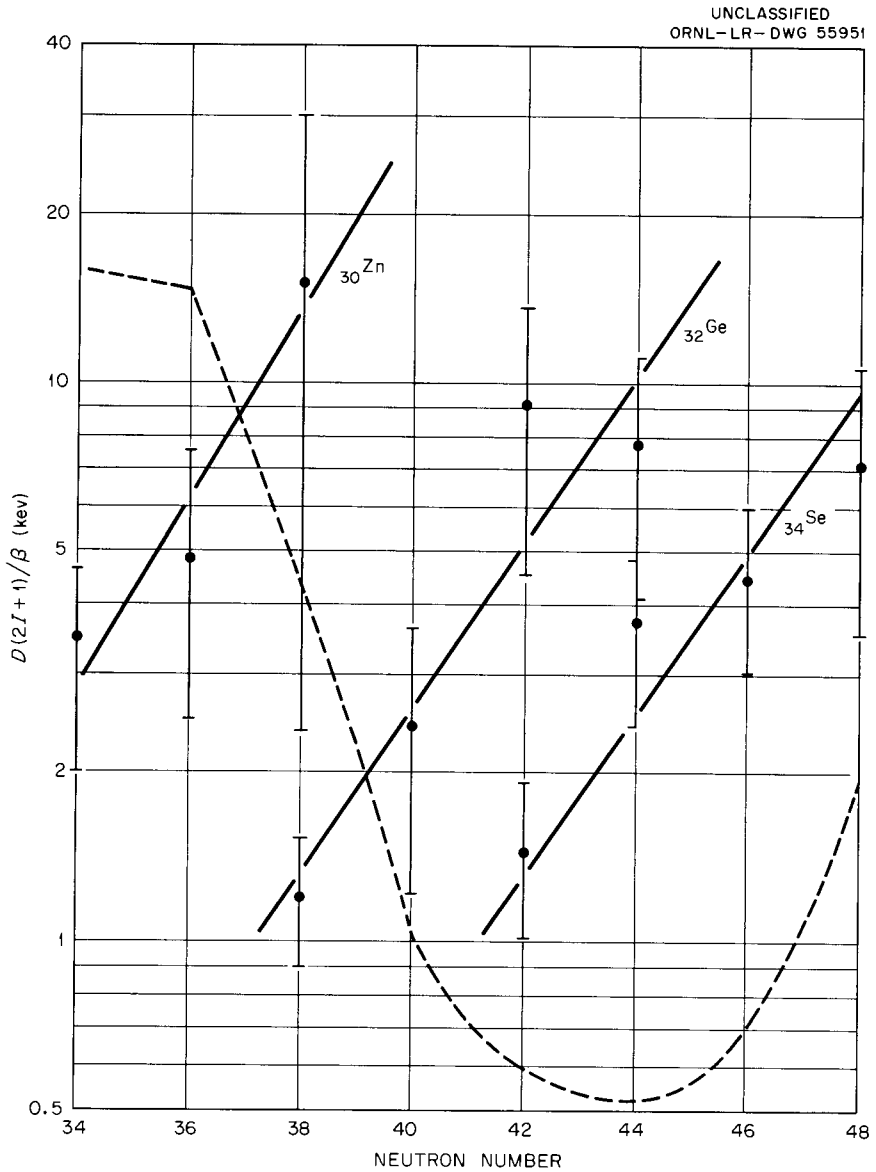

Fig. 2. Observed Mean Level Spacing in the Isotopes of Zn, Ge, and Se, as a Function of Neutron Number. For these nuclei $I = 0$, $\beta = 1$. The dashed curve is the reduced data for odd target nuclei.

STATISTICAL PARAMETERS OF MEDIUM-WEIGHT NUCLEI FROM kev NEUTRON TOTAL AND CAPTURE CROSS SECTIONS

P. D. Miller J. H. Gibbons J. H. Neiler W. M. Good R. L. Macklin

For several years the Oak Ridge National Laboratory has been engaged in a program of measuring kilovolt neutron cross sections by fast time-of-flight techniques with a 3-Mv Van de Graaff generator. Most of this effort has been concentrated on the study of (1) neutron total cross sections of separated

isotopes in the region of the s-wave giant resonance near $A = 50$, and (2) absolute neutron radiative capture cross sections of normal abundance samples in all regions of atomic weight except the lightest elements. Some of the earlier total cross-section measurements have been published, and the basic techniques used for these measurements have been described by Good, Neiler, and Gibbons.[1] Results of later measurements have been reported in cross-section compilations,[2] and strength functions[3] have been presented as well as results on average s-wave level spacing.[4] The experimental techniques and preliminary results on radiative neutron capture have been reported in several places.[5-8] Basically, the experiment involves the absolute measurement of radiative capture cross sections as a function of energy (by fast time-of-flight techniques) in the energy range about 7–170 kev. The equipment involves a terminal-pulsed proton accelerator, fast electronics, and a 1000-liter liquid scintillator counter with (0.97) 4π geometry. Results of the measurements include regularities of capture cross sections with atomic weight and correlation with major neutron and proton shells.

The average spacing of s-wave resonances has been determined for 15 separated isotopes in the region of $A = 45$ to $A = 88$ by transmission measurements within the energy range 3 to 50 kev.[1,3,4] The average spacings have been determined by counting resonances.

The formalism of Lane and Lynn for average radiative capture cross sections[9] has been utilized for fitting odd-Z capture cross sections ranging in atomic weight from bromine to gold. These fits have yielded spacings for s-wave resonances and strength functions for p waves subject to several plausible assumptions.

In general, the derived s-wave spacings have been slightly larger than the ev range spacings in the neighborhood of $A = 100$. We attribute this slight discrepancy to the presence of some p-wave resonances in the hundred ev range. In confirmation of this point, the latest high-resolution cross-section measurements at Columbia (Nb and I)[10] have statistically distinguished s-wave from p-wave resonances and have provided excellent fits to our capture cross-section data. In the rare-earth region, derived level spacings from capture cross sections are less than those observed in the ev range by up to a factor of 2 to 4. We attribute this discrepancy to narrow levels being missed in the ev range. This appears to be a range of A where it might be very fruitful to repeat with very high

---

[1] W. M. Good, J. H. Neiler, and J. H. Gibbons, *Phys. Rev.* **109**, 926 (1958).

[2] D. J. Hughes and R. B. Schwartz, *Neutron Cross Sections*, 2nd ed., and Supplement No. 1, BNL-325 (Jan. 1, 1960).

[3] P. D. Miller *et al.*, *Bull. Am. Phys. Soc.* **4**, 42 (1959).

[4] W. M. Good *et al.*, paper presented at the Southeastern Section Meeting of the American Physical Society, April 7–9, 1960.

[5] J. H. Neiler *et al.*, *Bull. Am. Phys. Soc.* **4**, 43 (1959).

[6] J. H. Neiler *et al.*, *Bull. Am. Phys. Soc.* **4**, 474 (1959).

[7] P. D. Miller *et al.*, *Bull. Am. Phys. Soc.* **4**, 474 (1959).

[8] R. L. Macklin *et al.*, *Bull. Am. Phys. Soc.* **4**, 474 (1959).

[9] A. M. Lane and J. E. Lynn, *Proc. Phys. Soc. (London)* **A70**, 557 (1957).

[10] J. L. Rosen *et al.*, *Bull. Am. Phys. Soc.* **4**, 473 (1959).

resolution the earlier ev range experiments. In Fig. 1 the results of the ORNL kev measurements of s-wave spacings as a function of neutron number are compared to a smooth line through the compilation of Newson and Gibbons.[11] The Bethe-Hurwitz factor β is taken as 1 for even-even nuclei, and 0.42 for odd-A nuclei.[12] The s-wave strength functions have been determined for 9 of the 15 isotopes studied by transmission. Some of these results have been reported,[3] and the analysis of the rest of the cross sections studied is in progress.

The p-wave strength functions which have been derived from curve-fitting the capture cross-section data are presented in Table 1. The peaking of the p-wave strength function in the region of $A = 100$ is very pronounced. We have not measured enough samples, since our technique has not yet been applied to separated isotopes, to confirm or deny the suspected splitting of the p-wave giant resonance.[13] The p-wave strength functions in the rare-earth region are upper limits only, as we suspect that the cross section positive inflections at about 100 kev are very possibly due to d waves.

[11] H. W. Newson and J. H. Gibbons, chap. V. L., "Neutron Cross Sections in the kev Region," in *Fast Neutron Physics*, Part II, ed. by J. B. Marion and J. L. Fowler, Interscience, New York (in press).

[12] J. H. Gibbons *et al.*, paper submitted to the *Physical Review*.

[13] L. W. Weston *et al.*, paper to be published in the *Annals of Physics*.

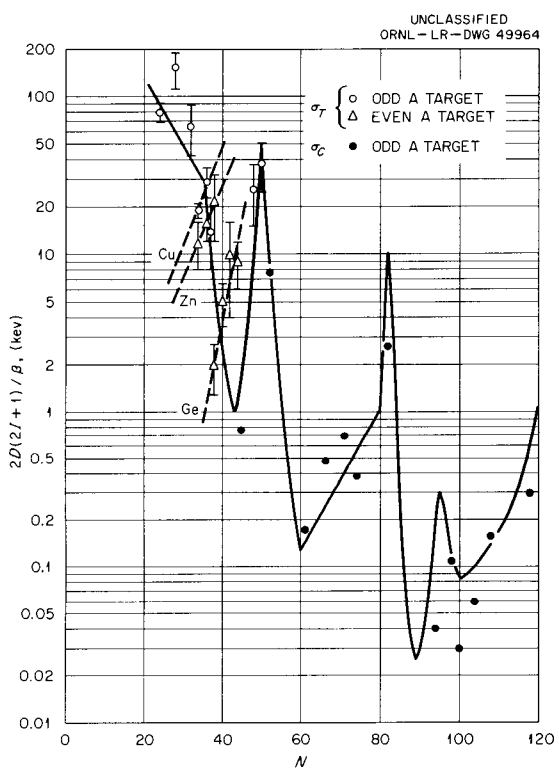

Fig. 1. Average Spacings of s-Wave Resonances as a Function of Neutron Number. Spin dependence and even-odd effects have been removed.

Table 1. p-Wave Strength Functions for Elements in the Neighborhood of the $2p$ Giant Resonances

Element	S_1	Element	S_1
	$\times 10^{-4}$		$\times 10^{-4}$
Br	0.05 ± 0.05	Tb	$0.2^{+0.1}_{-0.2}$
Nb	$6.0^{+1.5}_{-1.0}$	Ho	$0.4^{+0.1}_{-0.4}$
Ag	10^{+3}_{-2}	Tm	0.1 ± 0.1
In	8^{+1}_{-2}	Lu	0.1 ± 0.1
Sb	3 ± 1	Ta	$0.2^{+0.1}_{-0.2}$
I	$3^{+1}_{-1.5}$	Au	$0.2^{+0.1}_{-0.2}$
Pr	0.05 ± 0.05		

TOTAL NEUTRON CROSS SECTION OF B^{10} IN THE THERMAL-NEUTRON ENERGY RANGE[1]

H. W. Schmitt R. C. Block R. L. Bailey[2]

A precise determination of the total neutron cross section of B^{10} has been made by means of transmission measurements of boron samples highly enriched in B^{10}. The ORNL fast chopper time-of-flight spectrometer was used to obtain results in the neutron energy range $0.018 \leqq E \leqq 0.4$ ev. It is found that the total cross section of B^{10} in this energy range follows the relation σ_t (barns) = $(612 \pm 6)/\sqrt{E\,(\text{ev})}$. The total cross section of B^{10} for neutrons of energy 0.0253 ev (velocity = 2200 m/sec) is found to be 3848 ± 38 barns.

[1]Abstract of published paper: *Nuclear Phys.* 17, 109 (1960).
[2]Isotopes Division.

HIGH-RESOLUTION TOTAL CROSS SECTION MEASUREMENTS ON Np^{237} AND Am^{241}

G. G. Slaughter J. A. Harvey R. C. Block

The ORNL fast chopper and associated 180-m flight path were utilized in measuring the total neutron cross sections of Np^{237} (from 4 to 100 ev) and Am^{241} (from 5.4 to 43 ev). The neutron detector was a group of 65 BF_3 counters, each 1 in. in diameter and 40 in. long, segregated into four banks in the direction of the beam. The flight path error between banks was compensated by a time-dependent delay circuit. The data were taken at a resolution varying from 12 to 67 nanoseconds/m, giving an energy resolution of 0.2 to 0.6%, depending upon energy and rotor speed.

The neptunium sample had a total of 18.34 g of Np^{237} in the form of the oxide, with a reciprocal sample thickness of 570 barns/atom. The americium sample had a total of 1.66 g of Am^{241} in the form of the trifluoride, with reciprocal sample thicknesses of 522 and 3480 barns/atom, depending upon beam direction through the sample.

The transmission data were analyzed using an IBM 704 area analysis code which computes the neutron widths of resonances for an assumed total width. This code also convolutes Doppler and resolution shapes with the line shape in calculating a transmission which is compared with the observed transmission. In the case of nuclides with high level density and overlapping resonances, routine application of the code yields information which could not be obtained without laborious hand calculations.

For Np^{237} a total of 75 levels was found in the energy range 0–100 ev. Considering the range 0–29 ev, the average level spacing, D, was found to be 1.15 ± 0.12 ev per spin state. The strength function $(\overline{\Gamma}_n^0/D)$ obtained was $(0.96 \pm 0.13) \times 10^{-4}$ per spin state, considering the range 0–100 ev.

A total of 53 levels in the range 0–43 ev was found in the total neutron cross section of Am^{241}. The average level spacing derived from the data in the range 0–11 ev was $D = 0.87 \pm 0.13$ ev per spin state. The strength function, considering the range 0–40 ev, was $(1.1 \pm 0.2) \times 10^{-4}$ per spin state.

The large energy range of these measurements and the high level density made it possible to plot level spacing distributions and reduced neutron width distributions for these nuclides; these distributions were in qualitative agreement with expected theoretical distributions. The reduced neutron width distributions were consistent with a Porter-Thomas distribution. Since both nuclei have a spin of $5/2$, the level spacing distribution was compared to, and found consistent with, a random superposition of two Wigner distributions of the same density.

The resonance parameters measured for Np^{237} and Am^{241} are given in Tables 1 and 2.

Table 1. Resonance Parameters of $_{93}Np^{237}$

Resonance parameters up to 3.885-ev resonance are from previous data

E_0 (ev)	$g\Gamma_n^0$ (ev)	E_0 (ev)	$g\Gamma_n^0$ (ev)	E_0 (ev)	$g\Gamma_n^0$ (ev)
	$\times 10^{-3}$		$\times 10^{-3}$		$\times 10^{-3}$
0.489	0.023 ± 0.001	17.62	0.03 ± 0.01	49.90	0.31 ± 0.04
1.326	0.013 ± 0.006	19.22	0.005 ± 0.002	50.53	0.65 ± 0.06
1.48	0.044 ± 0.009	19.62	0.006 ± 0.002	56.25	0.10 ± 0.01
1.97	0.006 ± 0.001	19.89	0.012 ± 0.004	59.6	0.07 ± 0.02
3.885	0.073 ± 0.005	20.42	0.130 ± 0.013	60.18	0.146 ± 0.015
4.293	0.007 ± 0.002	21.12	0.055 ± 0.006	61.13	0.063 ± 0.009
4.77	0.0022 ± 0.0014	22.04	0.135 ± 0.014	62.63	0.06 ± 0.03
4.89	0.007 ± 0.003	22.88	0.040 ± 0.004	63.01	0.062 ± 0.026
5.81	0.16 ± 0.02	23.71	0.213 ± 0.025	65.91	0.24 ± 0.02
6.41	0.022 ± 0.002	25.01	0.51 ± 0.05	67.72	0.59 ± 0.09
6.73	0.004 ± 0.001	26.23	0.037 ± 0.004	70.48	0.15 ± 0.02
7.22	0.0033 ± 0.0013	26.59	0.31 ± 0.03	71.50	0.29 ± 0.03
7.46	0.026 ± 0.002	30.47	0.38 ± 0.04	74.53	0.13 ± 0.04
8.31	0.005 ± 0.002	30.73	0.021 ± 0.002	78.62	0.10 ± 0.02
8.37	0.013 ± 0.005	31.34	0.009 ± 0.003	79.50	0.13 ± 0.03
9.02	0.022 ± 0.004	33.50	0.045 ± 0.004	83.88	0.49 ± 0.05
9.33	0.09 ± 0.01	34.05	0.029 ± 0.003	86.73	0.40 ± 0.04
10.69	0.10 ± 0.03	35.24	0.031 ± 0.003	87.99	0.22 ± 0.03
10.84	0.20 ± 0.08	37.17	0.127 ± 0.013	89.73	0.31 ± 0.05
11.10	0.20 ± 0.06	38.24	0.114 ± 0.011	91.12	0.25 ± 0.04
12.25	0.007 ± 0.003	39.07	0.130 ± 0.013	93.52	0.10 ± 0.02
12.63	0.121 ± 0.012	39.37	0.044 ± 0.006	97.99	0.10 ± 0.02
15.84	0.021 ± 0.002	41.41	0.175 ± 0.018	100.43	0.33 ± 0.06
16.10	0.132 ± 0.013	46.43	0.18 ± 0.02	101.36	0.30 ± 0.06
16.88	0.030 ± 0.005	47.43	0.149 ± 0.015		

Table 2. Resonance Parameters of $_{95}Am^{241}$

Resonance parameters up to 5.44-ev resonance are from previous data

E_0 (ev)	$g\Gamma_n^0$ (ev)	E_0 (ev)	$g\Gamma_n^0$ (ev)	E_0 (ev)	$g\Gamma_n^0$ (ev)
	$\times 10^{-3}$		$\times 10^{-3}$		$\times 10^{-3}$
0.305	0.054 ± 0.003	10.38	0.053 ± 0.005	27.68	0.06 ± 0.02
0.575	0.049 ± 0.005	10.98	0.054 ± 0.007	28.36	0.045 ± 0.014
1.275	0.172 ± 0.009	12.86	0.020 ± 0.006	28.93	0.050 ± 0.015
1.93	0.045 ± 0.002	14.70	0.31 ± 0.06	29.56	0.075 ± 0.025
2.375	0.026 ± 0.004	15.60	0.022 ± 0.013	30.79	0.04 ± 0.03
2.60	0.062 ± 0.006	15.73	0.020 ± 0.012	31.21	0.11 ± 0.03
3.99	0.065 ± 0.006	16.02	0.018 ± 0.011	32.14	0.05 ± 0.04
4.40	0.006 ± 0.002	16.38	0.120 ± 0.024	34.02	0.07 ± 0.04
5.00	0.048 ± 0.005	16.82	0.05 ± 0.02	35.02	0.06 ± 0.04
5.44	0.224 ± 0.006	17.68	0.030 ± 0.012	35.53	0.045 ± 0.023
6.06	0.026 ± 0.008	18.37	0.05 ± 0.02	37.01	0.43 ± 0.14
6.78	0.045 ± 0.018	19.48	0.014 ± 0.014	38.39	0.23 ± 0.08
7.64	0.022 ± 0.015	20.64	0.03 ± 0.02	39.71	0.17 ± 0.05
7.97	0.14 ± 0.06	23.09	0.04 ± 0.02	40.42	0.14 ± 0.05
8.11	0.14 ± 0.06	23.28	0.080 ± 0.024	41.71	0.05 ± 0.05
8.28	0.022 ± 0.013	24.17	0.11 ± 0.02	42.64	0.9 ± 0.4
9.09	0.066 ± 0.008	25.61	0.10 ± 0.04	43.25	0.19 ± 0.08
9.84	0.053 ± 0.008	26.60	0.06 ± 0.02		

ANALYSIS OF BREIT-WIGNER RESONANCES USING AN IBM 704 COMPUTER

J. A. Harvey S. E. Atta[1]

High-resolution time-of-flight spectrometers can now make transmission measurements over energy regions which contain hundreds of resonances. The analysis of transmission data to obtain the parameters of the resonances is complicated because of Doppler and resolution broadening. The existing techniques are time-consuming and sometimes not very accurate when the resonances are not well resolved from one another. Two programs (which include Doppler and resolution) have been written for the IBM 704 computer in order to analyze transmission data.

[1]Mathematics Panel.

We have used the single-level Breit-Wigner formula. The total cross section is computed from the sum of single-level formulas,

$$\sigma(E'') = \left[4\pi r^2 + \frac{6.52 \times 10^5}{\sqrt{E''}} \sum_{\lambda} \frac{\Gamma^{\lambda}(fg\,\Gamma_n^{0\lambda})}{(E^{\lambda} - E'')^2 + (\Gamma^{\lambda}/2)^2} - 5.725 \times 10^3 \sum_{\lambda} \frac{(E^{\lambda} - E'')(fg\Gamma_n^{0\lambda})a}{(E^{\lambda} - E'')^2 + (\Gamma^{\lambda}/2)^2} \right], \quad (1)$$

where

E^{λ} is the resonance energy, in ev,

Γ^{λ} is the total width, in ev, of resonance λ,

$\Gamma_n^{0\lambda}$ is the reduced neutron width, in ev, of resonance λ,

r is the effective neutron radius, in 10^{-12} cm,

a is the nuclear scattering amplitude, in 10^{-12} cm,

f is the fractional abundance of the isotope,

g is the statistical weight factor.

Equation (1) includes interference between resonance and potential scattering, but there is no interference between resonances. Assuming that the Doppler broadening follows a Gaussian function, the Doppler-broadened cross section $\sigma_{\Delta}(E')$ is computed by convoluting the nuclear cross section $\sigma(E'')$ and a Gaussian:

$$\sigma_{\Delta}(E') = \frac{1}{\Delta\sqrt{\pi}} \int_0^{\infty} \sigma(E'')\, e^{-[(E'-E'')/\Delta]^2}\, dE'', \quad (2)$$

where Δ is the Doppler width.

Assuming that the resolution function can also be represented by a Gaussian, the theoretical transmission is computed by another convolution:

$$T(E_i) = \frac{1}{R\sqrt{\pi}} \int_0^{\infty} e^{-N\sigma_{\Delta}(E')}\, e^{-[(E_i-E')/R]^2}\, dE', \quad (3)$$

where R is the resolution width and N is the sample thickness, in atoms/barn.

The method adopted to solve for the parameters of the resonances was the estimation of the parameters of the resonances, the computation of the transmission at each E_i, and the comparison of the calculations with the experimental data. If the agreement between the experimental data and the theoretical calculations did not meet a pre-established criterion, corrections to the parameters were computed by the computer and the program would recompute $T(E_i)$. It would iterate until sufficiently good agreement was obtained.

The main difficulty with this approach to the problem is the large amount of computer time needed to evaluate so many double integrals. However, by representing the convolution of the

Breit-Wigner total cross section with a Gaussian as the real and imaginary parts of the complex probability integral and by the use of recurrence formulas and tables, the integrals could be evaluated accurately with a small amount of computer time.

SHAPE ANALYSIS

For low-energy neutron resonances where the Doppler widths and resolution widths are small compared with the natural widths of the resonances, the width, Γ, of each resonance can be determined as well as its E_0 and Γ_n^0. In this low-energy region the problem was to find an adequate and practical method of analysis of such a nonlinear function [Eq. (3)]. The least-squares method for solving such a nonlinear problem used Gauss's method of reducing the problem to one in which linear methods could be applied. The nonlinear function was linearized with respect to each of its parameters by expanding it in a truncated Taylor's series. Improved estimates for the parameters are obtained by using the initial estimates of the parameters to evaluate the coefficients in the expansion. The process is repeated until some convergence criterion is satisfied. This shape-fit program can solve a transmission curve for as many as four resonances at once for approximately $40.

AREA ANALYSIS

For higher-energy resonances where Δ or $R > \Gamma$, it is not possible to obtain meaningful values of Γ from the experimental data, since the observed widths of the resonances are determined mainly by Δ or R. Resonances at these higher energies are analyzed by an area-analysis technique to give Γ_n^0 for an assumed Γ, and the area analysis does not depend on the resolution. However, if the resonances are close together, the accuracy of the area method can be increased if the resolution is included in the analysis.

In the area-analysis code, the number of resonances as well as the number of channels which each resonance covers is fed into the machine with estimates of the parameters. The computer calculates the sum of the calculated transmissions over each resonance and compares it to the sum of the experimental transmissions over each resonance. If it meets a certain criterion, it stops; if not, it computes corrections to be applied to each resonance and again calculates the transmissions. It will iterate until it meets the criterion. When the criterion is met the code will type out the values it has computed for the neutron widths, as well as the input information. The output from a sample run containing four resonances is shown in Fig. 1. The last column gives the answers, $fg\Gamma_n^0$, for the four resonances. The IBM 704 also gives a curve plotter output, as shown in Fig. 2. The theoretical and experimental transmissions over these four resonances are in very good agreement. The program can analyze a transmission curve for as many as 12 resonances at one time. The cost for analyzing a typical 1024-channel analyzer transmission curve with $\sim$30 resonances is $\sim$$100.

AREA ANALYSIS OF TRANSMISSION DATA JOB 1910

RUN 164C

ELEMENT SM151

NUMBER OF ITERATIONS 2

C1	C2	GAMMA	C0	E0	FGXGAMMA N 0
262	272	0.850000E-01	0.267000E 03	0.104546E 02	0.368254E-04
273	331	0.180000E-00	0.302500E 03	0.804536E 01	0.879787E-02
332	345	0.750000E-01	0.337000E 03	0.642174E 01	0.182411E-04
361	374	0.980000E-01	0.368500E 03	0.533322E 01	0.107187E-05

A= 0.70000E 00
N= 0.26600E-02
AW= 0.15100E 03
R= 0.70000E 00
DIST= 0.45381E 02
T= 0.40000E 01
T DELAY=-0.53250E 02
D0= 0.31800E-00
B0= 0.43932E-02
B1=-0.
CN=1023
CF= 230
CL= 399
NO= 4
IF= 1
IM= 3

K0= 0.972525E 00
K1= -0.250407E-00
K2= 0.598599E 00

Fig. 1. Printed Output from IBM 704 for Area Analysis Code. The computed parameters $fg\Gamma_n^0$ for the four resonances are given in the last column; the other data are input information.

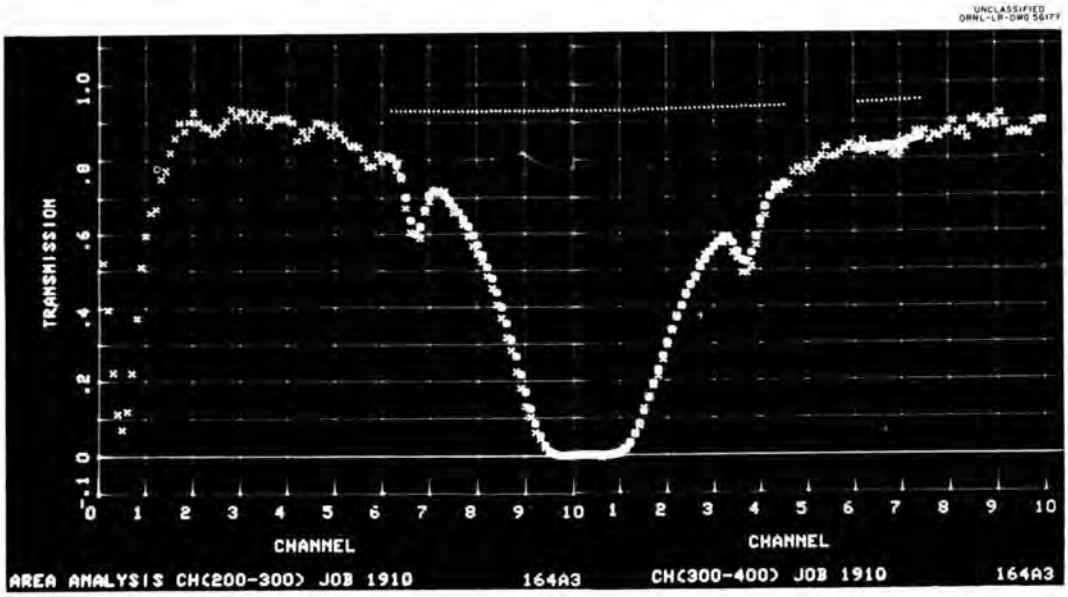

Fig. 2. Curve Plotter Output from IBM 704 for Area Analysis Code. The experimental points are the x's and the computed points are the •'s.

ENERGY SPECTRA OF CORRELATED FRAGMENT PAIRS FROM THE SPONTANEOUS FISSION OF Cf^{252}[1]

W. T. Joyner[2] H. W. Schmitt J. H. Neiler R. J. Silva[3]

Silicon surface-barrier counters have been used in conjunction with specially designed low-noise amplifiers to measure the energies of correlated fragment pairs from the spontaneous fission of Cf^{252}. The silicon counters, $\frac{1}{4} \times \frac{1}{4}$ in. in size and prepared from 3600-ohm-cm material, exhibit rise times for fission pulses of a few nanoseconds; the pulse-height resolution obtained for natural alpha particles is 0.5%. The energy response of the present counters to fission fragments appears to be slightly nonlinear. Pulses from coincident fragment pairs are analyzed and recorded in a 100×100 channel coordinate recorder. Approximately 3×10^5 events have been recorded on punched paper tape and sorted on the Oracle. Preliminary results including the deduced relative mass yields are shown, as well as pulse-height and energy spectra.

---

[1]Abstract of published paper: *IRE Trans. on Nuclear Sci.* **NS-8**, 54 (1961).
[2]1960 summer research participant.
[3]Chemistry Division.

NEUTRON RADIATIVE CAPTURE MEASUREMENTS

R. C. Block F. C. VonderLage L. W. Weston

Additional radiative capture measurements have been carried out with the 28-in.-diam spherical liquid scintillator installed at the 11.5-m flight station of the ORNL fast chopper.[1] The scintillation detector has been slightly modified over the past year to reduce the background produced by neutrons which scatter into the scintillator, moderate down to thermal energies, and produce 2.2-Mev capture gamma rays when captured in hydrogen. (Even though the scintillation solution is boron-loaded to reduce the hydrogen captures, approximately 5% of the neutrons which enter the tank can get captured by hydrogen.) A recent drawing of this detector is shown in Fig. 1; the improvements to be noted are the argon-filled beam tube through which the neutron beam passes through the scintillator tank, the 1.75-in.-thick Li^6H beam-tube liner (recommended by L. Cranberg to reduce the neutron inscattering), and the 4-in.-thick lithiated-paraffin shield to the left of the lead wall surrounding the scintillator. The Li^6H liner proved highly superior to an equally thick B_4C liner in reducing the inscattering background. Experiments with air, argon, and helium atmospheres inside the beam tube through the scintillator showed that the scattering from the gas inside this tube was approximately the same for air and helium but was considerably less for argon.

---

[1]*Phys. Div. Ann. Progr. Rept. Feb. 10, 1960*, ORNL-2910, p 35.

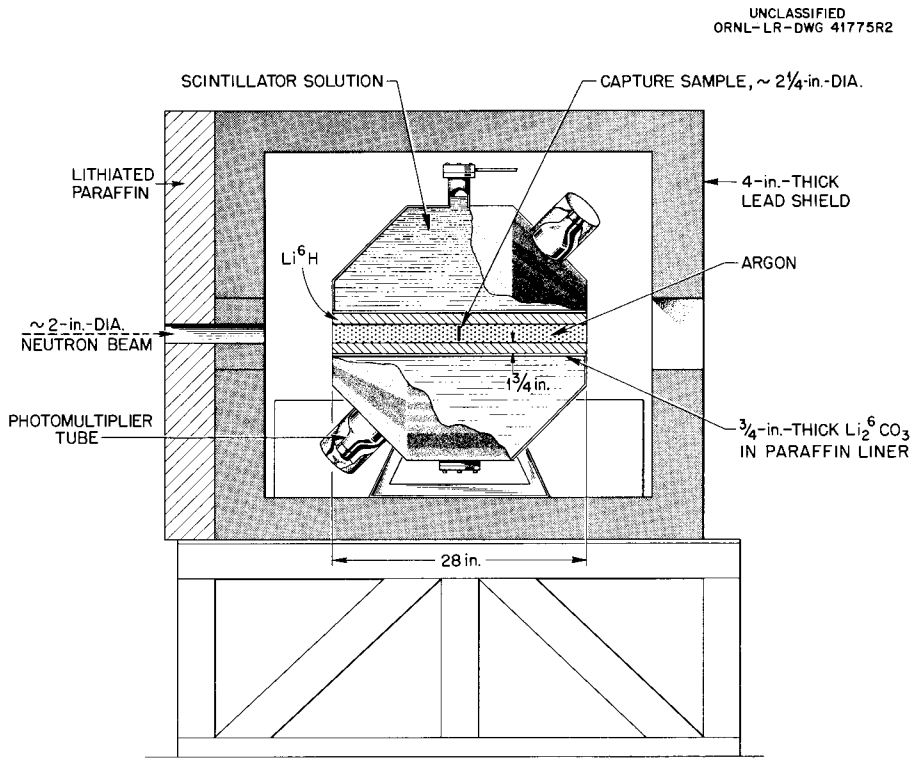

Fig. 1. The 28-in.-diam Liquid Scintillator Detector.

Since argon and helium have small scattering cross sections relative to that of air for resonance-energy neutrons, but helium and air have essentially high scattering cross sections relative to argon for neutrons of ~ 1 Mev in energy, it was concluded that the inscattering background is caused predominately by fission-energy neutrons which pass through the rotor slits when the chopper is in the "open" position and enter the beam tube. Hence, the beam tube through the tank was filled with argon to minimize the gas scattering for these measurements. It was also determined that the 4-in.-thick lithiated-paraffin wall reduced the background from other fission-energy neutrons, which also pass through the chopper when it is open, "splatter" over the front face of the lead shield surrounding the detector, and diffuse into the scintillator tank to produce hydrogen capture gamma rays. These three modifications to the detector have resulted in reduction by a factor of ~3 in this inscattering effect. (This corresponds to a reduction from ~30% down to ~ 10% in the correction to the indium capture-cross-section data at ~ 5 kev.)

The M1 high-intensity chopper[2] was used for these capture measurements. A rotor speed of 9050 rpm was employed, resulting in a resolution of 0.17 μsec/m. The capture samples were prepared by F. L. Layton under the direction of W. R. Laing of the Analytical Chemistry Division. The metallic samples were cut from sheets into 2.50-in.-diam disks. The powdered metals or compounds (mostly oxides) were pressed into 2.25-in.-diam disks with a 10-ton hydraulic press; then each was vacuum-sealed into an aluminum can with 0.003-in.-thick windows.

[2]R. C. Block, G. G. Slaughter, and J. A. Harvey, *Nuclear Sci. and Eng.* 8, 112 (1960).

The neutron flux was measured with a bank of six BF_3 proportional counters placed at the end of a 12.5-m flight path. The scintillator detector was biased at ~2.6 Mev, as determined by the 1.57-Mev Pr^{142} gamma ray. However, unlike the results reported last year,[1] because of electronic difficulties it was not possible to measure the efficiency of the scintillator tank at a given bias setting by observing the differential pulse-height spectrum resulting from capture in each sample and correcting for the counts "lost" below the bias setting on the amplifier. As a result, the radiative capture cross sections of Ag, Sb, Tb, Ta, W, and Au were each normalized at ~6000 ev to the results reported by Gibbons *et al.*[3] The normalization factors for each of these elements turned out to be within ~15% of a single "mean" normalization factor. Since only an accuracy of 20 to 25% is estimated for these measurements, this "mean" normalization factor was taken to be the same for all elements measured in the intermediate to heavy atomic weight range.

The radiative capture cross sections of those intermediate and heavy weight naturally abundant elements which had moderate capture cross sections are plotted in Figs. 2, 3, and 4. (Measurements were also undertaken for some of the elements which had either a small capture cross section or a large level spacing, but the capture cross section sensitivity of this apparatus, ~0.2 barn, and the limited energy range covered by these measurements did not allow a significant measurement to be made in many of these cases.) These results repeat some of the measurements reported a year ago,[1] and with the exception of the rhodium capture-cross-section results the two sets of measurements agree quite well with each other. In the case of the rhodium capture-cross-section data an arithmetical error was present in last year's presentation of the data; the rhodium results reported then were too high and should be disregarded. It is to be noted that with the resolution of 0.17 μsec/m employed in this experiment the capture cross sections plotted in Figs. 2, 3, and 4 show evidence of resolved or partially resolved resonance structure near the lower energies and exhibit reasonable "averages" over many resonances in the kev energy region. These data have not as yet been corrected for multiple scattering or resonance-self-protection effects with the sample thicknesses chosen these effects in general lead to less than ~10% corrections the data above ~400 ev; hence, in the region where resonance structure is averaged out these data are not seriously affected by these corrections.

The data cover the transition range from low energies where the capture cross section is almost exclusively due to s-wave neutrons to kev energies where p-wave contributions become important. By combining these data with the higher energy data of Gibbons *et al.*[3] it is possible to extract information about the s- and p-wave strength functions for these elements. These calculations, however, are not yet completed for inclusion in this report.

---

[3] J. H. Gibbons *et al.*, "Average Radiative Capture Cross Sections for 7- to 170-kev Neutrons," scheduled for publication in the April 1, 1961, issue of the *Physical Review*.

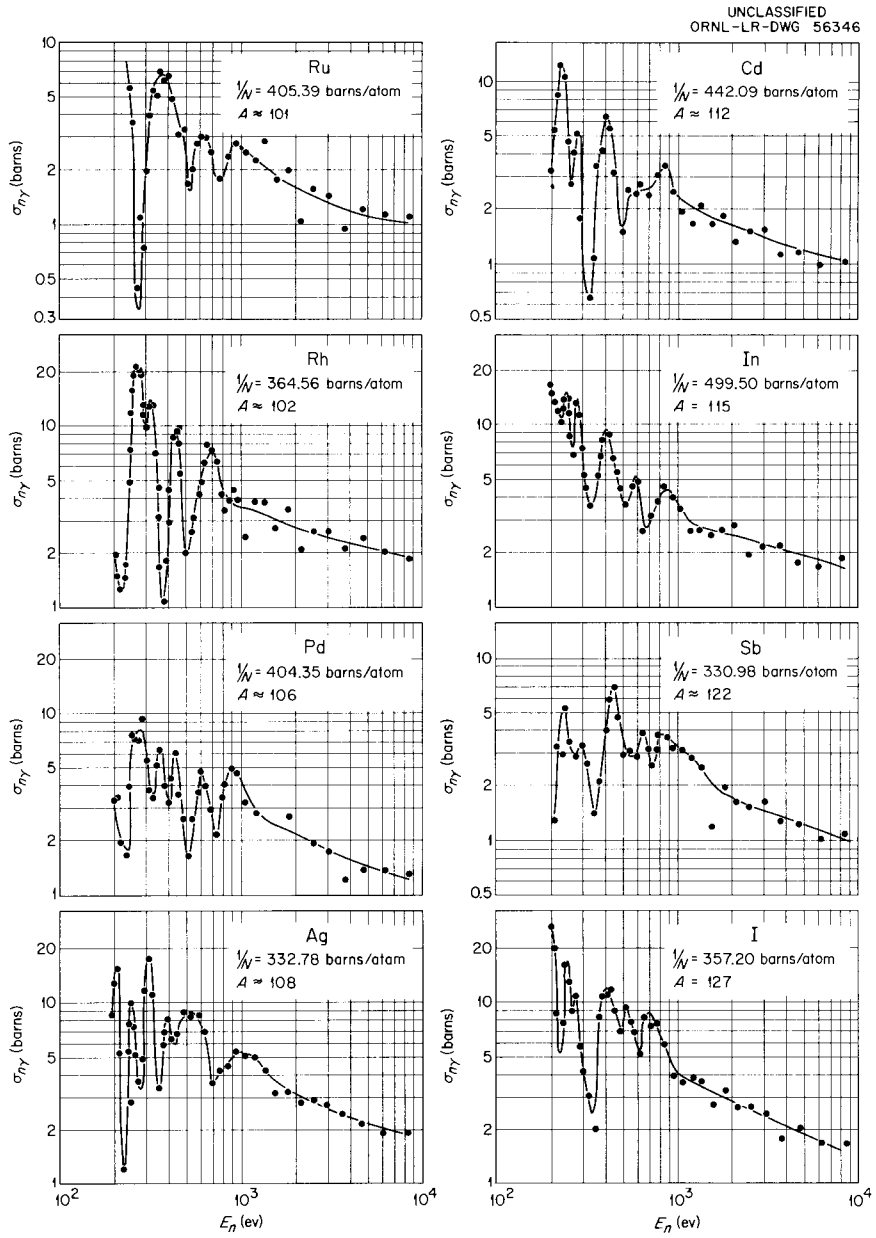

Fig. 2. Radiative Capture Cross Sections of Elements Near Atomic Weight 115.

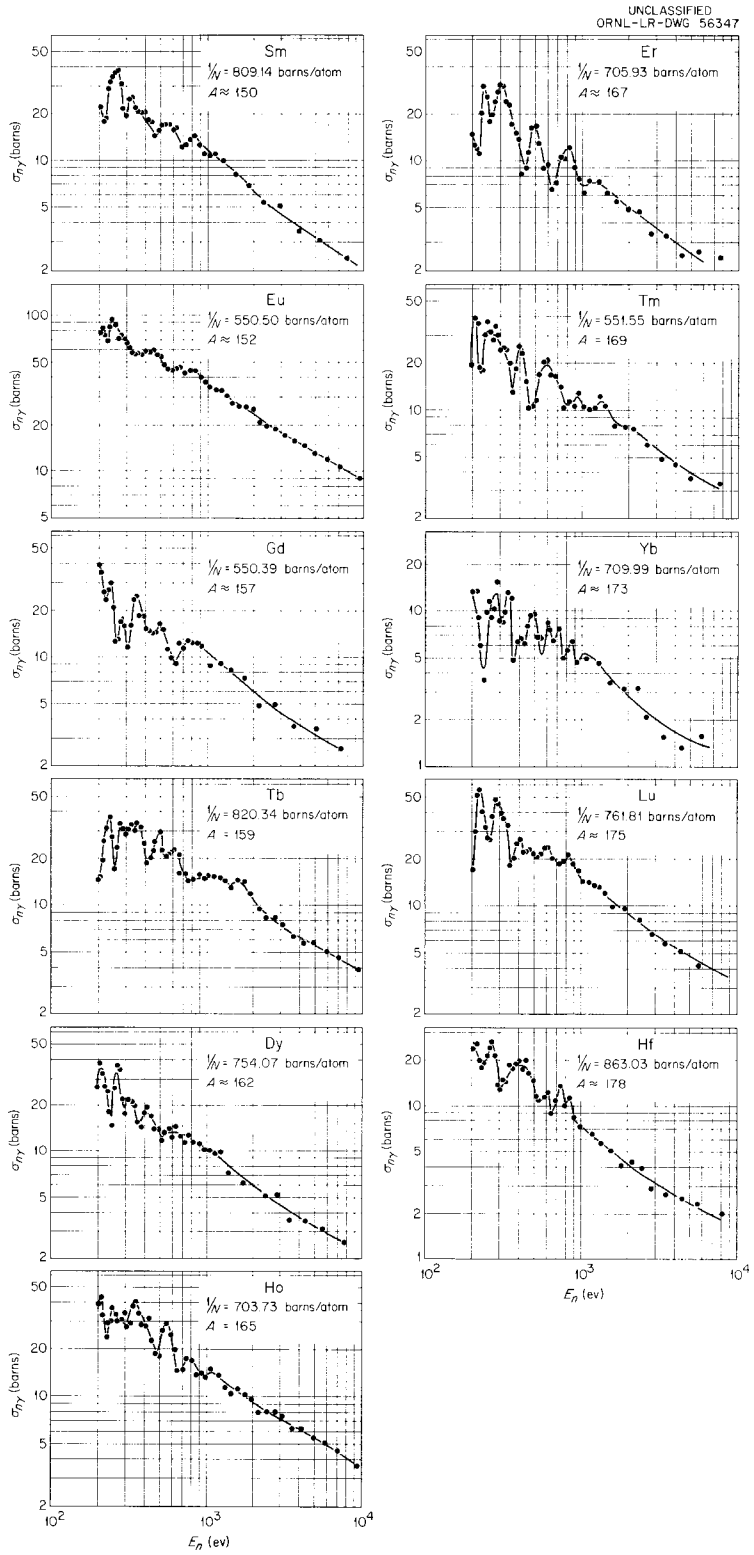

Fig. 3. Radiative Capture Cross Sections of the Rare-Earth Elements.

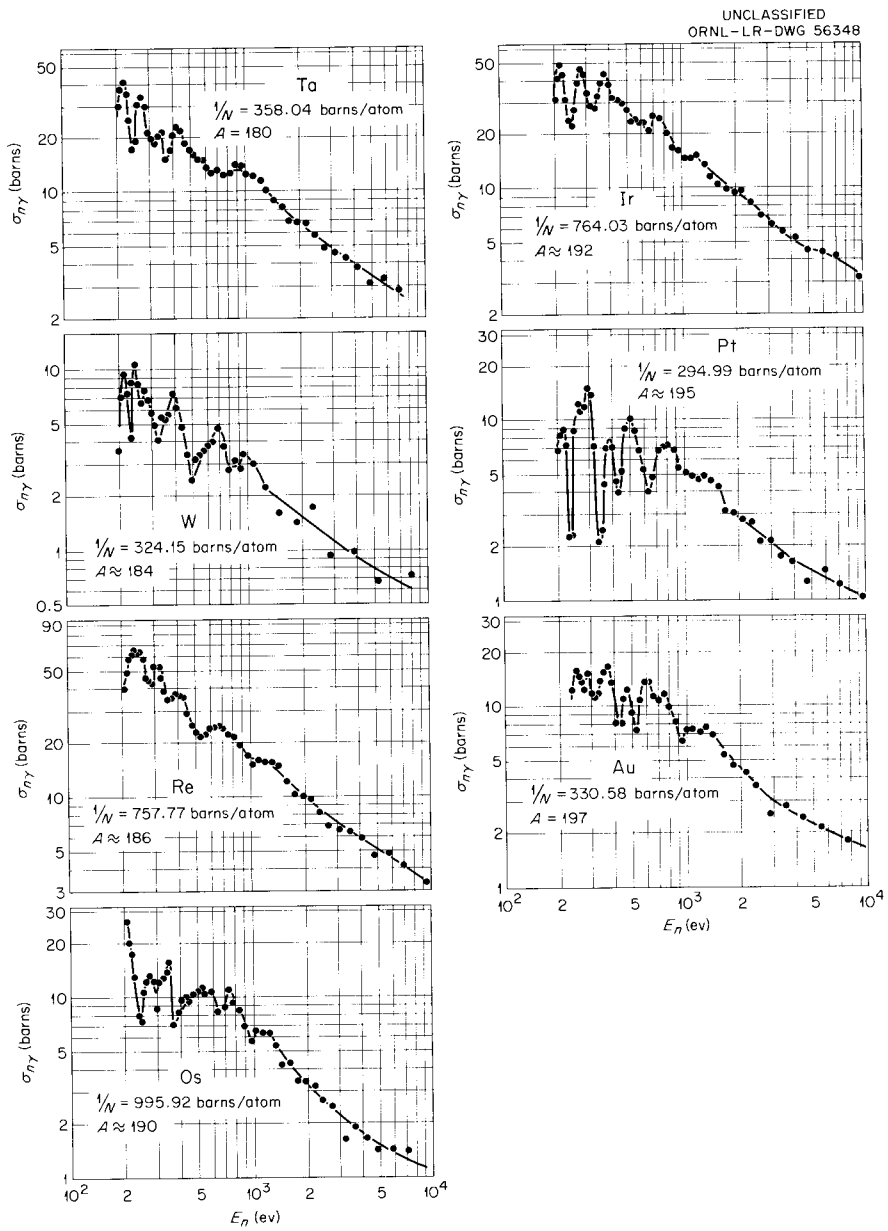

Fig. 4. Radiative Capture Cross Sections of Some Heavy Elements.

GAMMA-RAY SPECTRA FROM 30-kev NEUTRON CAPTURE

F. W. K. Firk[1] J. H. Gibbons

The study of prompt gamma rays from radiative neutron capture has been almost solely restricted to thermal- or ev-range neutrons, principally because of lack of sufficiently intense neutron sources at other energies. There are at least four motivations for similar investigations at higher neutron energies. First, it is known that spectra are dependent upon the spin of the capturing state and can thus change considerably with energy and neutron l wave. Second, recent discussions of possible "direct" capture effects[2] indicate a sensitive dependence of the intensity of high-energy gamma-ray transitions on neutron energy; the predicted intensity is higher in thermal than in fast neutron capture. Third, the determinations of radiative capture cross sections by use of large liquid scintillators are sensitive to gross changes in the spectra of gamma rays. Last, the general problem of efficient reactor shielding is strongly dependent upon a knowledge of capture gamma-ray spectra.

The $Li^7(p,n)Be^7$ reaction can be used as an extremely intense source of 30-kev neutrons due to kinematic collimation. Since the cross section for this reaction rises so rapidly from its threshold, approximately 5×10^8 neutrons/sec can be produced into a forward cone ($\pm 10°$) *during the*

[1]Visiting scientist from A.E.R.E., Harwell, England.

[2]A. M. Lane and J. E. Lynn, *Nuclear Phys.* 17, 563 (1960).

UNCLASSIFIED
ORNL-LR-DWG 55428

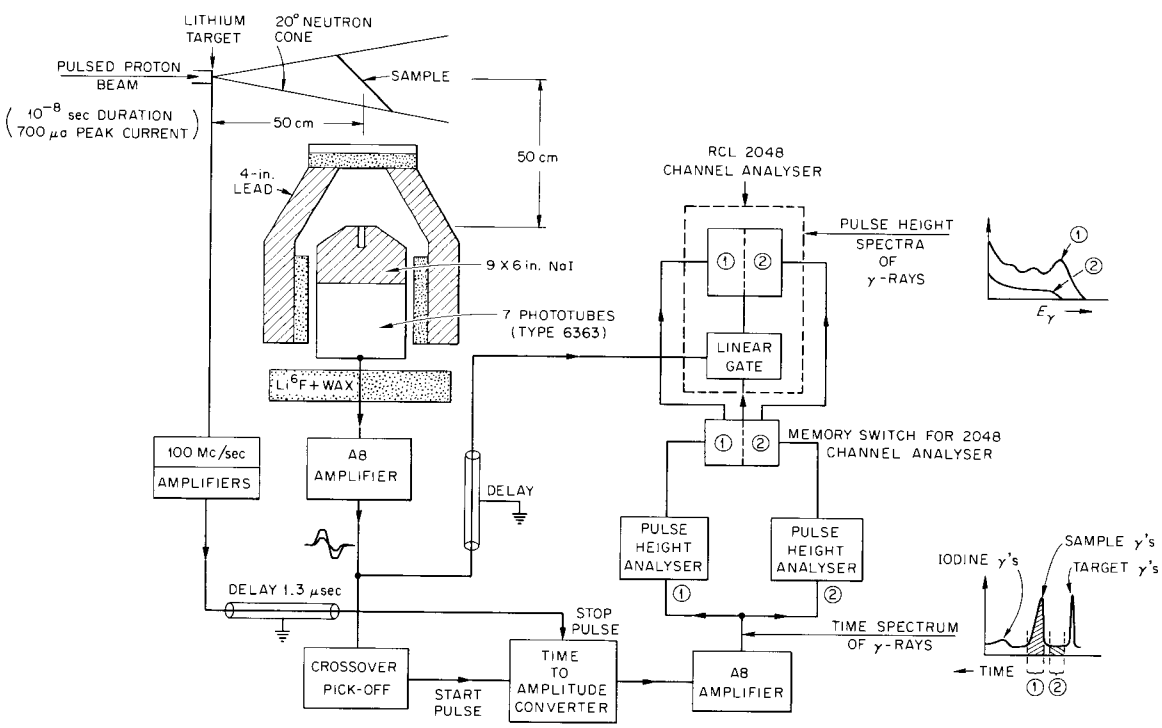

Fig. 1. Block Diagram of Electronics Used in the Experiment.

pulse with a 1-ma pulsed proton beam. Beam pulsing enables not only use of higher instantaneous beam currents, but also time separation of events. In our case this last point is essential to the experiment.

The experimental arrangement (Fig. 1) consists of a large massively shielded NaI crystal[3] which views the capturing sample. Distances from neutron source to sample and from sample to detector are both about 50 cm. Far more neutrons are, of course, scattered by the samples than are captured. These scattered neutrons can give rise to a later time peak (Fig. 2) due to prompt capture of scattered neutrons by the iodine in the NaI crystal. This peak and some small amount of longer-time-constant background can be removed with a small amount (2 in.) of Li^6F plus paraffin (Fig. 2).

Time gates are set corresponding to the time of capture (gate 1) and to a time interval a few tens of nanoseconds before or after the neutrons arrive at the sample (gate 2). These gates dynamically operate a 2 × 512 channel analyzer, allowing simultaneous accumulation of gross counts and background.

Typical spectra measured in this fashion are given in Figs. 3–7. These have *not* yet been corrected for detector peak efficiency, energy resolution, etc. However, the crystal has a reasonably good peak-to-total ratio (Fig.

[3]Loaned by the Neutron Physics Division.

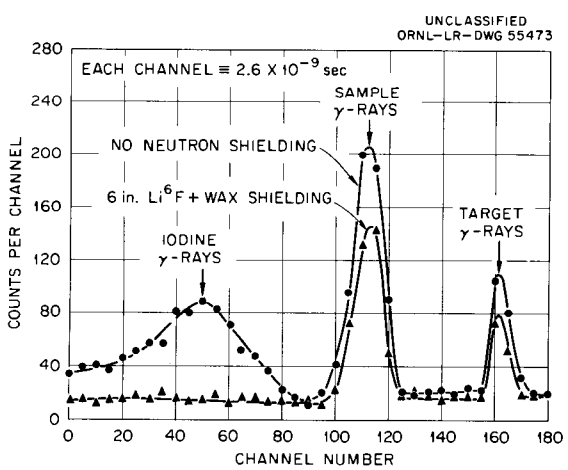

Fig. 2. Detector Counts as a Function of Time, Both With and Without Li^6F Neutron Shielding.

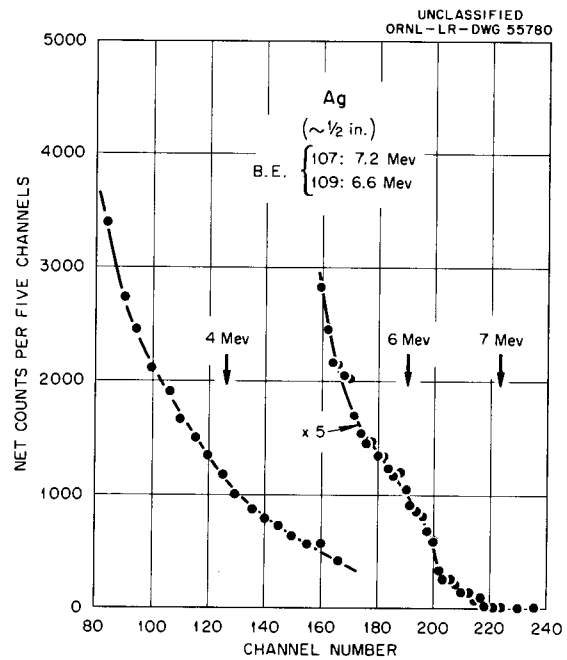

Fig. 3. Capture Gamma-Ray Spectra from Silver.

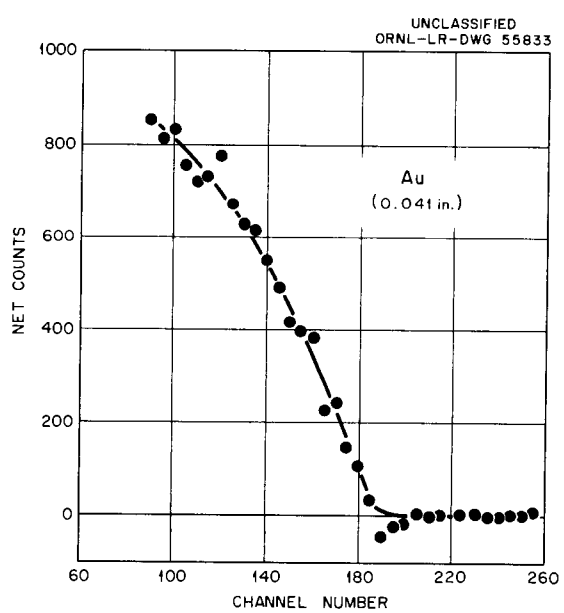

Fig. 4. Capture Gamma-Ray Spectra from Gold.

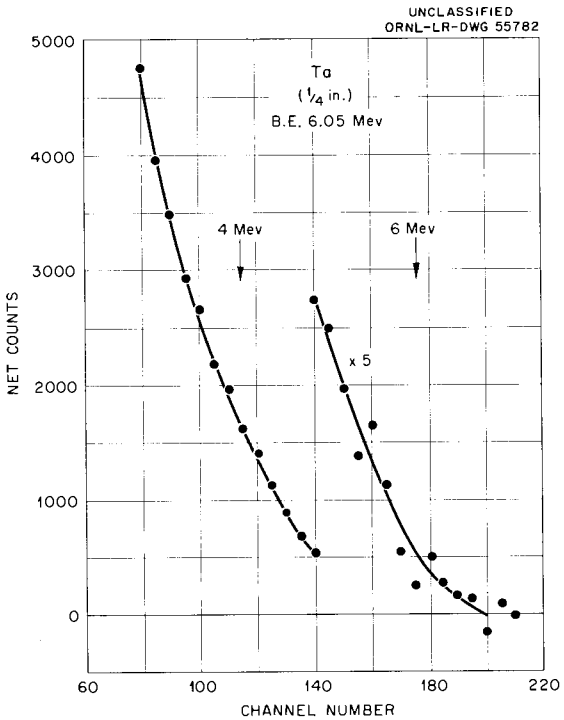

Fig. 5. Capture Gamma-Ray Spectra from Tantalum.

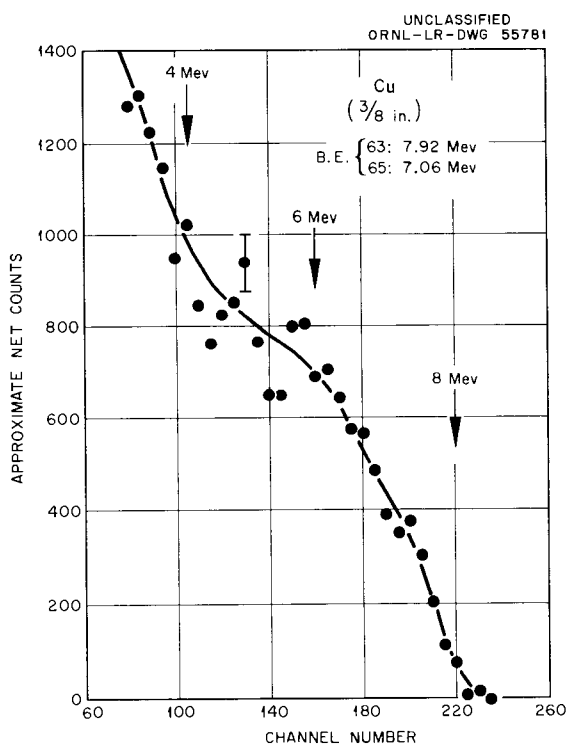

Fig. 6. Capture Gamma-Ray Spectra from Copper.

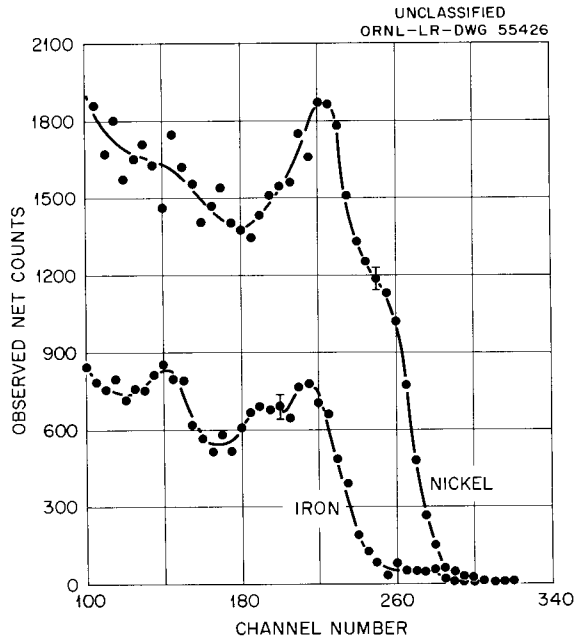

Fig. 7. Capture Gamma Rays from Fe and Ni.

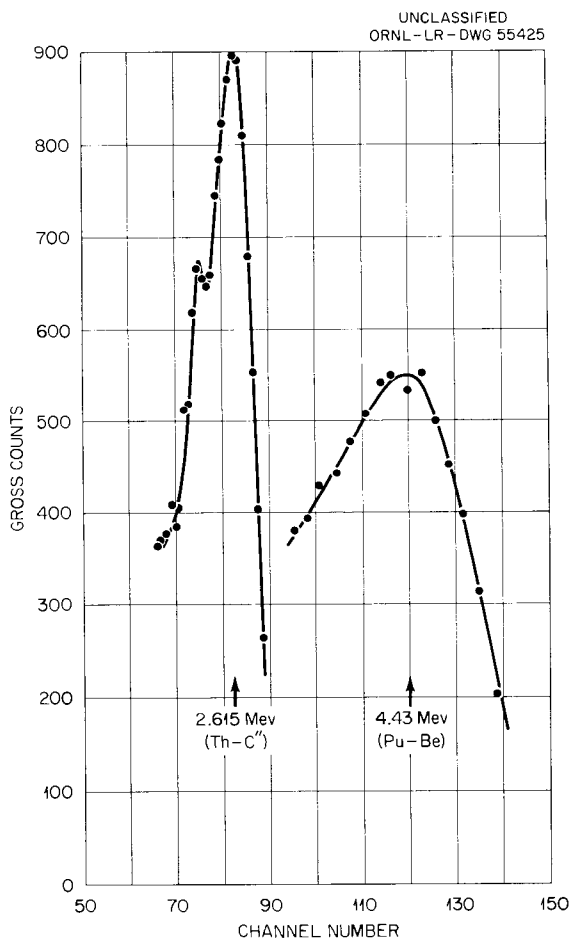

Fig. 8. Total Absorption Spectra for Single Gamma Rays on the 9 × 12 in. NaI Crystal.

8) for single gamma rays. Thus a predominant high-energy gamma ray should be detected. An example of this (Fig. 7) is the spectrum of gamma rays from capture in iron, where strong ground state and low-lying state transitions are observed. It is interesting to note that, for the case of iron, the gamma rays are essentially due to capture by the $\frac{1}{2}^+$ resonance at 29 kev. Examples in striking contrast to the spectrum from iron are those of gamma rays from capture in silver (Fig. 3) and tantalum (Fig. 5). Here, as expected, there is a smoothly decreasing curve all the way up to the neutron binding energy. While the silver and tantalum curves are concave, the spectrum of gammas from gold (Fig. 4) exhibits a convex shape, probably caused by a greater predominance of higher energy transitions. Finally, although the data are preliminary, there appears to be a definite lack of high-energy gamma-ray transitions in nickel (Fig. 7) and copper (Fig. 6) compared with thermal capture. These data may possibly be explained in terms of "direct" capture processes.

COULOMB EXCITATION OF THE SECOND 2^+ STATES IN W, Os, AND Pt NUCLEI[1]

F. K. McGowan P. H. Stelson

The location of a second 2^+ state has been established for six even-even nuclei by means of Coulomb excitation produced by 4- to 5-Mev protons. The relatively weak excitation of these states is detected by a measurement of the gamma-ray yields from singles spectra and from coincident measurements of the cascade gamma rays. The $B(E2)$'s for decay of the second 2^+ state to ground state by the crossover transition exhibit some uniformity for the even-even isotopes of W and Os, being about six times the single-particle value. The cascade/crossover ratio for the decay of the second 2^+ state is known for these nuclei. The upper cascade $B(E2)$'s exhibit enhancements of 10 to 60 times the single-particle value. The ratios of the $B(E2)$'s for decay of the first and second 2^+ states are compared to the predictions of several collective models. For five of these nuclei the $E2/M1$ ratio is known for the upper cascade transition. The $B(M1)$ values obtained are exceedingly small compared to the single-particle estimate. This result is in qualitative agreement with the collective models, which predict that $M1$ radiation is forbidden in the decay of vibrational excitations.

---

[1] Abstract of paper to be published in the *Physical Review*.

COULOMB EXCITATION OF SECOND 2^+ STATES IN EVEN-EVEN MEDIUM-WEIGHT NUCLEI[1]

P. H. Stelson F. K. McGowan

The location of a second 2^+ state has been found for 13 even-even medium-weight nuclei by means of Coulomb excitation produced by 8-, 9-, and 10-Mev alpha particles. The relatively weak excitation of these states is detected by a coincident measurement of the cascade gamma rays. From the observed gamma-ray yields information is obtained on the $B(E2)$'s for the crossover transitions. The crossover $B(E2)$'s exhibit some uniformity and are all rather weak, being about single-particle value or a little less. For some nuclei the cascade/crossover ratio for the second 2^+ state is known from other work and it is then possible to extract the $B(E2)$ for the upper cascade transition. These upper-cascade $B(E2)$'s exhibit enhancements comparable to those for the lower-cascade transitions. Evidence is obtained for the "double $E2$" Coulomb excitation of the 4^+ state in Cd^{114} and this requires an enhanced $4 \rightarrow 2$ $B(E2)$. In general, the measurements reported support a collective model interpretation, but it is as yet difficult to draw conclusions concerning the shape of the collective potential energy surface governing this motion.

[1]Abstract of published paper: *Phys. Rev.* 121, 209 (1961).

COULOMB EXCITATION OF Li^7, F^{19}, AND Na^{23} BY Ne^{20} IONS[1]

P. H. Stelson F. K. McGowan

Neon-20 ions of 9 to 11 Mev obtained by the acceleration of doubly charged ions in the ORNL 5.5-Mv Van de Graaff have been used to study Coulomb excitation in light nuclei. Excitation of . following states has been observed: Li^7, 478 kev; F^{19}, 110 and 197 kev; Na^{23}, 440 kev. Absolute values for the reduced electromagnetic transition rates have been obtained with an accuracy of ±20%.

[1]Abstract of published paper: *Nuclear Phys.* 16, 92 (1960).

COULOMB EXCITATION OF STATES IN Th^{232} AND U^{238}[1]

F. K. McGowan P. H. Stelson

The yield of gamma rays resulting from Coulomb excitation of states in Th^{232} and U^{238} with protons of 4- to 6-Mev energy has been measured. Gamma rays of 790-, 740-, and 613-kev energy from Th^{232} and of 1.02-Mev energy from U^{238} are observed. For Th^{232}, the variation in gamma-ray yields with proton energy, the results from gamma-ray angular distributions, and the linear polarization measurements are consistent with the direct excitation of a 2^+ state at 790 kev which decays by means of $E2$ radiation to the $I = 0^+$ and 2^+ members of the ground-state rotational band. In view of the recent results from internal conversion electron measurements at Rice University, the 613-kev gamma ray is interpreted to be a transition from a 2^+ β-vibrational state at 773 kev to the 4^+ state at 163 kev. An interpretation of the observed gamma-ray yields is carried out taking a γ-vibrational state at 790 kev and a β-vibrational state at 773 kev. The $B(E2)_d$ of the 2^+ state at 50 kev in Th^{232} is about 150 times the single-particle estimate. The $B(E2)_d$ of the vibrational states in Th^{232} and U^{238} are between two and four times the single-particle estimate. Combining Bernstein's relative internal conversion electron yields with our gamma-ray data, a value of $(8 \pm 2) \times 10^{-2}$ for the strength parameter ρ is obtained for the $E0$ transition between the 2^+ state at 773 kev and the 2^+ state at 50 kev in Th^{232}.

[1]Abstract of published paper: *Phys. Rev.* 120, 1803 (1960).

VIBRATIONS IN SPHERICAL AND NEARLY SPHERICAL NUCLEI[1]

P. H. Stelson

Experimental information on level positions and transition rates is summarized for nuclei which exhibit enhanced $E2$ transition rates and yet do not belong to the spheroidal groups. The $E2$ transition rates indicate that the dynamic quadrupole deformations of many nuclei in this group are comparable to the permanent quadrupole deformations of spheroidal nuclei. It is well known that the concept of phonon vibrations has considerable success in describing the properties of the low-lying states of a large fraction of the nuclei in this group. Several theoretical studies have been made to obtain better quantitative agreement with experimental results. The effects of the coupling of intrinsic states to the phonon states have been considered. Alternatively, the expected spectra and transition rates have been worked out for several quite different shapes for the nuclear potential

[1]Abstract of published paper: pp 787–800 in *Proceedings of the International Conference on Nuclear Structure*, ed. by D. A. Bromley and E. W. Vogt, University of Toronto Press, Toronto, Canada, 1960.

energy surface. The different theoretical results are compared to experimental results for some nuclei. The comparable magnitudes of the changes in level spectra and transition rates, caused either by interference from intrinsic states or by different shapes for the energy surface, make it difficult, with the still limited experimental information, to extract preferred descriptions for these nuclei.

COULOMB EXCITATION WITH Ne^{20} IONS[1]

P. H. Stelson F. K. McGowan

The ORNL 5.5-Mv Van der Graaff has been used to obtain Ne^{20} ions with energies up to 11 Mev. The Coulomb excitation produced by these ions has been studied in a number of nuclei ranging from Li^7 to Ir^{193}. Neon-20 ions in this energy range have the advantage that nuclear reactions other than Coulomb excitation have extremely small cross sections. However, with the presently available ion-beam intensities (e.g., 0.2 μa of Ne^{5+}), the Coulomb excitation gamma-ray yields are so low that room background counting rates are often troublesome. To alleviate this problem, a lead shield for the scintillation detector has been built which has 4-in. walls and inside dimensions of $48 \times 40 \times 18$ in. To obtain information on spins and decay modes of excited states, the 0–90° asymmetry ratios were measured for the 128-kev state of Mn^{55} and the 440-kev state of Na^{23}. Since the Ne^{20} ions produce relatively few K x rays during the slowing down process in the target, they are useful for measuring K-shell conversion coefficients of Coulomb excited states. K-shell conversion coefficients for the 136-kev state of Ta^{181} and the 123-kev state of W^{186} have been measured.

---

[1]Abstract of published paper: pp 47–56 in *Reactions Between Complex Nuclei*, ed. by A. Zucker, F. T. Howard, and E. C. Halbert, Wiley, New York, 1960.

CONTROL OF GAMMA RADIATION IN HEAVILY SHIELDED TARGET ROOMS[1]

H. E. Banta[2] G. W. Leddicotte[3]

Consideration has been given to controlling the gamma backgrounds in a massively shielded target room for a Van de Graaff accelerator. Only limited attention seems to have been given to this

---

[1]Abstract of paper presented at a meeting of the Southeastern Section of the American Physical Society, Gatlinburg, Tennessee, April 7–9, 1960.

[2]Instrumentation and Controls Division.

[3]Analytical Chemistry Division.

problem.[4] Some control of those gamma backgrounds that occur naturally, due principally to K^{40} and thorium, is possible by the selection of building materials. A study was made of portland cement, locally available sand, and crushed rock. The study showed that the K^{40} activity was generally of the order of eight times the thorium activity and that these activities could be reduced by a factor of 20 by using crushed rock in place of sand in the concrete mix. Consideration was also given to activation due to neutron absorption. It was found that in general about 1% of the incident neutrons go into (n,γ) processes followed by undesirable activities. This level of activity could be reduced by a factor of ~ 4 by the addition of 5 lb of borax per yard of concrete mix. It was shown by strength tests that this amount of borax does not demonstrably affect the concrete; larger amounts are known to do so.[5]

[4] C. P. Swann, "Matters Pertaining to Elimination of Background in Low Energy Nuclear Physics Measurements, with Special Reference to the Bartol ONR Generator," Bartol Research Foundation Technical Report (June 1, 1959).

[5] R. B. Gallaher and A. S. Kitzes, *Summary Report on Portland Cement Concretes for Shielding*, ORNL-1414 (Mar. 2, 1953).

GAMMA-GAMMA ANGULAR CORRELATIONS IN Xe^{132}

R. L. Robinson E. Eichler[1] N. R. Johnson[1]

The angular correlations of three gamma-ray cascades in Xe^{132} have been measured. For these measurements a source of 6.2-day Cs^{132} which had been produced with the ORNL cyclotron by a (p,pn) reaction on Cs^{133} was used. The gamma-ray cascades studied are illustrated in the simplified energy level diagram in Fig. 1. Data which were taken at ten different angles were least-squares fitted on the IBM 704 computer to the function $W(\theta) = 1 + A_2P_2(\cos\theta) + A_4P_4(\cos\theta)$. The experimental angular correlation coefficients which have been corrected for the finite angular resolution of the detectors[2] are given below:

Cascade (E in Mev)	A_2	A_4
0.63-0.673	-0.19 ± 0.07	$+0.42 \pm 0.10$
1.14-0.673	$+0.05 \pm 0.04$	$+0.05 \pm 0.06$
1.32-0.673	$+0.31 \pm 0.03$	$+0.03 \pm 0.04$

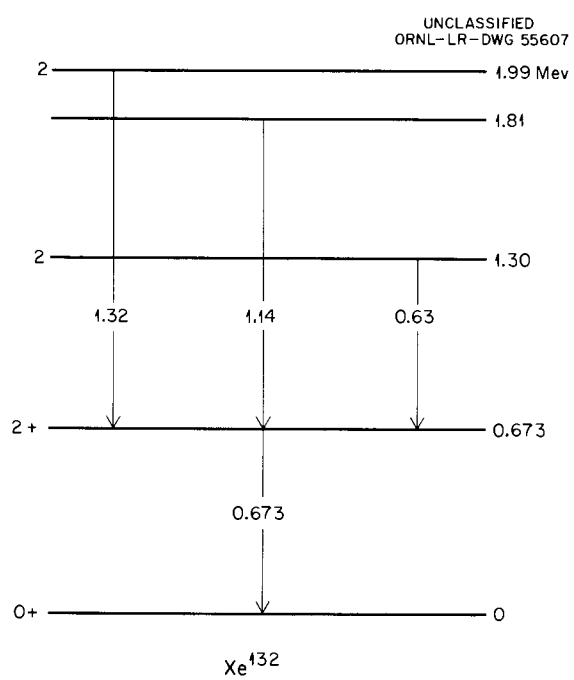

Fig. 1. Simplified Energy-Level Diagram of Xe^{132}.

[1] Chemistry Division.

[2] M. E. Rose, *Phys. Rev.* 91, 610 (1953).

A comparison of the experimental coefficients of the 0.63-0.673-Mev gamma-ray cascade with the theoretical correlation coefficients obtained for spin $I \leqq 4$ of the 1.30-Mev level establishes the spin of this level as 2. As can be seen in Fig. 2, the value of δ, where $\delta = (Q/D)^{1/2}$ in the notation of Biedenharn and Rose,[3] is -5.7. The predominantly quadrupole character of the transition between the second and first spin-2 levels is consistent with the collective behavior exhibited by even-even nuclei in this region.

The angular correlation of the 1.14-0.673-Mev cascade is compatible with a spin assignment of 1, 2, 3, or 4 for the 1.81-Mev level. The coefficients for the 1.32-0.673-Mev cascade are in best agreement with the theoretical coefficients for the spin sequence $2(D + Q)2(Q)0$ with $\delta = +0.089$ (see Fig. 2). This small value obtained for the mixing ratio suggests that the 1.99-Mev level may be due to excitation of the intrinsic structure of the nucleus.

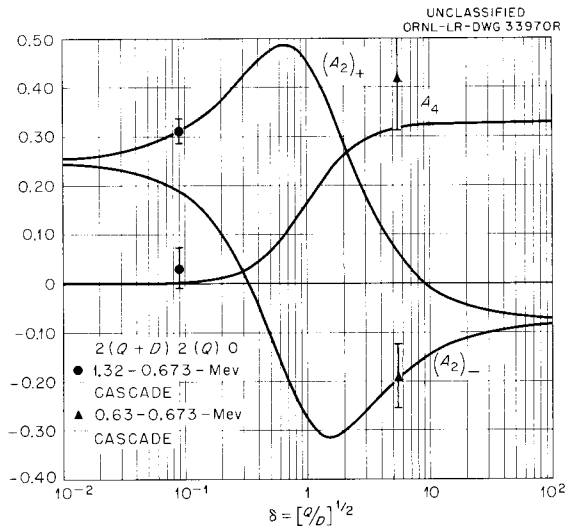

Fig. 2. Angular Correlation Coefficients as a Function of Dipole-Quadrupole Mixing for the Sequence $2(D + Q)2(Q)0$.

From our study of I^{132} (ref 4), which also decays to Xe^{132}, levels with energies similar to all of those given in Fig. 1 were observed. However, the level populated by I^{132} at 1.97 Mev was assigned spin 3. This was based on an angular correlation measurement and on the log *ft* value of the beta-ray group terminating at this level. The present correlation obtained for the 1.32-0.673-Mev cascade does not favor a spin-3 assignment for the 1.99-Mev level. It thus appears that there are two levels at approximately 1.98 Mev in Xe^{132}.

[3] L. C. Biedenharn and M. E. Rose, *Revs. Modern Phys.* **25**, 729 (1953).

[4] R. L. Robinson, E. Eichler, and N. R. Johnson (to be published in the *Physical Review*).

DECAY OF I^{132}[1]

R. L. Robinson E. Eichler[2] N. R. Johnson[2]

The decay of I^{132} has been investigated by means of scintillation spectrometers. Energies (and relative intensities) of the gamma rays which were observed are 0.240 (1.3), 0.518 (15), 0.667 (100), 0.72 (5), 0.775 (63), 0.953 (15), 1.14 (1.2), 1.142 (2.7), 1.30 (2.4), 1.392 (6.4), 1.45 (1.1), 1.75 (0.3),

[1] Abstract of paper submitted to the *Physical Review*.

[2] Chemistry Division.

1.91 (0.7), 1.99 (0.8), 2.08 (0.18), 2.18 (0.13), and 2.39 (0.11) Mev. Our data indicate that the gamma-ray peak at 0.667 Mev actually consists of four gamma rays with energies between 0.62 and 0.68 Mev. An energy-level diagram of Xe^{132} based on the present spectral studies and gamma-gamma angular correlation measurements has been proposed. Energies (and spins) of the levels are 0.673 (2^+), 1.32, 1.448 (4^+), 1.81, 1.966 (3), 2.10 (3, 4, or 5), 2.401 (4 or 5), 2.59 (3 or 5), and 2.84 (3, 4, or 5) Mev.

COULOMB EXCITATION OF LEVELS IN Se^{77}

R. L. Robinson F. K. McGowan P. H. Stelson

To study the properties of the low-lying levels in Se^{77}, it has been Coulomb-excited with alpha particles. Of particular interest is the Se^{77} level at 0.24 Mev. Previous investigations of the decays of As^{77} and Br^{77} (ref 1), which both populate levels in Se^{77}, and of Coulomb-excited levels in Se^{77} (ref 2) revealed inconsistencies in the spin assignment of this level and in the relative intensities of gamma rays de-exciting this level. One explanation which has been offered to account for the experimental results is that there are two levels at approximately 0.24 Mev.[1] The present study provides new evidence for such a doublet.

Doubly ionized helium ions of variable energy were obtained from the ORNL 5.5-Mv Van de Graaff generator. A thick selenium target, which was isotopically enriched in Se^{77} to 74.22%, was mounted at 45° with respect to the incident beam. In order not to melt the target it was necessary to keep the beam current below 0.02 μa. Gamma rays were detected by a 3×3 in. NaI crystal coupled to a Du Mont 6363 photomultiplier tube. The background was reduced by making the measurements in a lead shield with 4-in. wall thickness.

The gamma-ray spectra were measured for 14 different alpha-particle energies ranging from 2.1 to 8.0 Mev. For these investigations the angle between the incident beam and the gamma-ray detector was 235° and the target-to-detector distance was 5 or 10 cm. Figures 1 and 2 show the spectra obtained for alpha-particle energies of 4.034 and 8.018 Mev. Several of the peaks in the figures are not transitions of Se^{77}. The 74-kev gamma ray is believed to be the K x ray of lead; the 558-, 612-, and 662-kev gamma rays are transitions from the first excited states of Se^{76}, Se^{78}, and Se^{80}; the 859-kev gamma ray, which has also been observed with other targets, is not identified.

All spectra were decomposed as illustrated in Figs. 1 and 2, and the gamma-ray yields were determined. The variations of the gamma-ray yields with alpha-particle energy were compared with those expected for Coulomb excitation. Levels at 242, 440, and 515 kev were found to be directly excited by the electric quadrupole Coulomb excitation process. The ratio of the intensities of the

---

[1] *Nuclear Data Sheets*, National Academy of Sciences – National Research Council, Washington, D.C.
[2] G. M. Temmer and N. P. Heydenburg, *Phys. Rev.* 104, 967 (1956).

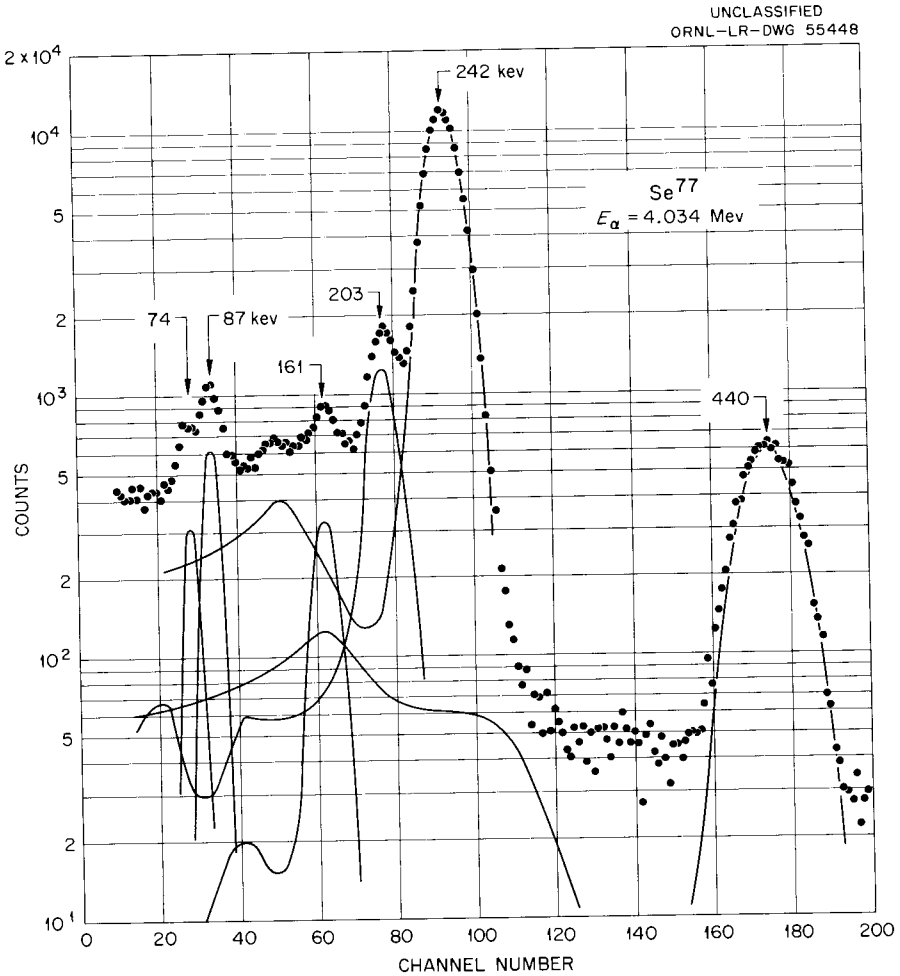

Fig. 1. Gamma-Ray Spectrum for 4.034-Mev Alpha Particles on Se^{77}.

203-kev gamma ray and the 440-kev gamma ray was found to be constant within the errors of experimental measurement for all energies of the alpha particles. This suggests that the 203-kev gamma ray originates at the 440-kev level. Similarly, the variation of the gamma-ray yield of the 87-kev transition indicates that it results from the de-excitation of the 242-kev level.

Spectra were also investigated for 11 alpha-particle energies with the beam turned off. The known 17.5-sec isomeric transition from the 161-kev level was observed. By repeating a cycle where the target was bombarded for 30 sec and then gamma rays were recorded for 30 sec, we were able to determine the yield of this gamma ray. The excitation curve of this transition was found to have the same shape as that obtained for direct excitation of a level at 242 kev.

The spectra in coincidence with the 242- and 203-kev gamma rays were investigated for $E_\alpha = 8.0$ Mev. These spectra are given in Fig. 3. A new gamma ray was observed at 283 kev in coincidence with gamma rays in the 242-kev peak. The 203-kev gamma ray was found to be in coincidence with a 242-kev gamma ray but, surprisingly, not in coincidence with the 87-kev

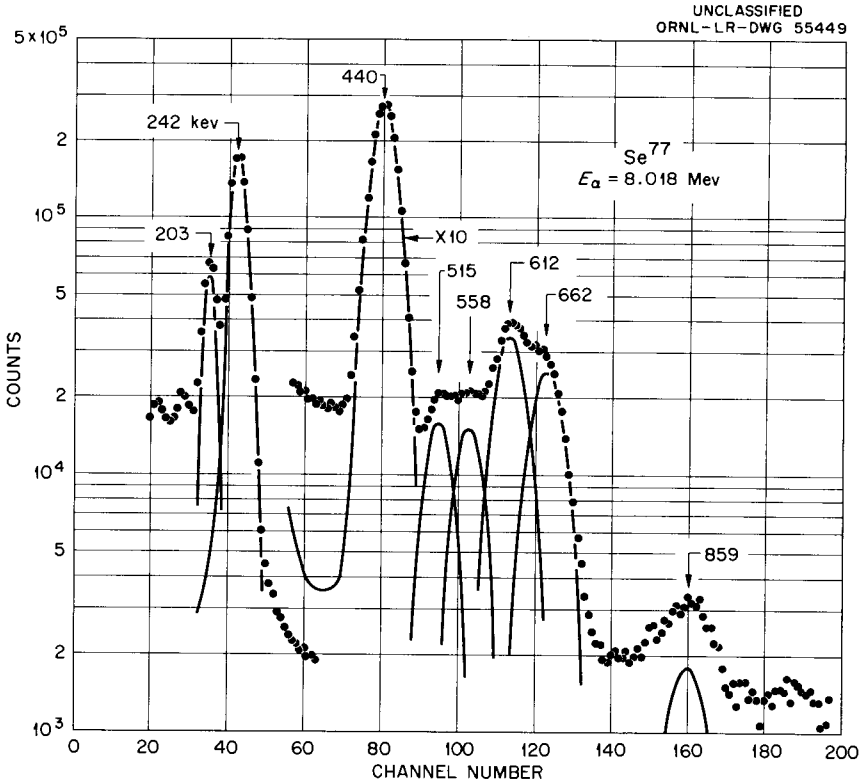

Fig. 2. Gamma-Ray Spectrum for 8.018-Mev Alpha Particles on Se^{77}.

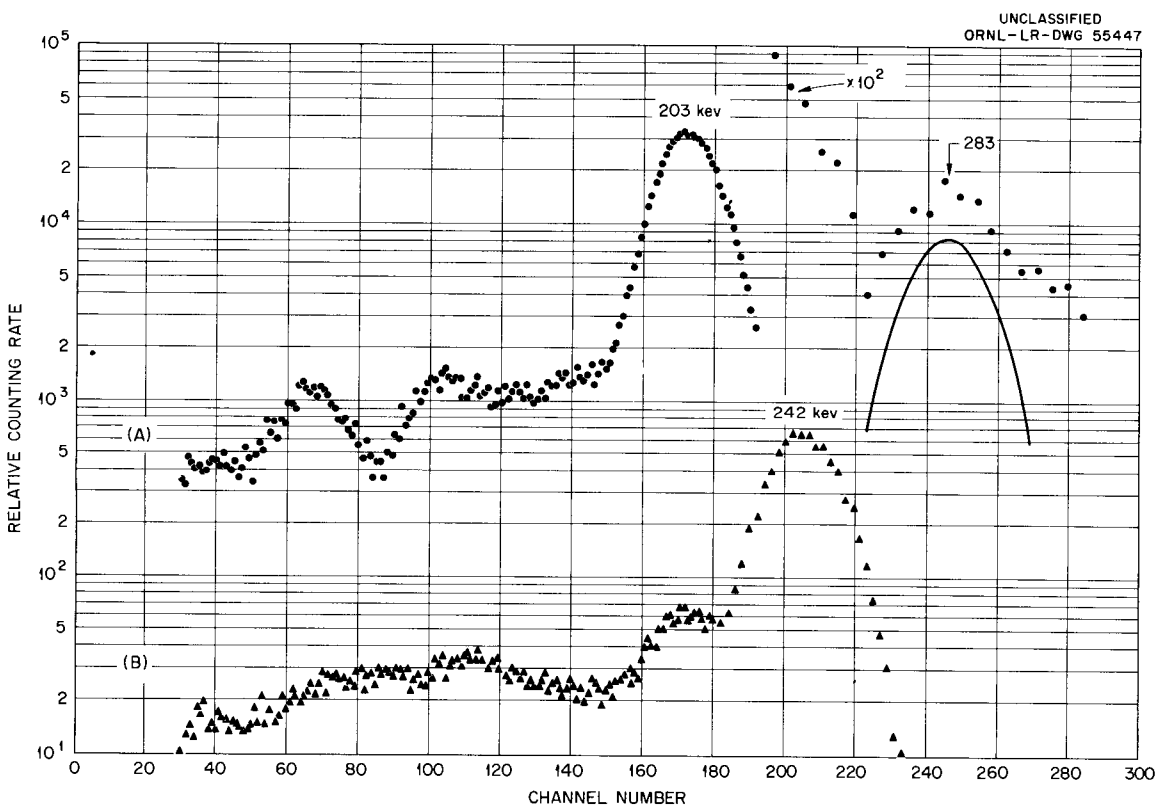

Fig. 3. Se^{77} Gamma-Ray Spectra in Coincidence with the (*A*) 242- and (*B*) 203-kev Gamma Rays for E_α = 8.0 Mev.

gamma ray. Since the gamma-ray yield of the 87-kev transition indicates it de-excites a level at 242 kev, this coincidence result requires that there be two levels at approximately this energy.

An energy-level diagram which includes only the transitions observed in the present study is shown in Fig. 4. The relative intensities are those found for $E_\alpha = 8.0$ Mev. The ground-state transitions from the level doublet at 242 kev could not be resolved. Instead, the energies of these two levels were deduced from the following gamma-ray energies: (440 ± 4) − (203 ± 4) = 237 ± 6 kev and (161 ± 3) + (87 ± 4) = 248 ± 5 kev. A careful energy determination was made of the peak of the transitions from this doublet for three alpha-particle energies. If the 248-kev level were more strongly excited, then this energy would be expected to vary with E_α. Energies obtained for the peak are 240.3 ± 2.5, 244.0 ± 3.4, and 242.5 ± 3.0 kev for E_α of 3.0, 5.0, and 7.0 Mev, respectively. The similarity of these energies suggests that either the energies of the two levels do not differ by 11 kev, as shown in Fig. 4, or that the 237-kev level is the more strongly excited. Spins and parities given in Fig. 4 for the ground state and the 161-kev state have been previously established.[3,4] Since the higher-energy states are excited by an electric quadrupole Coulomb excitation process, they can have only assignments of $\frac{3}{2}^-$ or $\frac{5}{2}^-$.

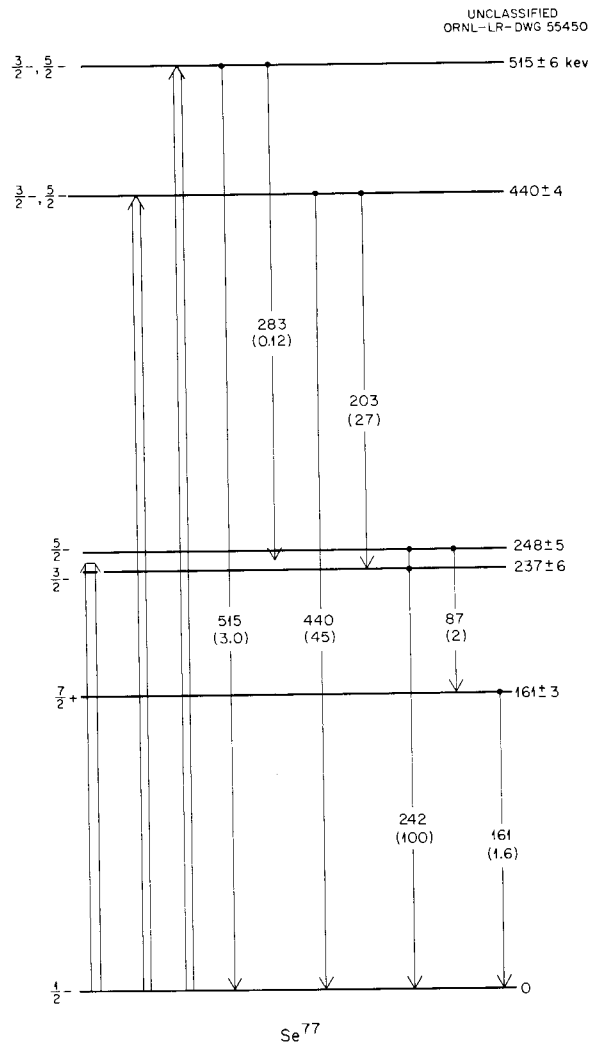

Fig. 4. Energy-Level Diagram of Se^{77}. The pair of numbers associated with each transition gives its energy in kev and relative intensity for $E_\alpha = 8.0$ Mev.

Angular distributions of the intense gamma rays were measured with respect to the incident beam for several alpha-particle energies. Data were taken at ten different angles and least-squares-fitted to the function $W(\theta) = 1 + a_2 A_2 P_2 (\cos\theta) + a_4 A_4 P_4 (\cos\theta)$, where a_2 and a_4 are the particle parameters. The experimental values of A_2 obtained for the distribution of the 203-, 242-, and 440-kev transitions are −0.145 ± 0.040, −0.095 ± 0.030, and +0.266 ± 0.025, respectively. The value given for the 242-kev gamma rays is that obtained for $E_\alpha = 3.0$ Mev. At higher energies, the population of a 242-kev level by the 203-kev gamma ray will change the angular distribution. Because the values for a_4 are always small,

[3] S. P. Davis and F. A. Jenkins, *Phys. Rev.* 83, 1269 (1951).

[4] M. Goldhaber and A. W. Sunyar, *Phys. Rev.* 83, 906 (1951).

the A_4 coefficients were very poorly determined and consequently do not provide any useful information. The A_2 coefficient for the 242-kev transitions establishes that at least one of the two levels at 242 kev must have spin $\frac{3}{2}$. If the other level has a spin of $\frac{5}{2}$, the coeffcient can be obtained only if the excitation of the spin $\frac{5}{2}$ level is not more than 55% of the total excitation of the two levels. The coefficients for the distributions of the 203- and 440-kev gamma rays are consistent with a spin assignment of $\frac{3}{2}$ or $\frac{5}{2}$ for the 440-kev level.

The intensity of the 87-kev transition relative to the intensity of the 242-kev transitions indicates its character is probably $E1$ rather than $M2$. Thus, the 248-kev level is assigned spin and parity of $\frac{5}{2}^-$. From the angular distribution results, the 237-kev level is then assigned spin $\frac{3}{2}$.

From the gamma-ray yields, the excitations per microcoulomb were determined for each alpha-particle energy. These are given in Table 1. They include corrections for the isotopic abundance of the target and for internal conversion of the transitions. Also included in the table are values of the thick-target integral Y and values of the reduced electric quadrupole transition probability $B(E2)$ for excitation. The procedure for determination of these quantities has been discussed in a previous paper.[5] The increase of the $B(E2)$ values for excitation of the 515-kev level for large E_α are believed to result from production of Br^{80} through an (α,p) reaction on Se^{77}. However, the contribution of this reaction is small for $E_\alpha \leqq 7.0$ Mev. The average $B(E2)$ values for excitation of the 242- (doublet), 440-, and 515-kev levels are (1.89 ± 0.16), (2.59 ± 0.17), and $(0.104 \pm 0.016) \times 10^{-49} e^2$ cm^4, respectively. These are 19, 26, and 1 times the single-particle estimates for excitation. For the single-particle transition probability, we have taken $B(E2)_{sp} = (5/4\pi)\,|\,\frac{3}{5}R_0^2\,|^2$ with $R_0 = 1.2 \times 10^{-13} A^{1/3}$ cm. It is interesting to note that the sum of these $B(E2)$ values is very similar to the average $B(E2)$ value obtained for the excitation of the first 2^+ levels in Se^{76} and Se^{78} (ref 6). This suggests that all strong quadrupole transitions have been detected in Se^{77}.

[5] F. K. McGowan and P. H. Stelson, *Phys. Rev.* 109, 901 (1958).

[6] P. H. Stelson and F. K. McGowan, *Phys. Div. Ann. Progr. Rept. Feb. 10, 1960*, ORNL-2910, p 12.

Table 1. Information on Variation of Gamma-Ray Yields from Coulomb Excitation

Level (kev)	E_α (Mev)	Excitations per Microcoulomb	Y, Thick-Target Integral (kev × mg/cm^2)	$\frac{B(E2)}{e^2}$ (cm^4)
				$\times 10^{-49}$
242	2.114	$(1.37 \pm 0.14) \times 10^3$	2.06×10	2.14 ± 0.29
	2.420	$(4.71 \pm 0.38) \times 10^3$	9.31×10	1.62 ± 0.23
	2.735	$(1.38 \pm 0.11) \times 10^4$	2.62×10^2	1.69 ± 0.20
	3.025	$(3.40 \pm 0.27) \times 10^4$	5.78×10^2	1.89 ± 0.20
	3.528	$(1.01 \pm 0.07) \times 10^5$	1.63×10^3	1.99 ± 0.19
	4.034	$(2.26 \pm 0.17) \times 10^5$	3.53×10^3	2.06 ± 0.20
	4.539	$(3.88 \pm 0.29) \times 10^5$	6.41×10^3	1.94 ± 0.18
	5.042	$(5.90 \pm 0.54) \times 10^5$	1.04×10^4	1.82 ± 0.19
	5.537	$(9.00 \pm 0.86) \times 10^5$	1.54×10^4	1.88 ± 0.21
	6.034	$(1.28 \pm 0.13) \times 10^6$	2.16×10^4	1.90 ± 0.22

Table 1 (continued)

Level (kev)	E_α (Mev)	Excitations per Microcoulomb	Y, Thick-Target Integral (kev × mg/cm^2)	$\frac{B(E2)}{e^2}$ (cm^4)
	6.528	$(1.70 \pm 0.16) \times 10^6$	2.90×10^4	1.88 ± 0.20
	7.055	$(2.24 \pm 0.20) \times 10^6$	3.82×10^4	1.88 ± 0.20
	7.532	$(2.84 \pm 0.25) \times 10^6$	4.77×10^4	1.91 ± 0.20
	8.018	$(3.52 \pm 0.29) \times 10^6$	5.86×10^4	1.93 ± 0.18
440	3.025	$(2.30 \pm 0.35) \times 10^3$	2.81×10	2.63 ± 0.41
	3.528	$(1.38 \pm 0.11) \times 10^4$	1.65×10^2	2.68 ± 0.28
	4.034	$(4.69 \pm 0.35) \times 10^4$	5.86×10^2	2.57 ± 0.24
	4.539	$(1.25 \pm 0.08) \times 10^5$	1.51×10^3	2.66 ± 0.23
	5.042	$(2.48 \pm 0.19) \times 10^5$	3.17×10^3	2.51 ± 0.24
	5.537	$(4.55 \pm 0.33) \times 10^5$	5.69×10^3	2.57 ± 0.24
	6.034	$(7.41 \pm 0.58) \times 10^5$	9.01×10^3	2.64 ± 0.25
	6.528	$(1.13 \pm 0.09) \times 10^6$	1.40×10^4	2.59 ± 0.24
	7.055	$(1.61 \pm 0.11) \times 10^6$	2.04×10^4	2.53 ± 0.22
	7.532	$(2.19 \pm 0.13) \times 10^6$	2.74×10^4	2.57 ± 0.20
	8.018	$(2.89 \pm 0.15) \times 10^6$	3.59×10^4	2.59 ± 0.19
515	5.041	$(5.9 \pm 2.2) \times 10^3$	1.92×10^3	0.10 ± 0.04
	5.537	$(1.25 \pm 0.32) \times 10^4$	3.74×10^3	0.11 ± 0.03
	6.034	$(1.99 \pm 0.55) \times 10^4$	6.48×10^3	0.10 ± 0.03
	6.528	$(3.14 \pm 0.90) \times 10^4$	1.02×10^4	0.10 ± 0.03
	7.055	$(5.9 \pm 1.4) \times 10^4$	1.58×10^4	0.12 ± 0.03
	7.532	$(8.0 \pm 1.8) \times 10^4$	2.16×10^4	0.12 ± 0.03
	8.018	$(13.3 \pm 2.4) \times 10^4$	2.91×10^4	0.15 ± 0.03

MÖSSBAUER EFFECT WITH Ni^{61}[1]

F. E. Obenshain H. H. F. Wegener[2]

The Mössbauer effect is observed in Ni^{61}. The Ni^{61*} was obtained by

$$Ni^{64}(p,\alpha)Co^{61} \xrightarrow{\beta^-(99\ \mathrm{min})} Ni^{61*}$$

giving a nickel Mössbauer nucleus in an Ni^{64} host lattice. The magnitude of the effect at $T = 80°K$ is about 4% for a 400-mg/cm^2 absorber foil (natural nickel). From the thickness dependence we obtain $f_{source} = f_{abs} = (9 \pm 1)\%$ for the Debye-Waller factor at $T = 80°K$. The temperature dependence yields a Debye temperature varying between 413 and 437°. The velocity dependence has a half-width of 1.65 mm/sec. The spectrum deviates from the Lorentz shape expected for a single

[1]Abstract of paper to be published in the *Physical Review*.

[2]On leave from University of Erlangen, Germany.

line. A recent electronic determination of the lifetime of this 71-kev state indicates a natural half-width of 0.37 mm/sec. The increased half-width and the shape of the spectrum observed in our experiment may be understood in terms of a magnetic hyperfine splitting. The moment of the ground state is known. The internal field H and the magnetic moment μ_e of the first excited state are unknown. An analysis of the data gives a connection between the two quantities, $\mu_e(H)$.

MÖSSBAUER EFFECT FOR Ni^{61} WITH APPLIED MAGNETIC FIELDS[1]

H. H. F. Wegener[2] F. E. Obenshain

The Mössbauer effect with Ni^{61} is observed in the presence of applied magnetic fields. The Ni^{61} nuclei, for both source and absorber, occupy normal lattice sites in the nickel crystal lattice. The application of external fields serves to polarize the internal fields, which are responsible for the hyperfine structure splitting in the source and absorber. Consequently, the nuclei involved in the Mössbauer emission and absorption act respectively as polarizer and analyzer of the individual gamma transitions. A measurement of the Mössbauer spectrum M(v) with applied magnetic fields yields certain information relating to the nuclear magnetic moments μ_e and μ_g and the internal magnetic field H. From this experiment we obtain the ratio $\mu_e/\mu_g = -0.47 \pm 0.08$, the product $(\mu_g \cdot H) = 26.0 \pm 2.6$ Mc/sec $\cdot j_g \cdot h$, and the sign of H with respect to the magnetization j. The directions of H and j are opposite, just as they are in the case of Fe^{57}. A general expression for M(v) is specialized, in the case of Ni^{61}, for several geometries which are particularly suitable for experimental investigation.

---

[1]Abstract of paper to be submitted to the *Zeitschrift für Physik.*

[2]On leave from University of Erlangen, Germany.

A STUDY BY THE MÖSSBAUER METHOD OF THE HFS SPLITTING OF Au^{197} ALLOYED IN Fe, Co, AND Ni

L. D. Roberts J. O. Thomson[1]

Previous investigations by Nagle *et al.*[2] have shown that a nuclear resonance fluorescence effect occurs in Au^{197}. Studies by Samoilov *et al.*[3] have shown that when gold is alloyed in iron, fields of the order of 10^6 gauss are found at the nucleus. Alloys of gold with ferromagnetic metals

---

[1]Consultant and research participant from University of Tennessee, Knoxville.

[2]D. Nagle *et al.*, *Phys. Rev. Letters* 4(5), 237 (1960).

[3]B. N. Samoilov, V. V. Sklyarevsky, and E. P. Stepanov, *International Conference on Low Temperature Physics, Toronto, September 1960*, p 415.

thus seem particularly suitable for studies by the Mössbauer method. For this purpose we built a simple compact electromechanical transducer capable of velocities in the range 0 to about 40 cm/sec over the temperature range from 4 to perhaps 400°K. In preliminary tests of this apparatus we reinvestigated the Mössbauer spectrum for Fe_2O_3, using an Fe^{57m} source. Our results are in good agreement with those of Kistner and Sunyar.[4] Also, using a Pt^{197} source we studied the nuclear resonant absorption of the 77-kev level in metallic Au^{197}. Our results gave a line width equivalent to a lifetime of 2 ± 0.2 mμsec, in agreement with a nuclear lifetime measurement by Sunyar[5] of 1.9 ± 0.2 mμsec, but in disagreement with the results of Nagle *et al.*,[2] who found a substantially broader Mössbauer line. This difference between the latter results and our own would seem to arise from the method of taking data.

Au^{197} has a $\frac{3}{2}^+$ ground state and a $\frac{1}{2}^+$ first excited state at 77 kev. Although gold is normally nonmagnetic, when it is alloyed with iron it partakes of the ferromagnetism of the latter through a magnetic polarization process. This polarization produces an hfs splitting of the above ground and excited states of gold. We have prepared 1 at. % alloys of Au in Fe, Co, and Ni. These alloys were cut to thicknesses of 200 mg/cm^2 of gold and were approximately $\frac{1}{4}$ in. thick. The gamma-ray source was Pt^{197} metal, prepared from enriched Pt^{196}, and each of the above alloys was used in turn as an absorber. In the transducer, the source was stationary and the absorber was set in motion. All the measurements were made at 4.2°K. A single-channel analyzer was used to isolate the 77-kev gamma ray, but this isolation was not perfect. Depending on the age of the source, there were x-ray and Compton scattering processes which reduced the size of the effect from that which would have been observed from a pure gamma ray. This reduction was quite roughly of the order of a factor of 2. The results of these studies are shown in Figs. 1, 2, and 3. Several observations may be made about these measurements.

Magnetic Field at the Nucleus

The ground state of gold is known to have quite a small magnetic moment (+0.14 nm). The moment of the 77-kev excited state has not been measured, however. On the basis of the shell model, it is expected to be an $s_{1/2}$ state with a large moment. Thallium-203 has two protons more than Au^{197}, and its ground state is $s_{1/2}$. Its measured magnetic moment is +1.5960. We make a preliminary assumption that the 77-kev excited state in gold has this value for the magnetic moment also. On this basis, one would expect the Mössbauer spectrum of gold in a strong magnetic field to consist of two lines, each being an unresolved triplet. In the case of the iron and of the cobalt alloys this is observed, but in the case of nickel a single line only is found. The observed splittings are given in terms of cm/sec of Doppler motion in the figures. For the iron alloy, these results correspond to $|\mu_n H_0| = 4.5 \times 10^5$; for cobalt, $|\mu_n H_0| = 3.5 \times 10^5$; and for nickel, $\mu_n H_0 \sim 0$. Making the above assumption about the magnetic moment of the excited state in gold, one may

---

[4] O. C. Kistner and A. W. Sunyar, *Phys. Rev. Letters* 4(8), 412 (1960).

[5] A. W. Sunyar, *Phys. Rev.* 98, 653 (1955).

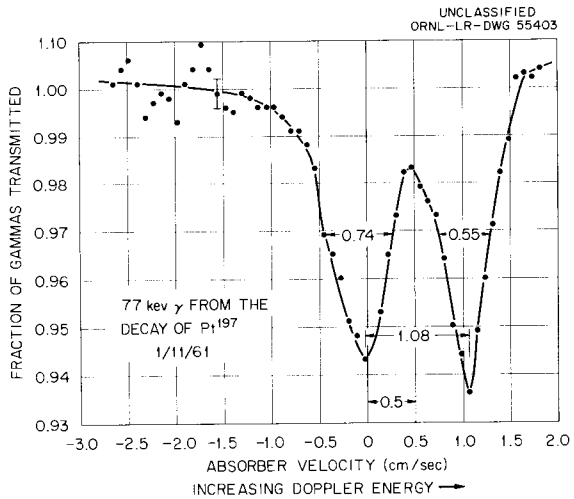

Fig. 1. Fraction of Gammas Transmitted as a Function of Absorber Velocity for 1 at. % Au^{197} in Fe.

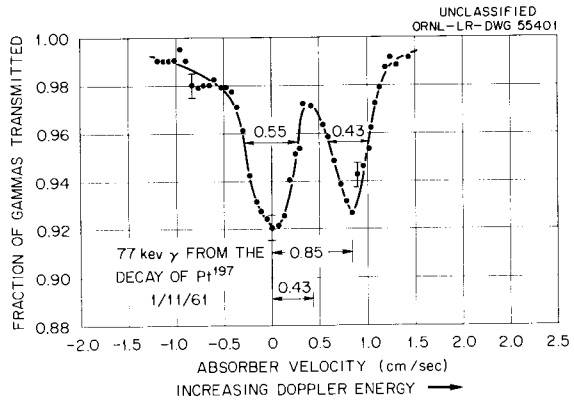

Fig. 2. Fraction of Gammas Transmitted as a Function of Absorber Velocity for 1 at. % Au^{197} in Co.

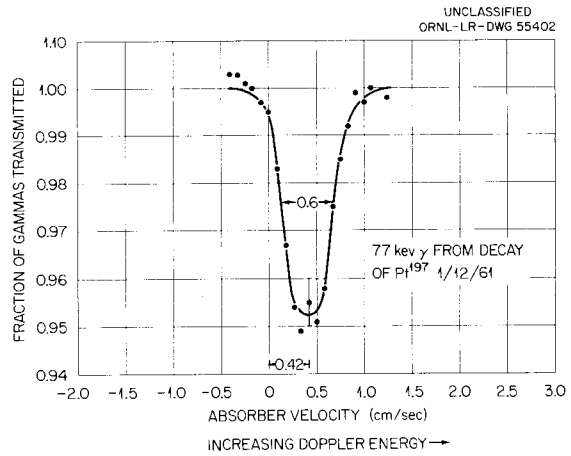

Fig. 3. Fraction of Gammas Transmitted as a Function of Absorber Velocity for 1 at. % Au^{197} in Ni.

calculate the effective magnetic fields at the nucleus as 280,000 gauss, 220,000 gauss, and unmeasurably small, respectively, for the three alloys. In a recent paper by Boyle *et al.*[6] on the polarization of the conduction electrons in ferromagnetic metals, a study quite similar to the above was made, using tin instead of gold. They found that in fact their results could be qualitatively understood in terms of current theory for the cases of iron and cobalt but not in the case of nickel. This is also true for our results where the magnetic field at the gold nucleus in the nickel alloy is approximately zero.

Chemical Shift

It will be noted on each of the three graphs that the spectra do not center around zero velocity but are displaced about 0.5 cm/sec to positive Doppler energy. This means that the gamma ray as it leaves the platinum metal source is of insufficient energy to resonate with the gold dissolved in the ferromagnetic materials. This chemical shift is the largest that has been so far observed. It arises in part from a nuclear volume change between the ground and excited states of gold and in part from the difference of $\psi^2(0)$ between source and absorber. The fact that gold is an odd-proton nucleus, the only one to be studied by the Mössbauer method so far, may be related to this large shift.

---

[6] A. J. F. Boyle, D. St. P. Bumbury, and C. Edwards, *Phys. Rev. Letters* 5(12), 553 (1960).

Line Widths

The natural line width for Mössbauer absorption in gold corresponds to a line width at half height of somewhat less than 0.3 cm/sec, and, as indicated above, this was observed in the experiment with the Pt^{197} metal source and Au^{197} metal absorber. In the case of the alloys, the line width is invariably greater than this, and, in the cases of iron and cobalt alloys, the two lines are observed to be of unequal width. This disparity of line width could be due to a distribution of chemical shifts and corresponding H_{eff} shifts for different gold-atom sites. The fact that the chemical shift is almost the same for the three alloys, which have such different magnetic effects, suggests that this may not be the explanation. An alternative, possibly more reasonable, explanation is that there are quadrupole splitting effects in the $\frac{3}{2}^+$ ground state of Au^{197} in the alloys. If this is the case, the experiments correspond to a substantial distortion of the gold atomic *p* or *d* electron shells. Assuming the magnetic moment of the gold excited state to be positive, our result requires that this distortion of the gold atom be of "cigar" shape.

MAGNETIC STRUCTURE PROPERTIES OF RARE-EARTH METALS[1]

W. C. Koehler E. O. Wollan M. K. Wilkinson J. W. Cable

Progress made through neutron diffraction techniques toward the solution of the magnetic structures of the heavier rare-earth metals is summarized.

[1]Abstract of paper presented at Rare Earth Seminar (proceedings to be published by McGraw-Hill, New York, April 1961).

NEUTRON DIFFRACTION INVESTIGATION OF MAGNETIC ORDERING IN DYSPROSIUM[1]

M. K. Wilkinson W. C. Koehler E. O. Wollan J. W. Cable

Neutron diffraction measurements on a single crystal of dysprosium show that the magnetic structure in the antiferromagnetic region between 179 and 87°K closely resembles a helical-type arrangement of the atomic moments. In this arrangement the moments within a hexagonal layer are aligned parallel and point in a direction perpendicular to the *c* axis of the crystal. The moment direction in adjacent layers is rotated by a specific angle which is dependent on the temperature of the sample. A slight modification of this structure exists below about 140°K, and a transition to ferromagnetism occurs at 87°K.

[1]Abstract of paper to be published in the *Journal of Applied Physics* (suppl).

NEUTRON DIFFRACTION STUDY OF METALLIC ERBIUM[1]

J. W. Cable E. O. Wollan W. C. Koehler M. K. Wilkinson

Neutron diffraction measurements were made on erbium single crystals in the temperature range 298 to 4.2°K. The material is antiferromagnetic below 80°K and ferromagnetic below 20°K. In the antiferromagnetic region, the magnetic scattering consists of satellite reflections corresponding to a modulation of the magnetic scattering amplitude along the c axis. The spacing and intensity distribution of these satellites show two distinct subregions of antiferromagnetism. In the upper region, between 80 and 52°K, the data suggest a sinusoidal modulation of the magnitude of the c-axis component of magnetic moment with a period of $3.5c_o$. Between 52 and 20°K the wavelength of the modulation varies continuously from $3.5c_o$ to $4.0c_o$. In addition, there is a squaring up of the modulation and a simultaneous ordering of the component of the moment normal to the c axis. Below 20°K the material is basically ferromagnetic, with a moment of $7.2\mu_B$ directed parallel to the c axis.

[1]Abstract of paper to be published in the *Journal of Applied Physics* (suppl).

MAGNETIC ORDERING IN RARE-EARTH INTERMETALLIC COMPOUNDS

H. R. Child M. K. Wilkinson J. W. Cable E. O. Wollan W. C. Koehler

Although a large amount of data has been obtained in recent years on rare-earth compounds, the magnetic properties of these systems are not well understood. In most of these compounds the interpretation of the experimental results has been complicated by crystal distortions or by the presence of other magnetic ions. Therefore, it was of interest to investigate the existence of magnetic ordering at low temperatures in some rare-earth intermetallic compounds[1] with the simple NaCl-type structure. The first investigations[2] were made on HoN and TbN, and later experiments have included other nitrides, antimonides, phosphides, and arsenides. The results of these investigations are summarized in Table 1.

All the nitrides except TmN were found to experience ferromagnetic ordering at low temperatures, and the Curie temperatures are given in the table. Although the paramagnetic scattering from each compound was in good agreement with that calculated for the paramagnetic moment of the free trivalent ion, the ferromagnetic moments were smaller than the maximum ordered moments associated with these ions. These results indicate that the moment values at low temperatures are affected by crystalline field interactions, and calculations by Trammell[3] of the energy levels which

[1]We are very much indebted to D. E. LaValle, Analytical Chemistry Division, for preparing the samples used in this investigation.

[2]M. K. Wilkinson *et al.*, *J. Appl. Phys.* (suppl) 31, 358S (1960).

[3]G. T. Trammell, *J. Appl. Phys.* (suppl) 31, 359S (1960).

Table 1. Summary of Neutron Diffraction Results of Rare-Earth Intermetallic Compounds

Compound	a_0 (A)	T_C (°K)	T_N (°K)	Paramagnetic Moment		Ordered Magnetic Moment		
				Calculated (μ_B/ion)	Observed (μ_B/ion)	Calculated (μ_B/ion)	Observed (μ_B/ion)	Magnetic Axis
TbN	4.93	42		9.7	9.7	9.0	6.7, 7.0	[111]
TbP	5.69		9	9.7		9.0	6.2	[111]
TbAs	5.82		12	9.7		9.0	7.7	[111]
TbSb	6.17		14	9.7	9.9	9.0	8.2	[111]
HoN	4.87	18		10.6	10.8	10.0	6.8, 8.9	[100]
HoSb	6.13		9	10.6		10.0	9.3	[100]
ErN	4.83	5		9.6	9.4	9.0	3.5, 6.0	
ErSb	6.11		3.7	9.6	9.8	9.0	7.0	⊥ to [111]
TmN				No observable magnetic order at 1.3°K				

result from these interactions are consistent with this interpretation. These calculations showed that crystal field effects could reduce the moment value in both HoN and TbN and that the magnetic moment in the ordered state of TmN would be zero. His calculations also predicted that the magnetic moments would be directed along the edges of the cubic unit cell in HoN and along the cube diagonal in TbN and that large energies would be required to move them from these specific directions. These predictions were verified experimentally by examining the effect of an external magnetic field on the ferromagnetic reflections from both compounds.

In the diffraction patterns obtained from all the rare-earth nitrides in the ferromagnetic state, there was a very pronounced small-angle scattering and a large increase in diffuse scattering in the angular regions of the ferromagnetic reflections. These effects are indicative of a short-range ferromagnetic correlation, and they existed at temperatures far below the magnetic transition temperatures. In fact, experiments on the small-angle scattering from HoN showed that it occurred at temperatures above the Curie point and increased with decreasing temperatures to 1.3°K, which was the lowest temperature obtained. Consequently, it does not have the characteristics associated with critical magnetic scattering, and the mechanism for producing it is not understood. Furthermore, this large variation in the diffuse scattering causes considerable uncertainty concerning the calculation of the ferromagnetic moment at low temperatures. The assumption that the long-range ferromagnetic order produces reflections with a resolution comparable to the nuclear reflections gives a specific moment value, but a larger value is obtained when the large background humps are included in the reflections. Both values are given in Table 1, and it is evident that the relative importance of this effect increases regularly from TbN to ErN.

The investigations of the other intermetallic compounds were initiated in an effort to clarify the peculiar ordering behavior observed in the nitrides. Although these compounds also have the

rock-salt structure, there is a large increase in the separation of rare-earth atoms with the larger anions, and the antimonides have lattice spacings which are about 25% larger than those of the corresponding nitrides. These other compounds also exhibit magnetic ordering at low temperatures, but all of them become antiferromagnetic with an MnO-type antiferromagnetic structure in which ferromagnetic sheets of moments exist along the cube diagonal and adjacent ferromagnetic planes are antiparallel. The values of the atomic moments in these structures are lower than the maximum expected for the trivalent ions and thereby indicate that crystal field interactions are also important in these materials. The moment values in the antiferromagnetic terbium compounds are consistent with this interpretation, since the values become larger as the lattice spacing is increased and the crystal field effects correspondingly decreased. Moreover, the orientation of the magnetic moments in the holmium and terbium compounds are identical to those predicted by the crystal field calculations. These calculations have not yet been performed for erbium compounds, but the experimental results indicate that the moment direction is perpendicular to the cube diagonal. This is a definite determination for ErSb, and the data on ErN are inconclusive with respect to moment direction. There were no observable short-range-order effects in the antiferromagnetic structures, which suggests that these effects in the nitrides are probably associated with their ferromagnetic behavior.

It is interesting to speculate on the magnetic coupling which exists in these rare-earth intermetallic compounds. If it is assumed that only nearest neighbor and next nearest neighbor interactions are important, then all the magnetic structures can be correlated by the same type of coupling scheme. According to this picture, there is a ferromagnetic interaction between nearest neighbors, an antiferromagnetic interaction between next nearest neighbors, and the nearest neighbor interaction decreases more rapidly as the distance between magnetic ions is increased by larger anions. Of course, such a situation would predict a critical value of the lattice spacing in which the nearest neighbor and next nearest neighbor interactions were equal, and any magnetic ordering would then be influenced by higher-order interaction terms. It is possible that this is exactly the situation that exists in HoP, which has a lattice spacing near the critical value. Preliminary results on this compound show that magnetic ordering exists below about 5.5°K, and the diffraction pattern contains both ferromagnetic and antiferromagnetic reflections. While the exact details of the structure have not been calculated, the effects of an external magnetic field indicate that the reflections do not come from separate ferromagnetic and antiferromagnetic clusters but are the result of a single ferrimagnetic structure.

NEUTRON DIFFRACTION BY HELICAL SPIN STRUCTURES[1]

W. C. Koehler

A summary is given of neutron diffraction techniques as applied to helical-type and related spin structures. Illustrations are drawn from results of recent investigations of metallic holmium and $MnAu_2$.

[1]Abstract of paper to be published in the *Journal of Applied Physics.*

NEUTRON DIFFRACTION INVESTIGATIONS OF METALLIC CERIUM AT LOW TEMPERATURES[1]

M. K. Wilkinson H. R. Child C. J. McHargue W. C. Koehler E. O. Wollan

Neutron diffraction experiments have been performed on metallic cerium at a series of temperatures between room temperature and 4.2°K in an attempt to clarify the anomalous behavior which has been observed in previous specific heat and magnetic susceptibility measurements. Results on three specially prepared samples show that the interesting magnetic behavior can be correlated with the three crystallographic phases present in the samples. There is a change in the electronic configuration of the cerium atoms when the collapsed face-centered-cubic phase is formed, and antiferromagnetic ordering occurs in the hexagonal-close-packed phase at about 12.5°K.

[1]Abstract of paper submitted to the *Physical Review.*

A NEUTRON DIFFRACTION INVESTIGATION OF THE MAGNETIC ORDER IN MnI_2[1]

J. W. Cable M. K. Wilkinson E. O. Wollan W. C. Koehler

Neutron diffraction measurements were made on polycrystalline and single-crystal samples of anhydrous MnI_2 at sample temperatures from 298 to 1.3°K. The results show an unusual type of antiferromagnetic order below the Néel temperature of 3.40°K for this hexagonal layer-type crystal. The indicated magnetic structure is a helical type in which the moments within (307) planes are aligned ferromagnetically but rotate by $2\pi/16$ in successive (307) planes. This structure is supported both by intensity measurements of the antiferromagnetic reflections and by the domain transformations effected with an applied magnetic field.

[1]Abstract of paper to be published in the *Physical Review.*

VIBRATIONAL SPECTRUM OF THE $NCSe^-$ ION[1]

H. W. Morgan

The infrared and Raman spectra of the selenocyanate ion have been observed and studied in solid KNCSe and in aqueous solution. The fundamental vibrational modes in the solid are assigned to the following frequencies: $\nu_{(CN)} = 2070\ cm^{-1}$, $\nu_{(CSe)} = 558\ cm^{-1}$, and $\nu_{(NCSe\ bend)} = 416, 424\ cm^{-1}$. The bending mode is split by the crystal field. Assuming a valence force field, the calculated potential constants are $K_{(CN)} = 15.1$, $K_{(CSe)} = 3.9$, and $K_{(bend)} = 0.25$, each times 10^5 dynes/cm.

[1]Abstract of paper to be published in the *Journal of Inorganic and Nuclear Chemistry.*

APPLICATIONS OF SOLID SOLUTION INFRARED SPECTRA: THE FREQUENCY CALIBRATION OF PRISM SPECTROMETERS AND THE MEASUREMENT OF SPECTRAL SLIT WIDTH

P. A. Staats H. W. Morgan

The comparison of frequency and intensity data recorded by commercial infrared spectrometers has been made difficult not only by the different types of instruments now in use, but by the variations among identical models operated under equivalent settings of the various parameters. There is a definite need for a simple and reliable standard by which frequency or spectral slit width, or preferably both, may be calibrated at regular intervals. The dependence of these characteristics upon minor adjustments to the optical systems indicates that such calibrations should be made frequently. At present, frequency calibration and the estimation of effective slit width are time-consuming operations requiring a series of gas samples, each at a particular pressure. Ideally, a solid is required, easily obtained and stable indefinitely, which exhibits a series of absorption bands throughout the infrared region. These bands should be sufficiently symmetric and narrow in width so that band centers may be estimated to about $0.1\ cm^{-1}$, and the observed peak heights should be simply related to the spectral slit width of the instrument used. The characteristics of solid solution spectra, particularly the spectra of simple inorganic ions in alkali halide matrices, suggest that these spectra may provide such a standard.

Previous work on these spectra[1] showed that the intense absorptions of the cyanide and cyanate ions should be satisfactory and also indicated that only an impure single crystal would exhibit long-term chemical stability. Thus, in the search for other absorption frequencies, the samples and the alkali halides were heated to the melting point. Over 100 different inorganic salts were fused in this manner, yielding approximately 45 very sharp absorption bands and a roughly

[1]H. W. Morgan, *Stable Isotopes Div. Semiann. Progr. Rept. May 20, 1956*, ORNL-2114, pp 4–5.

equivalent number of broader bands. The bandwidths can be qualitatively explained by the following factors: the ratio of the ionic and lattice dimensions and the symmetries of the ion and the lattice site which it occupies. The process of fusion with an alkali halide has generated several new ionic species giving sharp absorption bands; however, due to the relatively few data on high-temperature chemistry, the identification of these species will form a separate study.

From the observed spectra, the 16 sharp bands listed in Table 1 have been chosen to provide calibration points spaced throughout the region 2200 to 700 cm^{-1}. This is the region normally studied with an NaCl prism. The frequencies shown are characteristic of ions in a KBr matrix. These bands are produced by the addition of six compounds, identified in Table 1, to the alkali halide melts. The amount required is in every case less than 1 mg of the compound per gram of alkali halide. Preliminary studies of these bands indicate that they will be satisfactory for the measurement of spectral slit width. Precise contours of these absorptions will be determined by R. N. Jones, NRC, Ottawa, Canada.

Table 1. KBr Solid Solution Spectra for Spectrometer Calibration

Frequency (cm^{-1})	Compound Added
2172	Cyanate
2032	Borate (B^{10})
1960	Borate (B^{11})
1695	CuO
1550	PbO
1418	CuO
1414	PbO
1382	Nitrate
1312	PbO
1180	Silicate
1149	Silicate
1080	Silicate
1036	PbO
957	CuO
857	PbO
727	PbO

APPLICATIONS OF SOLID SOLUTION INFRARED SPECTRA: THE DETERMINATION OF TRACE AMOUNTS OF POLYATOMIC INORGANIC IONS[1]

J. R. Lawson[2] R. L. Barnett, Jr.[2] H. W. Morgan

The infrared spectra of polyatomic inorganic ions in dilute solid solution in alkali halide crystals have been obtained by a method which employs the pressed-disk technique. The alkali halide and sample are mixed, heated in a platinum crucible until complete solution is attained, and then quenched to form a solid solution. The solid is ground and pressed to form a transparent disk and the infrared spectrum recorded in the usual manner.

The solid solution bands are, in most cases, narrower and show increases in peak absorption coefficients which allow quantitative determinations in the microgram range. The infrared spectra of the OCN^-, SO_4^{2-}, and CO_3^{2-} ions have been studied in some detail in solution in KBr, KCl, and NaCl. Comparisons have been made with spectra of the pure solute crystals, obtained by the usual technique of grinding with the alkali halides and pressing to form a disk. Beer's law plots have been made for several of the stronger absorption bands and the quantitative accuracy of the method determined.

[1]Abstract of paper to be published in *Analytical Chemistry*.

[2]Department of Physics, Fisk University, Nashville, Tennessee.

VAPOR-PHASE INFRARED ABSORPTION SPECTRA OF TiF_4, ZrF_4, AND HfF_4

M. Blander[1] H. W. Morgan

The study of one-component salt vapors constitutes a preliminary investigation of the infrared spectra of salt vapors at high temperatures. In future work, it is planned to investigate mixtures of salt vapors, with emphasis on the study of associated vapor species. The salts TiF_4, ZrF_4, and HfF_4 were chosen for this initial study because they are believed to form stable compounds with alkali fluorides in the vapor phase and because the spectra of these molecules, assumed to be tetrahedral in structure, are relatively simple and are expected to show absorptions at wavelengths less than 40 μ.

Infrared spectra were recorded with a Perkin-Elmer model 12 C spectrometer, using NaCl, KBr, and CsBr prisms to cover the region 3000 to 300 cm^{-1}. The spectrometer optics were modified to allow the use of a 42-in. heated absorption cell between the infrared source and the entrance slit of the monochromator. Radiation from the source was interrupted by a chopper before passing through the cell, in order to prevent radiation from the sample and cell from contributing to the background. The sample cell was constructed of mullite and Pyrex tubing and was heated at its center with a conventional tube furnace. Temperatures up to 1000°C were obtained at the center of the cell, which

[1]Reactor Chemistry Division.

was kept filled with dry helium and fitted with windows of CsBr or polyethylene. The salt under study was vaporized in the heated center section of the cell, and the vapor was examined as it diffused to the cooler ends where it condensed to a fine powder.

Numerous bands were observed for each sample; however, upon eliminating absorptions from impurities and from the condensed crystallites of the sample, only one absorption was observed for each of the three compounds. On the basis of "reasonable" force constants, these bands have been assigned to the asymmetric stretching fundamental, ν_3. Frequencies of the estimated band centers are: TiF_4, 794 $\pm$3 cm^{-1}; ZrF_4, 670 $\pm$3 cm^{-1}; HfF_4, 650 $\pm$3 cm^{-1}. Estimated frequencies for the bending mode, ν_4, lie in the range 150 to 250 cm^{-1}, and thus beyond the region reported in this study.

AN IMPROVED Li^6-LOADED GLASS SCINTILLATOR FOR NEUTRON DETECTION[1]

F. W. K. Firk[2] G. G. Slaughter R. J. Ginther[3]

A cerium-activated, Li^6-loaded glass scintillator of improved scintillation efficiency and Li^6 content has been developed and used for detecting neutrons with energies from 1 ev to 80 kev by time-of-flight techniques. The following properties of a glass scintillator were determined:

1. an efficiency of 25% for detecting neutrons of 1 kev energy,
2. a complete absence of background due to gamma rays of energy <1.3 Mev,
3. a resolution of 18% for the $Li^6(n,\alpha)T$ peak,
4. a pulse with rise time $\sim$5 nanosec and a decay time $\sim$100 nanosec into an impedance of 100 ohms, and
5. a time resolution $\lesssim$5 nanosec when using a "fast-slow" coincidence system.

These properties have been exploited in measuring the neutron energy spectrum from the reaction $Li^7(p,n)Be^7$, using the ORNL pulsed Van de Graaff and the associated nanosecond time-of-flight spectrometer. For a proton energy 15 kev above the reaction threshold, the neutron energy spectrum extended from 5 to 80 kev. Total neutron cross section measurements up to several kev also demonstrate the use of the scintillator with a fast-chopper neutron spectrometer. Lithium- and boron-loaded glass scintillators have been compared, and it is concluded that lithium glass is, in general, more suitable for neutron detection.

---

[1]Abstract of paper to be submitted to *Nuclear Instruments & Methods.*

[2]Visiting ORNL from AERE, Harwell, England.

[3]Naval Research Laboratory, Washington, D.C.

DEVELOPMENT OF A POLARIZED-ION SOURCE

J. E. Sherwood S. J. Ovenshine R. F. King

Inasmuch as there is considerable interest at this time in nuclear reactions of polarized particles, we wish to announce that preliminary results have been obtained with our polarized-ion source. Our experiment is similar in principle to that of Brown *et al.*[1] Polarization of deuterons has been detected by observing anisotropy in the neutrons resulting from the $T(d, n)He^4$ reaction, as suggested by Galonsky *et al.* [2] of this laboratory.

Figure 1 shows the experimental arrangement. Deuterium gas is dissociated by means of a Wood discharge. A vertical slit in the wall of the discharge tube permits the gas to escape into a vacuum chamber where it is collimated to form a beam of atomic deuterium. Our measurements indicate that the beam is 70% dissociated (or less, depending on the condition of the discharge tube). The atomic beam is then sent through a strong inhomogeneous magnetic field which is divided into two sections. The fields are of a dipole or "two-wire" type familiar to molecular beamists. These magnetic fields split the beam into its Zeeman components. From the polarizer, one of the component beams enters the ionizer where a small fraction of the deuterium atoms is ionized by electron bombardment in a weak magnetic field. Figure 2 shows schematically the ionizer arrangement.

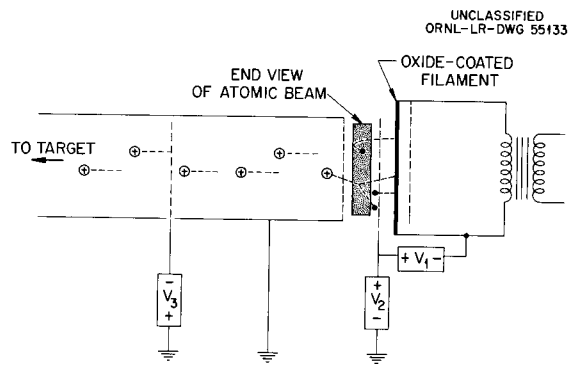

Fig. 1. Schematic Diagram of Ionizer.

The polarizer has been designed for use as a Rabi magnetic resonance machine which will provide a maximum of 83% polarization. However, it was convenient at this time simply to ionize one of the Zeeman components.

The atomic states as separated by the magnetic deflection, and the weak field states into which these convert adiabatically, are listed in Table 1, along with the deuteron spin states produced by ionization. The table also shows the calculated anisotropies resulting from the $T(d, n)He^4$ reaction, and the expected neutron polarization.

It should be noted that experiments in which deflection is obtained by means of quadrupole or sextupole magnets will ordinarily use the $m_j = \frac{1}{2}$ states since these states are focused toward the axis of symmetry. The maximum neutron polarization is somewhat greater for these states but is obtained at the angle of minimum neutron yield. For $m_j = -\frac{1}{2}$, maximum polarization is obtained at the angle of maximum neutron yield.

---

[1] L. Brown *et al.*, *Phys. Rev. Letters* 5(4), 154 (1960).

[2] A. Galonsky, H. B. Willard, and T. A. Welton, *Phys. Rev. Letters* 2(8), 349 (1959).

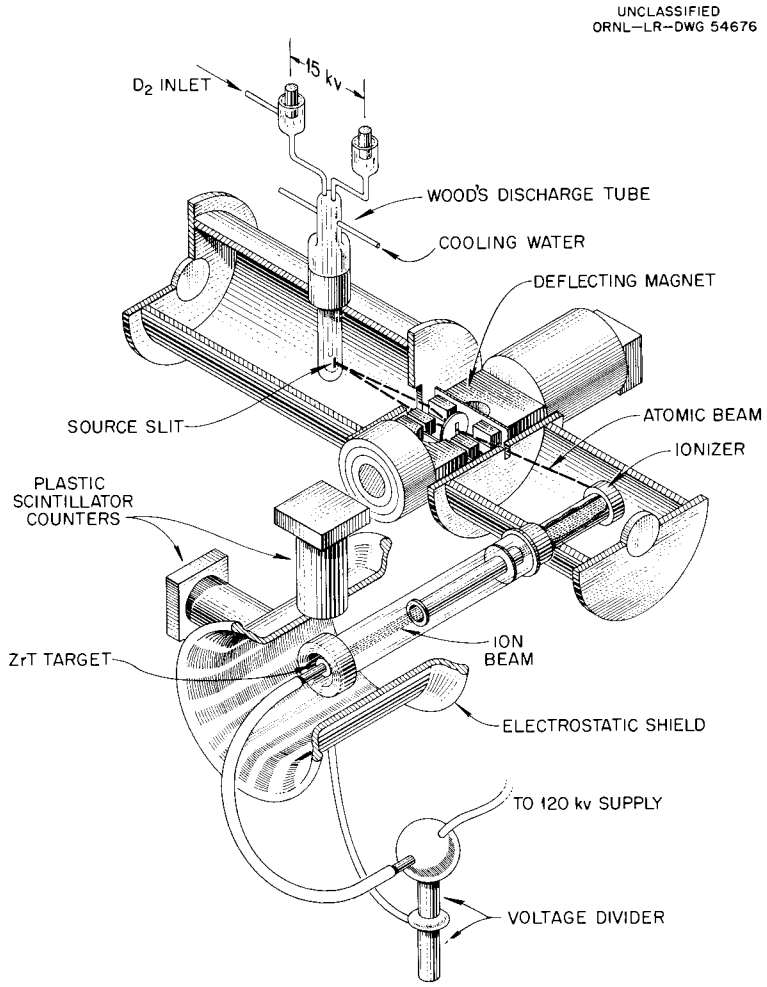

Fig. 2. Neutron Anisotropy Setup.

Either $m_j = \frac{1}{2}$ or $m_j = -\frac{1}{2}$ states may be selected when using the two-wire field.

This fact has been used to exhibit the polarization of the deuterons as follows: Collimation of the atomic beam was so arranged that both (diverging) Zeeman components were permitted to enter the ionizer. A mask, which contained a vertical slit $\frac{1}{2}$ mm wide, was then interposed between polarizer and ionizer. The ions were accelerated to 115 kev energy and allowed to strike a tritium target. Table 2 shows the net neutron counts and their ratio obtained in the direction of polarization (channel 1) and at right angles to it (channel 2) as the slit was traversed across the beam. Thus, although the performance was erratic, it appears clear that the Zeeman components yield polarized ions as expected. The erratic neutron yield is thought to be due to exchange between deuterium and hydrogen in some hydrogenous materials of which the source is constructed. These materials are being replaced.

The above results are, of course, preliminary and are submitted to support the feasibility of an ion source of this type. The ion yield has been greatly increased recently and appears now to be about 10^{-8} amp.

Table 1. Calculated Deuteron Polarizations and Neutron Anisotropies for the $T(d,n)He^4$ Reaction

Strong-Field States, (m_i, m_j)	Weak-Field States, (f, m_f)	Population of Deuteron Spin States			Deuteron Polarization	$\sigma_{90°}/\sigma_{0°}$	Neutron Polarization	
		$m_i = 1$	$m_i = 0$	$m_i = -1$			0°	90°
$(+1, \frac{1}{2})$	$(\frac{3}{2}, \frac{3}{2})$	1	0	0				
$(0, \frac{1}{2})$	$(\frac{3}{2}, \frac{1}{2})$	$\frac{1}{3}$	$\frac{2}{3}$	0	$\frac{1}{3}$	0.76	0.231	−0.414
$(-1, \frac{1}{2})$	$(\frac{3}{2}, -\frac{1}{2})$	0	$\frac{2}{3}$	$\frac{1}{3}$				
	Total	$\frac{4}{3}$	$\frac{4}{3}$	$\frac{1}{3}$				
$(-1, -\frac{1}{2})$	$(\frac{3}{2}, -\frac{3}{2})$	0	0	1				
$(0, -\frac{1}{2})$	$(\frac{1}{2}, -\frac{1}{2})$	0	$\frac{1}{3}$	$\frac{2}{3}$	$-\frac{1}{3}$	1.3	−0.273	0.324
$(+1, -\frac{1}{2})$	$(\frac{1}{2}, \frac{1}{2})$	$\frac{2}{3}$	$\frac{1}{3}$	0				
	Total	$\frac{2}{3}$	$\frac{2}{3}$	$\frac{5}{3}$				

Table 2. Observed Neutron Anisotropy vs Slit Position

Slit Position (in.)	n_1 per 10 min	n_2 per 10 min	n_1/n_2
0.600	384	287	1.33
0.580	930	791	1.18
0.560	587	311	1.89
0.540	1610	1151	1.40
0.520	353	314	1.12
0.500	−52	10	
0.480	103	194	0.53
0.460	58	122	0.48
0.440	20	48	0.42
0.420	62	110	0.56

LARGE-AREA GERMANIUM SURFACE-BARRIER COUNTERS[1]

F. J. Walter J. W. T. Dabbs L. D. Roberts

A description is given of a solid-state counter of good resolution, long-term stability, and fast rise time which is suitable for heavy charged particles, for example, alpha particles and fission fragments. A simple theoretical model for the counter behavior is presented which is found to describe the observed behavior of the counter very well. The importance of germanium purity in connection with pulse height, rise time, and counter area is discussed. Counters with sensitive areas up to 5 cm^2 have been successfully used.

[1]Abstract of published paper: *Rev. Sci. Instr.* 31, 756 (1960).

PULSE CHARACTERISTICS OF SOME FAST PHOTOTUBES

C. W. Williams[1] R. P. Cumby[1] J. H. Neiler

Tests have recently been performed on a group of phototubes to determine their pulse characteristics, such as rise time and transit time differences for photoelectrons emitted from different points on the photocathode. The combination of the rise time and transit time difference within a given photocathode area determines the ultimate timing resolution that may be expected in use. Types checked include the RCA 7046 and Philips 58AVP, which have nominal 5-in. photocathodes; the Du Mont 6363 and the CBS CL-1016, which are 3-in. tubes; and the 2-in. RCA C7251-7264 and Philips 56AVP.

The tubes are tested by means of a UCRL mercury-capsule light-pulse generator.[2] This pulser furnishes a pulse of light of $\sim 5 \times 10^{-10}$ sec rise time and width at half maximum. The light is masked so that a small spot is directed onto the photocathode of the tube under test, which is located in a light-proof chamber. The chamber is equipped with a traversing mechanism, by which the tube may be positioned to cause the pulsed light spot to fall on a selected point of the photocathode. Time measurement is performed on the anode pulse by means of a Lumatron sampling oscilloscope. Calibration of the scope against calibrated delay-line lengths permits measurement with a fair degree of confidence to about $\pm 10\%$.

Table 1 lists transit time difference, rise time, and pulse width for the 7046, showing the effect of a change in grid-2 voltage with constant cathode to anode voltage ($E = 3400$ v). This table also gives comparative data for the 58AVP for two values of cathode to anode voltage. Useful photocathode diameter is ≈ 4 in. for the 7046 and ≈ 4.3 in. for the 58AVP. Results of the measurements on the 6363, CL-1016, 7264, and 56AVP are shown in Table 2.

[1]Instrumentation and Controls Division.

[2]Q. A. Kerns, F. A. Kirsten, and G. C. Cox, *A Generator of Fast-Rising Light Pulses for Phototube Testing*, UCRL-8227 (Mar. 24, 1958).

Table 1. Time Response Characteristics of the 7046 and 58AVP

	7046		58AVP	
	$V_{g2} = 1250$ v	$V_{g2} = 1750$ v	$E = 3000$ v	$E = 2500$ v
Transit time difference (in nanoseconds) for the specified distance from center of photocathode				
Center	0	0	0	0
0.50 in.	0.10	0	0	0
0.75 in.	0.20	0.10	0.10	0.10
1.0 in.	0.30	0.15	0.25	0.30
1.25 in.	0.40	0.30	0.30	0.45
1.5 in.	0.70	0.50	0.45	0.70
1.75 in.	1.25	1.0	0.75	0.90
2.0 in.	1.90	1.5	1.10	1.20
Associated rise time, nanosec	2.0	2.4	1.5	1.5
Width (half-max), nanosec	6.2	5.0	2.4	2.2
Approximate gain	3×10^6		$>10^8$	
Maximum linear pulse amplitude, ma	~ 60		>300	

Table 2. Time Response Characteristics of the 6363, CL-1016, C7251-7264, and 56AVP

	6363	CL-1016	C7251-7264	56AVP
Transit time difference (in nanoseconds) for the specified distance from center of photocathode				
Center	0	0	0	0
0.25 in.	0.5	0.2	0	0
0.50 in.	1.5	0.7	0.15	0.05
0.75 in.	3.5	1.8	0.35	0.20
0.80 in.	3.9	2.0	0.45	0.25
0.90 in.	4.9	2.6	0.80	0.55
0.95 in.	5.5	3.1	1.0	0.75
1.0 in.	6.0	3.7		
1.25 in.	11.0	5.9		
1.50 in.		4.8		
Associated rise time, nanosec	7.0	3.0	2.3	1.6
Cathode-to-anode voltage, v	1700	2000	2000	2400
Nominal cathode diameter, in.	3	3	2	2

PROPERTIES OF SEMICONDUCTOR DETECTORS

J. W. T. Dabbs F. J. Walter L. D. Roberts

In previous annual reports[1,2] a theoretical model describing the behavior of semiconductor particle detectors was given which seemed to agree rather well with our experimental results on germanium surface-barrier detectors over a wide range of parameters. More recently, work in the Physics Division has been extended to the use of silicon detectors at room temperature and at 77°K.

Epoxy-potted detectors[3] were found unsatisfactory for applications requiring cooling because of the large difference in expansion coefficients. Several other methods for mounting relatively large silicon crystals have been developed for low-temperature use. The first is illustrated in Figs. 1 and 2. The ohmic contact (back side) was made by using electroless nickel plating on a lapped surface and soldering a platinum wire to the nickel with 60-40 solder. This connection was protected with Apiezon W wax during subsequent etching operations. A room-temperature test of a series of crystals having two such contacts failed to show any noise in excess of that attributable to the associated circuits, at currents up to 25 $\mu a/cm^2$. These tests were made using the ORNL low-noise Q2069B-3RO preamplifier.[3] The crystal was supported at three points by insulating beads of epoxy resin at the upper ends of three small-diameter wires. In order to make electrical contact to the front surface, a small bead of epoxy resin was used to attach a 1-mil copper strip to the etched silicon surface, and gold was evaporated across the copper-epoxy-silicon region and the counting region simultaneously. To eliminate possible high resistance in an oxide layer, the upper surface of the copper strip

UNCLASSIFIED
PHOTO 51386

Fig. 1. Flexible Mounting of Silicon Crystal.

UNCLASSIFIED
PHOTO 51385

Fig. 2. Detector of Fig. 1 with Cover.

[1] F. J. Walter *et al.*, *Phys. Div. Ann. Progr. Rept. Mar. 10, 1959*, ORNL-2718, p 53.
[2] F. J. Walter *et al.*, *Phys. Div. Ann. Progr. Rept. Feb. 10, 1960*, ORNL-2910, p 70.
[3] *Low Noise Amplifiers for Use with Solid State Detectors*, TID-6119 (1960).

had previously been gold plated. Front electrodes of this type have exhibited point-to-strip resistance of a few ohms for ~200-A-thick gold over distances of ~1 cm. The front cover shown in Fig. 2 serves to prevent the particles being counted from reaching the silicon immediately outside the gold-coated area, where smaller-than-normal pulses have been observed to originate.

The second and third methods of mounting take advantage of the small and similar expansion coefficients of silicon, germanium, Kovar metal, and the glasses used in Kovar seals. In the second method, after attachment of the back electrode and etching, the silicon crystal was mounted on the end of the glass-tube portion of a Kovar feedthrough glass-to-metal seal, using epoxy resin. The back electrode lead was passed through the central Kovar tube, and the copper strip to the front electrode was soldered to the Kovar surround of the seal. The third method consisted of soldering the central tube of another type of Kovar feedthrough seal directly to the back of a germanium crystal, and attaching copper strip as before. These mountings are shown in Figs. 3 and 4.

High-Resolution Studies

An exploration of the feasibility of the use of silicon detectors (operated in the temperature range 77 to 300°K) in connection with experiments which require separation of alpha-particle fine structure and various alpha-particle groups has been made.

As expected, leakage currents were reduced by large factors in cooling to 77°K. Factors of 100 were found on cooling to −20°C. The peak width resulting from bombardment with alpha particles, as well as the peak width resulting from electrical noise from the detector and amplifier, was measured

Fig. 3. Glass-Epoxy Mounting.

Fig. 4. Soldered Mounting (8 cm^2 Germanium Crystal).

as a function of detector temperature. These tests were made using the low-noise Q2069B-3RO amplifier system.[3] The noise width of this "charge-sensitive" amplifier system, as a function of input capacitance, is shown in Fig. 5. (The stepwise behavior of the pulser measurements at small peak widths is a result of rounding off to the next larger integral number of channels.) As can be seen from Fig. 6, the electrical noise from the detector was reduced to $\leqq$3 kev full width of half maximum (fwhm) by cooling to 77°K. This fact may be used to advantage in cases where this noise is the controlling factor in peak widths. For alpha particles with detectors of relatively large area, the electrical noise is important in this sense. For lightly ionizing particles (e.g., electrons or minimum ionizing particles) further improvements in

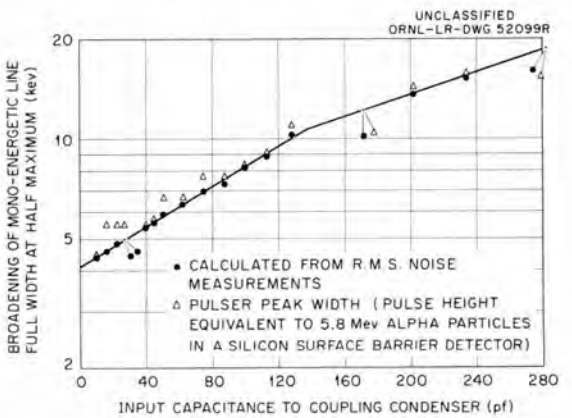

Fig. 5. Electronic Noise as a Function of Input Capacitance for ORNL Preamplifier Q-2069B-3 with Selected Input Tube and 20-Megohm Load Resistor.

amplifier noise levels would permit an approach to the situation indicated by the bottom curve in Fig. 6.[4]

For certain experiments, the problems of long-time stability and peak shape are important. A study of these aspects, with particular attention to variation in measured peak areas, was made. Figure 7 shows a typical multichannel pulse-height spectrum, representing 4 hr of counting near the middle of a 20-hr stability test made with the detector at room temperature. The peak locations remained constant within ten channels, or 16 kev, during the entire period. During the 20-hr counting period, the electrical noise contribution increased from 13 kev (fwhm) to 16.5 kev (fwhm), and the alpha peak widths increased from 17.5 kev (fwhm) to 23 kev (fwhm). (The latter change may have been caused by the gradual accumulation of contaminants from the untrapped vacuum system.) A separate test of the amplifier system and analyzer showed only a few kev peak location drift during a comparable interval.

A study of the peak shapes was made by fitting the sum of two Gaussian functions to the alpha peaks associated with the ground and first excited states of Pu^{240}. In the four-parameter fit, the width of both peaks was required to be the same. The five-parameter fit allowed individual variation of the widths and subjectively appears to be a better fit. However, a comparison of the Gaussian areas under the two fine-structure peaks revealed that the four-parameter fit not only gave an area ratio in closer agreement with magnetic spectrograph data, but also showed much less variation in the ratio during the 20-hr period. Using the four-parameter fit, the

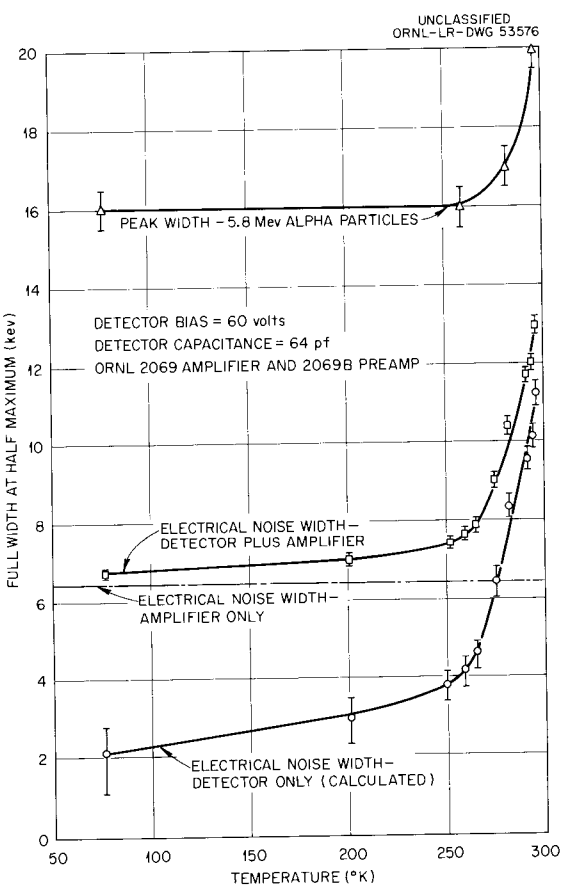

Fig. 6. Energy Resolution and Noise for 40-mm^2 Silicon Surface Barrier Detector as a Function of Detector Temperature.

[4]G. Amsel, "Semiconductor Nuclear Particle Detectors," ed. by J. W. T. Dabbs and F. J. Walter, paper 5 in *NAS–NRC Nuclear Science Series Rept. No. 32*, National Academy of Sciences, Washington, D.C., February 1961.

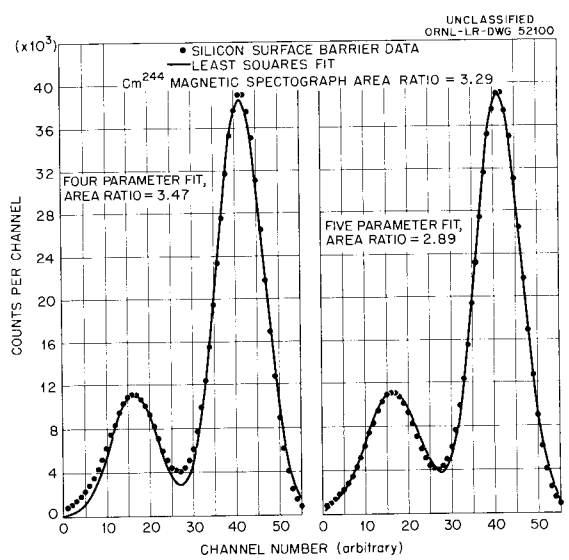

Fig. 7. Curium-244 Alpha Fine Structure.

variation in area ratio was less than 0.7%, while the five-parameter fit gave a variation of 9%. It is clear that the peaks shown in Fig. 7 are not Gaussian; the disagreement with the Gaussian sum curve in the valley cannot be caused by conversion electrons because of the small solid angle.

Pulse Rise Times

Under certain circumstances, the charge-carrier transit times in semiconductor particle detectors can be quite short.[2,5] This presents the possibility of using such detectors in nanosecond timing applications. Even though the transit times of the charge carriers across the depletion region may be short, the rise time at the amplifier input may be relatively long. An estimate of the observable rise time requires that one consider not only the charge transit times, but the time required to transmit the information to the amplifier through the undepleted base material and through any contact or sheet resistances which may exist.

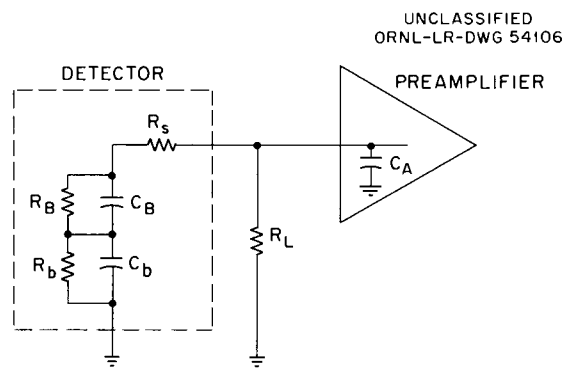

Fig. 8. Equivalent Circuit for a Junction Detector.

Figure 8 shows an equivalent circuit for a junction detector.[2,5] The effective capacitance and resistance of the depletion region are denoted by C_B and R_B, respectively, while C_b and R_b represent these quantities for the undepleted bulk region. The input capacitance of the amplifier, including any stray capacitances, is denoted by C_A; R_L is the load resistor; and R_S is any additional series resistance. In Fig. 8, let $V_A(t)$ be the voltage across C_A resulting from a current $I(t)$ which corresponds to the transit of charge carriers across C_B. $V_A(t)$ is given by

$$V_A(t) = L^{-1}\left\{[L\ I(t)] \cdot \frac{1}{R_S C_A C_B} \cdot \left[\frac{s + (\tau_D)^{-1}}{s^3 + 2\alpha s^2 + \gamma^2 s}\right]\right\}, \tag{1}$$

where

$\tau_D = R_b C_b = \rho\kappa\xi_0$ (the "dielectric" relaxation time),

$\alpha = \frac{1}{2}[(R_S C_S)^{-1} + (R_S C_b)^{-1} + (\tau_D)^{-1}]$,

$\gamma^2 = (\tau_D)^{-1}(R_S C_S)^{-1}$,

$C_S = (C_A C_B)/(C_A + C_B)$,

ρ = resistivity of bulk semiconductor,

κ = dielectric constant,

---

[5] F. J. Walter, J. W. T. Dabbs, and L. D. Roberts, *Rev. Sci. Instr.* 31, 756 (1960).

ξ_0 = permittivity of free space,

L = Laplace transform operator ($s = \sigma + j\omega$).

In Eq. (1), R_B and R_L are neglected, since they normally contribute only to the pulse decay.

Consider the case where the charge-carrier transit time is sufficiently short that $I(t)$ may be represented by a delta function, that is, $I(t) = \delta(t - t_0) \cdot Q$ or $I(s) = L\ I(t) = Q$. Then the voltage at the amplifier is given by

$$V_A(t) = \frac{Q}{C_A + C_B} \left\{ 1 - \left[\cosh \beta t - \frac{1}{\beta} \left(\frac{1}{R_S C_S} - \alpha \right) \sinh \beta t \right] \cdot \exp(-\alpha t) \right\}, \tag{2}$$

where $\beta = (\alpha^2 - \gamma^2)^{1/2}$.

For the case where R_S is negligibly small (e.g., with an evaporated metal front electrode), the voltage at the amplifier becomes

$$V_A(t) = \frac{Q}{C_A + C_B} \left\{ 1 - \left[1 - \left(\frac{C_b}{C_b + C_S} \right) \right] \exp \left(\frac{-t}{\tau_D + R_b C_S} \right) \right\}. \tag{3}$$

It is apparent from the above that the rise time can only approach the transit times if C_A, R_S, τ_D, and R_b are sufficiently small. The pulse height predicted by Eq. (3) for very large values of R_b (and τ_D) has been observed in germanium detectors at very low temperatures.[6]

In the above, the carrier current has been represented by a delta function in order to delineate the effects of various circuit parameters. In practice, transit times are by no means always as short as a few nanoseconds, and detailed consideration of the mobilities, electric fields, and transit distances is required. It should also be noted that in the case of densely ionizing particles, the internal electric fields may be strongly perturbed by the charge carriers. Another difficulty in realizing this potential application to fast-timing problems is connected with the unresolved question of obtaining satisfactory signal-to-noise ratios when semiconductor detectors are used with very fast amplifiers.

---

[6]Ref 2, Fig. 2 and Eq. (2); ref 5, Fig. 9 and Eq. (10).

RESPONSE OF SILICON DETECTORS TO FISSION FRAGMENTS

H. W. Schmitt J. H. Neiler F. J. Walter R. J. Silva

The response of silicon surface-barrier detectors to fission fragments is under investigation. Preliminary findings indicate that the measured pulse height is not strictly proportional to fragment energy but that an empirical relation of the form $E = a \times \mathrm{PH} + \delta$ is followed, where E = fragment energy, a = a constant, PH = pulse height, and δ has been termed "pulse height defect." Values of δ range from 6 to 26 Mev for the values of detector bias and silicon resistivity employed.

Method

Fission fragments from the spontaneous fission of Cf^{252} were incident on the surface of a detector, as shown schematically in Fig. 1. The source was approximately 1 cm in diameter and was positioned routinely about 1 cm from the detector. For any given set of operating conditions, the shape of

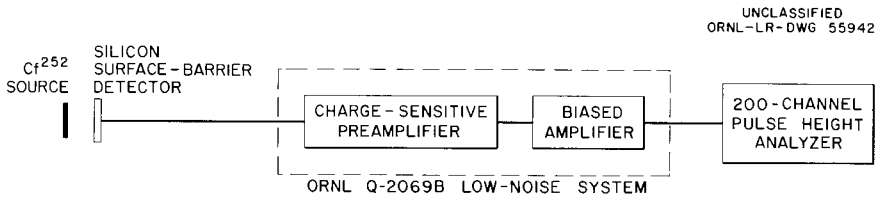

Fig. 1. Schematic Diagram of Experimental Arrangement.

the fission spectrum did not change with source-to-detector distance above ~6 mm. The detectors were in general 5 × 5 mm in size; in most cases they were mounted as shown in Fig. 3 of the previous paper, so that the effective detection area was somewhat smaller. The low-noise, charge-sensitive preamplifier, main amplifier, and biased amplifier were of the modified ORNL Q-2069 type.[1] Calibration in every case was made relative to an ORNL Q-1212 mercury-relay pulser which was experimentally known to be linear with zero intercept.

On the basis that the normalized pulse-height spectra obtained in these measurements agreed in shape with the energy spectrum deduced from double time-of-flight measurements,[2,3] seven points over the spectrum were selected for the pulse-height-vs-energy correlation for each set of operating conditions. These were the heavy- and light-fragment peaks, the valley, the points at half maximum on the low- and high-energy edges of the spectrum, and extrapolated minimum and maximum energies obtained from these edges. It has been considered that the heavy and light fragments may exhibit different pulse-height-vs-energy relations; reasonable physical considerations, however, indicate that such an effect should be of second or higher order. It is noted that in the ionization-vs-energy measurements for fission fragments in gases,[4] the same relation is followed by the heavy and light fragments in the range of initial fragment energies.

Results

A typical pulse-height-vs-energy plot is shown in Fig. 2. Note that the empirical equation

$$E = a \times \mathrm{PH} + \delta \tag{1}$$

describes the data, although the values of a and δ depend on whether one uses the energy spectrum of Milton and Fraser[2] or that of Stein and Whetstone.[3] We have found essentially a constant difference in the value of δ for all runs, the energies of Stein and Whetstone yielding smaller values of δ.

---

[1] *Low Noise Amplifiers for Use with Solid State Detectors*, TID-6119 (1960).

[2] J. C. D. Milton and J. S. Fraser, *Phys. Rev.* 111, 877 (1958).

[3] W. E. Stein and S. L. Whetstone, *Phys. Rev.* 110, 476 (1958).

[4] H. W. Schmitt and R. B. Leachman, *Phys. Rev.* 102, 183 (1956).

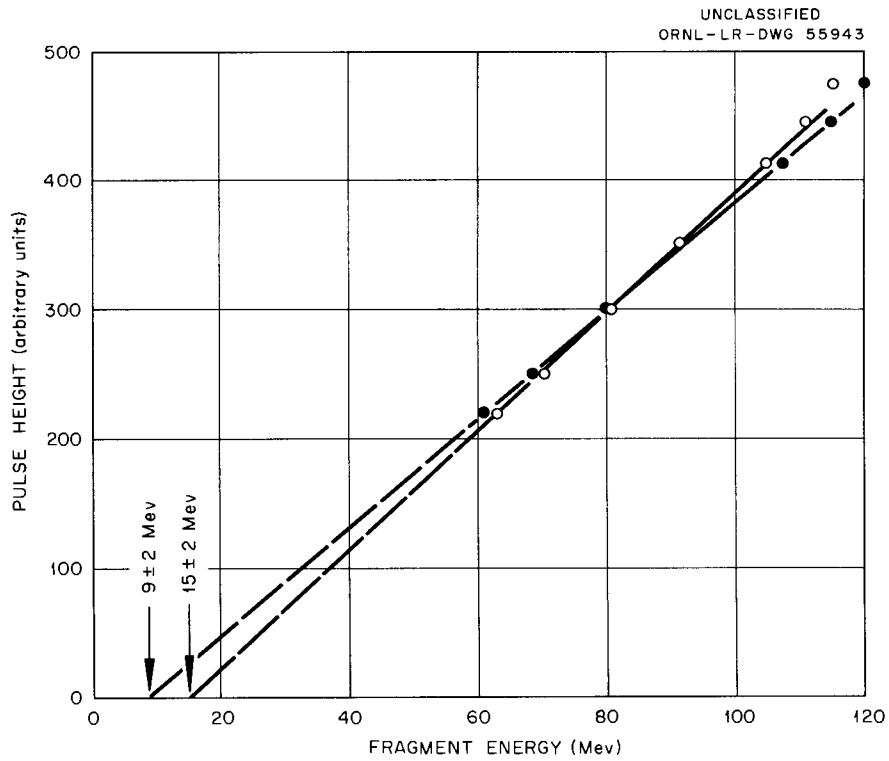

Fig. 2. Typical Pulse Height vs Energy Relation. Open circles are used with the energy measurements of ref 2; closed circles are used with the energy measurements of ref 3.

The latter energies have been arbitrarily chosen for purposes of plotting the pulse-height defect δ vs maximum electric field E_0 in the barrier region. The maximum field E_0 for silicon detectors is given by

$$E_0 = 4.2 \times 10^4 \sqrt{V/\rho} \text{ v/cm} , \tag{2}$$

where V = detector bias in volts = applied bias plus 0.6 v, and ρ = resistivity in ohm-cm.

The results of measurements to date are shown in Fig. 3. We note only that a trend appears, namely, that larger values of δ are observed for high-resistivity silicon than for low-resistivity material, for E_0 constant. Also for the high-resistivity material, δ decreases as E_0 or detector bias is increased. The large variation in δ between the 3600 ohm-cm and 100–300 ohm-cm measurements indicates a strong dependence on resistivity; however, the variations in δ among the lower-resistivity detectors are probably not significant because of the large uncertainty in the resistivity measurements. Further work is in progress to determine the systematics of this behavior and its physical basis.

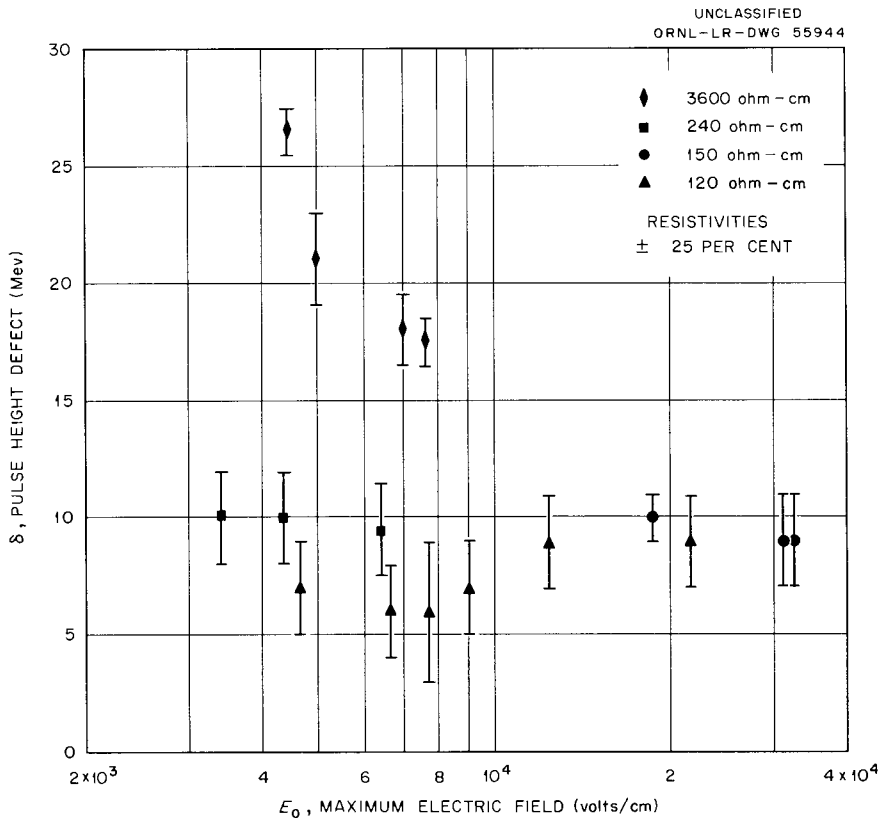

Fig. 3. Pulse-Height Defect δ vs Maximum Electric Field E_0 in Barrier Region.

PUBLICATIONS

Ajzenberg-Selove, F., and P. H. Stelson, "The $Be^9(\alpha,n)C^{12}$ Reaction and the Parameters of the 7.66-Mev State of C^{12}," *Phys. Rev.* **120**, 500 (1960).

Alburger, D. E., "Nuclear Pair Emission from the 7.656-Mev Level in C^{12}," *Phys. Rev.* **118**, 235 (1960).

Bair, J. K., H. O. Cohn, and H. B. Willard, "Level Structure of N^{14}," *Phys. Rev.* **119**, 2026 (1960).

Bair, J. K., R. D. Edge, and H. B. Willard, "Reaction $C^{14}(p,n)N^{14}$," *Phys. Rev.* **119**, 1948 (1960).

Bhalla, C. P., and M. E. Rose, "Pseudoscalar Interaction in Nuclear Beta Decay," *Phys. Rev.* **120**, 1415 (1960).

Block, M. M., E. B. Brucker, R. Gessaroli, T. Kikuchi, C. M. Meltzer, A. Pevsner, P. Schlein, R. Strand, H. O. Cohn, E. M. Harth, J. Leitner, A. Minguzzi-Ranzi, L. Monari, and G. Puppi, "Search for Evidence of Parity Nonconservation in K-He Interactions," *Phys. Rev.* **120**, 570 (1960).

Block, R. C., G. G. Slaughter, and J. A. Harvey, "Thermal Neutron Cross Section Measurements of U^{233}, U^{235}, Pu^{240}, U^{234}, and I^{129}," *Nuclear Sci. and Eng.* **8**, 112 (1960).

Block, R. C., and R. H. Ward, "Sealing Photomultipliers to Liquid Scintillator with Indium Gaskets," *Rev. Sci. Instr.* **31**, 66 (1960).

Cable, J. W., M. K. Wilkinson, and E. O. Wollan, "Neutron Diffraction Studies of Antiferromagnetism in CrF_2 and $CrCl_2$," *Phys. Rev.* **118**, 950 (1960).

Carlson, T. A., "Dissociation of C_6H_5T following Beta Decay," *J. Chem. Phys.* **32**, 1234 (1960).

Dabbs, J. W. T., S. H. Hanauer, L. D. Roberts, F. J. Walter, and G. W. Parker, "Alpha-Particle Emission from Oriented Np^{237}," p 936 in *Proceedings of the International Conference on Nuclear Structure* (ed. by D. A. Bromley and E. W. Vogt), University of Toronto Press, Toronto, Canada, 1960.

Dabbs, J. W. T. and F. J. Walter (eds.) *Semiconductor Nuclear Particle Detectors* (Proceedings of an Informal Conference Held in Asheville, N.C., September 28–30, 1960), Natl. Acad. Sci. – Natl. Research Council, Nuclear Sci. Series, Report No. 32 (February 1961).

Dazai, T., "An Analysis of the $F^{19}(d,p)F^{20}$ Reaction," p 936 in *Proceedings of the International Conference on Nuclear Structure* (ed. by D. A. Bromley and E. W. Vogt), University of Toronto Press, Toronto, Canada, 1960.

Felsner, G., and M. E. Rose, "Electron Polarization in Allowed Beta-Transitions with Coulomb Corrections," *Z. Physik.* **159**, 505 (1960).

Fowler, J. L., E. G. Corman, and E. C. Campbell, "Neutron Scattering from Closed Shell Nuclei," p 474 in *Proceedings of the International Conference on Nuclear Structure* (ed. by D. A. Bromley and E. W. Vogt), University of Toronto Press, Toronto, Canada, 1960.

Fowler, T. K., and W. M. Good, "A Theory on Obtaining Short Bursts of Ions from a Beam of Ions," *Nuclear Instr. & Methods* **7**, 245 (1960).

Good, W. M., "Millimicrosecond Pulsing – Its Application and Technique," *Nuclear Instr. & Methods* **6**, 323 (1960).

Gordon, M. M., and T. A. Welton, "The Oak Ridge Relativistic Isochronous Cyclotron. Part III. Analysis of Ion Orbits in the Isochronous Cyclotron," *Nuclear Instr. & Methods* **6**, 221 (1960).

Harvey, J. A., "Donald J. Hughes (1915–60)," *Nuclear Phys.* **20**, 1 (1960).

Harvey, J. A., "Slow Neutron Resonances," p 659 in *Proceedings of the International Conference on Nuclear Structure* (ed. by D. A. Bromley and E. W. Vogt), University of Toronto Press, Toronto, Canada, 1960.

Herpin, Andre, W. C. Koehler, and Pierre Meriel, "Structure Magnétique du Grenat d'Holmium A Basse Température (Magnetic Structure of Holmium Garnet at Low Temperatures)," *Compt. rend.* **281**, 1359 (1960)

Joyner, W. T., H. W. Schmitt, J. H. Neiler, and R. J. Silva, "Energy Spectra of Correlated Fragment Pairs from the Spontaneous Fission of Cf^{52}," *IRE Trans. on Nuclear Sci.* **NS-8**, 54 (1961).

Koehler, W. C., E. O. Wollan, and M. K. Wilkinson, "Neutron Diffraction Study of the Magnetic Properties of Rare Earth–Iron Perovskites," *Phys. Rev.* **118**, 58 (1960).

LaValle, D. E., R. M. Steele, M. K. Wilkinson, and H. L. Yakel, Jr., "The Preparation and Crystal Structure of Molybdenum(III) Fluoride," *J. Am. Chem. Soc.* **82**, 2433 (1960).

McGowan, F. K., and P. H. Stelson, "Coulomb Excitation of Vibrational States in Th^{232} and U^{238}," p 957 in *Proceedings of the International Conference on Nuclear Structure* (ed. by D. A. Bromley and E. W. Vogt), University of Toronto Press, Toronto, Canada, 1960.

McGowan, F. K., and P. H. Stelson, "Coulomb Excitation of States in Th^{232} and U^{238}," *Phys. Rev.* **120**, 1803 (1960).

Macklin, R. L., "Volcanic Energy Resources," *Nuclear Sci. and Eng.* **7**, 553 (1960).

Macklin, R. L., G. deSaussure, J. D. Kington, and W. S. Lyon, "Manganese Bath Measurements of η of U^{233} and U^{235}," *Nuclear Sci. and Eng.* **8**, 210 (1960).

Mann, R. A., and M. E. Rose, "Depolarization of Negative Mu Mesons," *Phys. Rev.* **121**, 293 (1961).

Miller, P. D., J. H. Gibbons, J. H. Neiler, W. M. Good, and R. L. Macklin, "Statistical Parameters of Medium Weight Nuclei from Kev Neutron Total and Capture Cross Sections," p 959 in *Proceedings of the International Conference on Nuclear Structure* (ed. by D. A. Bromley and E. W. Vogt), University of Toronto Press, Toronto, Canada, 1960.

Moak, C. D., "Space Charge Effects in Cylindrical Beams with Uniform Acceleration," *Nuclear Instr. & Methods* **8**, 19 (1960).

Pattenden, N. J., and J. A. Harvey, "The Resonance Energy Cross Section of U^{233}," p 882 in *Proceedings of the International Conference on Nuclear Structure* (ed. by D. A. Bromley and E. W. Vogt), University of Toronto Press, Toronto, Canada, 1960.

Pearlstein, L. D., Y. C. Tang, and K. Wildermuth, "Energy Levels of He^5 and Li^5," p 962 in *Proceedings of the International Conference on Nuclear Structure* (ed. by D. A. Bromley and E. W. Vogt), University of Toronto Press, Toronto, Canada, 1960.

Pinkston, W. T., and G. R. Satchler, "Collective Effects in Inelastic Scattering," p 963 in *Proceedings of the International Conference on Nuclear Structure* (ed. by D. A. Bromley and E. W. Vogt), University of Toronto Press, Toronto, Canada, 1960.

Roberts, L. D., J. W. T. Dabbs, and G. W. Parker, "Alpha-Particle Emission from Oriented Neptunium-237 and Uranium-233 Nuclei," *Proc. U.N. Intern Conf. Peaceful Uses Atomic Energy, 2nd, Geneva, 1958* **15**, 322–30 (1958).

Roberts, L. D., F. J. Walter, J. W. T. Dabbs, G. W. Parker, and J. O. Thomson, "Fission Fragments from Oriented U^{233} and U^{235}," p 884 in *Proceedings of the International Conference on Nuclear Structure* (ed. by D. A. Bromley and E. W. Vogt), University of Toronto Press, Toronto, Canada, 1960.

Robinson, R. L., F. K. McGowan, and W. G. Smith, "Decays of Rh^{106} and Ag^{106}," *Phys. Rev.* **119**, 1692 (1960).

Rose, M. E., *Relativistic Electron Theory*, Wiley, New York, 1961.

Rose, M. E., and R. H. Good, Jr., "Angular Distribution of Recoils from Mu Meson Capture," *Ann. Phys. (N.Y.)* **9**, 211 (1960).

Satchler, G. R., "Circularly Polarized Gamma Rays from Direct Nuclear Reactions," *Nuclear Phys.* **16**, 674 (1960).

Satchler, G. R., "Symmetry Properties of the Distorted Wave Theory of Direct Nuclear Reactions," *Nuclear Phys.* **18**, 110 (1960).

Satchler, G. R., "Spin-Orbit Coupling for Spin-1 Particles," *Nuclear Phys.* **21**, 116 (1960).

Satchler, G. R., and W. Tobocman, "Gamma Rays from Deuteron Stripping Reactions," *Phys. Rev.* **118**, 1566 (1960).

Schmitt, H. W., "Determination of the Energy of Antimony-Beryllium Photoneutrons," *Nuclear Phys.* **20**, 220 (1960).

Schmitt, H. W., R. C. Block, and R. L. Bailey, "Total Neutron Cross Section of B^{10} in the Thermal Energy Range," *Nuclear Phys.* **17**, 109 (1960).

Schmitt, H. W., and C. W. Cook, "Absolute Neutron Absorption Cross Sections for Sb-Be Photoneutrons," *Nuclear Phys.* **20**, 202 (1960).

Schmitt, H. W., and R. B. Murray, "Neutron-Induced Fission Cross Section of Np^{237}," *Phys. Rev.* **116**, 1575 (1959).

Shull, C. G., M. K. Wilkinson, and M. H. Mueller, "Slow Neutron Scattering by the Titanium Isotopes," *Phys. Rev.* **118**, 797 (1960).

Snell, A. H., F. Pleasonton, and J. L. Need, "Charge Spectrometry for Kr^{79}-Br^{79}," *Phys. Rev.* **116**, 1548 (1959).

Stelson, P. H., "Vibrations in Spherical and Nearly Spherical Nuclei," p 787 in *Proceedings of the International Conference on Nuclear Structure* (ed. by D. A. Bromley and E. W. Vogt), University of Toronto Press, Toronto, Canada, 1960.

Stelson, P. H., and F. K. McGowan, "Coulomb Excitation of Li^7, F^{19}, and Na^{23} by Ne^{20} Ions," *Nuclear Phys.* **16**, 92 (1960).

Stelson, P. H., and F. K. McGowan, "Coulomb Excitation with Ne^{20} Ions," p 47 in *Proceedings of the 2nd Conference on Reactions Between Complex Nuclei*, Wiley, New York, 1960.

Stelson, P. H., and F. K. McGowan, "Coulomb Excitation of Second 2^+ States in Even-Even Medium Weight Nuclei," *Phys. Rev.* **121**, 209 (1961).

Trammell, G. T., "Theory of the Low-Lying States of some Rare Earth Compounds," *J. Appl. Phys.* **31**, 362S (1960).

Walter, F. J., J. W. T. Dabbs, and L. D. Roberts, "Large Area Germanium Surface-Barrier Counters," *Rev. Sci. Instr.* **31**, 756 (1960).

Walter, F. J., J. W. T. Dabbs, and L. D. Roberts, "Semiconductor Particle Counters at Low Temperatures," *IRE Trans. on Nuclear Sci.* **NS-8**, 79 (1961).

Wegener, H. H. F., "Schroedinger Equation in Multiply Connected Spaces and Phase Optics," *Z. Physik* **159**, 243 (1960).

Welton, T. A., "The Southern Regional Accelerator," pp 365–71 in *Proceedings of the International Conference on High Energy Accelerators and Instrumentation*, CERN, 1959.

Wildermuth, K., and H. Faissner, "Asymmetric Fission from the Viewpoint of the Cluster Model," p 972 in *Proceedings of the International Conference on Nuclear Structure* (ed. by D. A. Bromley and E. W. Vogt), University of Toronto Press, Toronto, Canada, 1960.

Wilkinson, M. K., "Neutron Diffraction," p 88 in *McGraw-Hill Encyclopedia of Science and Technology*, vol 9, McGraw-Hill, New York, 1960.

Wilkinson, M. K., H. R. Child, J. W. Cable, E. O. Wollan, and W. C. Koehler, "Neutron Diffraction Investigations of the Magnetic Ordering in Rare-Earth Nitrides," *J. Appl. Phys.* **31**, 358S (1960).

Wilkinson, M. K., E. O. Wollan, H. R. Child, and J. W. Cable, "Neutron Diffraction Investigation of Magnetic Ordering in the Trifluorides of 4d-Transition Elements," *Phys. Rev.* **121**, 74 (1961).

Wollan, E. O., "Magnetic Coupling in Crystalline Compounds – A Phenomenological Theory of Magnetism in 3d Metals," *Phys. Rev.* **117**, 387 (1960).

Zeldes, Henry, G. T. Trammell, Ralph Livingston, and R. W. Holmberg, "A Common Error Made in Treating Hyperfine Effects in Electron Paramagnetic Resonance Studies of Free Radicals," *J. Chem. Phys.* **32**, 618 (1960).

PAPERS PRESENTED AT SCIENTIFIC AND TECHNICAL MEETINGS

Conference on Analytical Chemistry and Applied Spectroscopy, Pittsburgh, Pennsylvania, February 29–March 4, 1960

J. R. Lawson and H. W. Morgan, "The Determination of Trace Amounts of Polyatomic Inorganic Ions by Infrared Spectroscopy."

American Physical Society Meeting, Houston, Texas, March 4–5, 1960

G. R. Satchler (invited paper), "Distorted Wave Effects on Direct Nuclear Reactions."

Midwest Conference on Theoretical Physics at Purdue University, Lafayette, Indiana, April 1–2, 1960

R. H. Good and M. E. Rose, "A Paradox Concerning Polarization in Beta Decay."

Southeastern Section of the American Physical Society, Gatlinburg, Tennessee, April 7–9, 1960

J. L. Fowler, "Neutron Scattering from Lead."

W. M. Good, J. H. Gibbons, P. D. Miller, and J. H. Neiler, "Total Cross Sections of $Ge^{70,72,74,76}$, Cu^{63}, and Co^{59}."

C. H. Johnson and A. Galonsky, "Thresholds for (p,n) Reactions."

F. K. McGowan and P. H. Stelson, "Decay of $Rh^{102} \rightarrow Ru^{102}$."

R. L. Robinson, E. Eichler, and N. R. Johnson, "Decay of I^{132}."

J. E. Sherwood, S. J. Ovenshine, and R. F. King, "A Polarized Ion Source."

Conference on Neutron Diffraction in Relation to Magnetism and Chemical Bonding (sponsored by the Oak Ridge National Laboratory, the Office of Naval Research, and the American Physical Society), Gatlinburg, Tennessee, April 20–22, 1960

J. W. Cable, M. K. Wilkinson, and E. O. Wollan, "Magnetic Ordering in $CrCl_3$ and $FeCl_3$."

W. C. Koehler, J. W. Cable, E. O. Wollan, and M. K. Wilkinson, "Magnetic Structure Properties of Metallic Holmium."

M. K. Wilkinson, H. R. Child, E. O. Wollan, J. W. Cable, and W. C. Koehler, "Magnetic Ordering in Rare Earth Nitrides and Antimonides."

M. K. Wilkinson, E. O. Wollan, and W. C. Koehler, "Current Work on Chromium at ORNL."

E. O. Wollan, M. K. Wilkinson, W. C. Koehler, J. W. Cable, and H. R. Child, "The ORNL Neutron Diffractometer for Magnetic Studies."

American Physical Society Meeting, Washington, D.C., April 25–28, 1960

F. Ajzenberg-Selove and P. H. Stelson, "Neutrons from the Alpha Bombardment of Be^9."

R. A. Mann and M. E. Rose, "Depolarization of Mu Mesons in Atomic Capture."

F. K. McGowan, P. H. Stelson, and W. G. Smith, "Total Reaction Cross Section for α-Particles on Ni^{58}."

P. H. Stelson and F. K. McGowan, "(α,n) Cross Sections for Ni, Cu, and Zn Nuclei."

H. H. F. Wegener, "Mott Scattering Asymmetry by Foils of Finite Thickness."

2nd Conference on Reactions Between Complex Nuclei (sponsored by the American Physical Society and the Oak Ridge National Laboratory), Gatlinburg, Tennessee, May 2–4, 1960.

P. H. Stelson and F. K. McGowan, "Coulomb Excitation with Ne^{20} Ions."

Chemical Institute of Canada Conference, Ottawa, Ontario, Canada, June 13–15, 1960

M. K. Wilkinson (invited paper), "Neutron Diffraction."

Symposium on Molecular Structure and Spectroscopy, Ohio State University, Columbus, Ohio, June 13–17, 1960

P. A. Staats and H. W. Morgan, "Vibrational Spectra of Solid Phosphine."

Gordon Conference on Nuclear Chemistry, New London, New Hampshire, June 27–July 1, 1960

L. D. Roberts (invited paper), "Alpha Particle Emission and Fission of Oriented Actinide Nuclei."

Symposium on Polarization Phenomena of Nucleons (sponsored by the International Union of Pure and Applied Physics), Basel, Switzerland, July 4–8, 1960

L. C. Biedenharn and G. R. Satchler (invited paper), "Polarization Phenomena in Deuteron Stripping Reactions."

H. B. Willard (invited paper), "Detection of Deuteron Alignment with S-Wave Reactions."

American Society for Engineering Education – Summer Institute at the University of Michigan, Ann Arbor, Michigan, July 13, 1960

S. Bernstein, "Slow Neutron Crystal Spectrometry."

11th Annual Infrared Institute, Fisk University, Nashville, Tennessee, August 8–12, 1960

H. W. Morgan, "Effects of Molecular Environment upon Vibrational Spectra."

P. A. Staats, "Qualitative and Quantitative Analysis by Infrared Spectroscopy."

International Union of Crystallography, Cambridge, England, August 20, 1960

W. C. Koehler, E. F. Bertaut, E. F. Forrat, and H. L. Yakel, "Erbium Manganite – A New ABO_3 Structure."

Gordon Research Conference on Infrared Spectroscopy, Meriden, New Hampshire, August 22–26, 1960

H. W. Morgan, "Spectroscopy Work at ORNL" (informal report).

International Conference on Nuclear Structure, Queen's University, Kingston, Ontario, Canada, August 29–September 3, 1960

J. A. Harvey (invited paper), "Slow Neutron Resonances."

P. H. Stelson (invited paper), "Vibrations in Spherical and Nearly Spherical Nuclei."

J. W. T. Dabbs, S. H. Hanauer, L. D. Roberts, F. J. Walter, and G. W. Parker, "Alpha-Particle Emission from Oriented Np^{237}."

T. Dazai, "An Analysis of the $F^{19}(d,p)F^{20}$ Reaction."

J. L. Fowler, E. G. Corman, and E. C. Campbell, "Neutron Scattering from Closed Shell Nuclei."

F. K. McGowan and P. H. Stelson, "Coulomb Excitation of Vibrational States in Th^{232} and U^{238}."

P. D. Miller, J. H. Gibbons, J. H. Neiler, W. M. Good, and R. L. Macklin, "Statistical Parameters of Medium Weight Nuclei from Kev Neutron Total and Capture Cross Sections."

N. J. Pattenden and J. A. Harvey, "The Resonance Energy Cross Section of U^{233}."

L. D. Pearlstein, Y. C. Tang, and K. Wildermuth, "Energy Levels of He^5 and Li^5."

L. D. Roberts, F. J. Walter, J. W. T. Dabbs, G. W. Parker, and J. O. Thomson, "Fission Fragments from Oriented U^{233} and U^{235}."

K. Wildermuth and H. Faissner, "Asymmetric Fission from the Viewpoint of the Cluster Model."

International Conference on Low Temperature Physics, Toronto, Canada, August 29–September 3, 1960

J. W. T. Dabbs, S. H. Hanauer, L. D. Roberts, F. J. Walter, and G. W. Parker, "Alpha-Particle Emission from Oriented Np^{237}."

L. D. Roberts, F. J. Walter, J. W. T. Dabbs, G. W. Parker, and J. O. Thomson, "Fission Fragments from Oriented U^{233} and U^{235}."

Conference on the Use of Radioisotopes in the Physical Sciences and Industry, Copenhagen, Denmark, September 6–17, 1960

L. D. Roberts, J. W. T. Dabbs, F. J. Walter, S. H. Hanauer, and G. W. Parker, Nuclear Orientation Experiments with U^{233}, U^{234}, U^{235}, and Np^{237} Isotopes."

American Chemical Society Meeting, New York, September 11–16, 1960

Milton Blander and H. W. Morgan, "Vapor Phase Infrared Spectra of ZrF_4 and HfF_4."

J. R. Lawson, R. L. Barnett, and H. W. Morgan, "Inorganic Analysis by Infrared Spectroscopy."

Conference on Solid State Radiation Detectors and Advanced Technique Amplifiers [sponsored by the Professional Group on Nuclear Science (IRE) and the Oak Ridge National Laboratory], Gatlinburg, Tennessee, October 3–5, 1960

W. T. Joyner, H. W. Schmitt, J. H. Neiler, and R. J. Silva, "Energy Spectra of Correlated Fragment Pairs from the Spontaneous Fission of Cf^{252}."

F. J. Walter, J. W. T. Dabbs, and L. D. Roberts, "Semiconductor Particle Counters at Low Temperatures."

Symposium on Pile Neutron Research and Physics (sponsored by the International Atomic Energy Agency), Vienna, Austria, October 17–21, 1960

R. C. Block, G. G. Slaughter, N. J. Pattenden, and J. A. Harvey, "The ORNL Fast Chopper Time-of-Flight Neutron Spectrometer."

J. W. Cable, H. R. Child, W. C. Koehler, M. K. Wilkinson, and E. O. Wollan, "Neutron Diffraction Studies of Rare Earth Metals and Compounds."

Rare Earth Seminar at the University of California, Lake Arrowhead, California, October 23–27, 1960

W. C. Koehler, E. O. Wollan, M. K. Wilkinson, and J. W. Cable (invited paper), "Magnetic Structure Properties of Rare Earth Metals."

Symposium on Chemical Effects of Nuclear Transformation (sponsored by the International Atomic Energy Agency), Prague, Czechoslovakia, October 24–27, 1960

T. A. Carlson, A. H. Snell, and F. Pleasonton, "Electron Shakeoff following Beta Decay."

A. H. Snell, F. Pleasonton, and T. A. Carlson, "Techniques of Radioactive Recoil Spectrometry and Charge Spectrometry; the Atomic Consequences of Internal Conversion and Electron Capture."

G. T. Trammell, "γ-ray Diffraction by Resonant Nuclei."

Southeastern Regional Meeting of the American Chemical Society, Birmingham, Alabama, November 3–5, 1960

W. G. Trawick and H. W. Morgan, "Infrared and Ultraviolet Spectra of the Nitrate and Nitrite Ions in the Solid State."

6th Conference on Magnetism and Magnetic Materials, New York, November 14–17, 1960

W. C. Koehler (invited paper), "Neutron Diffraction by Helical Spin Structures."

J. W. Cable, E. O. Wollan, W. C. Koehler, and M. K. Wilkinson, "A Neutron Diffraction Study of Metallic Erbium."

M. K. Wilkinson, W. C. Koehler, E. O. Wollan, and J. W. Cable, "Neutron Diffraction Investigation of Magnetic Ordering in Dysprosium."

American Physical Society Meeting, Chicago, Illinois, November 25–26, 1960

R. L. Becker, "Bound Pairs and Elimination of Reaction Matrix Singularities."

E. C. Campbell and J. L. Fowler, "Total Neutron Cross Section of Pb^{208}."

F. E. Obenshain and H. H. F. Wegener, " Measurement of the Mössbauer Effect in Ni^{61}."

70th Annual Meeting of the Tennessee Academy of Science, Knoxville, Tennessee, December 2–3, 1960

Jean H. Durfee, E. G. Corman, and J. L. Fowler, "Calculation of Phenomenological Nuclear Potentials for O^{17}."

American Physical Society Meeting, New York, February 1–4, 1961

R. H. Bassel, R. M. Drisko, and G. R. Satchler, "Numerical Study of Distortion Effects in Deuteron Stripping Reactions."

B. Buck and G. R. Satchler, "Distorted Wave Analysis of the Reaction $Si^{28}(d,p)Si^{29}$."

R. M. Drisko, R. H. Bassel, and G. R. Satchler, "Distortion Effects in the Scattering of High Energy Nucleons."

J. L. Duggan, R. F. Gabbard, and P. D. Miller, "Neutrons from the He^3 Bombardment of Some Light Nuclei. I. Techniques."

J. A. Harvey and S. E. Atta, "Analysis of Breit-Wigner Resonances Using the IBM-704 Computer."

F. S. Levin, "Mechanism for the $B^{10}(d,p_1)B^{11*}$ (2.14 Mev) Reaction."

P. D. Miller, J. L. Duggan, and R. F. Gabbard, "Neutrons from the He^3 Bombardment of Some Light Nuclei. II. $Li^7(He^3,n)B^9$, $Be^9(He^3,n)C^{11}$, and $C^{13}(He^3,n)O^{15}$."

F. E. Obenshain and H. H. F. Wegener, "Mössbauer Effect of Ni^{61} in Applied Magnetic Fields."

L. D. Roberts and J. O. Thomson, "A Study by the Mössbauer Method of the HFS Splitting of Au^{197} Alloyed in Fe."

G. R. Satchler, R. M. Drisko, and R. H. Bassel, "Gamma-Rays Following Direct Inelastic Scattering from Nuclei."

G. G. Slaughter, J. A. Harvey, and R. C. Block, "High Resolution Total Cross Section Measurements on Np^{237} and Am^{241}."

T. A. Welton and J. Kronsbein, "On the Correction of Electron Lenses."

ANNOUNCEMENTS

Additions and temporary assignments to the various groups within the Physics Division during the past year were as follows: F. E. Obenshain, Jr. (Scintillation Spectrometry and Instrument Development Group); A. Almen[1] of the Chalmers University of Technology, Gothenburg, Sweden (High Voltage Group); G. P. Felcher[1] of the Center for Nuclear Information, Studies and Experiments, Milan, Italy (Neutron Diffraction Group); F. W. K. Firk[1] of the Atomic Energy Research Establishment, Harwell, England (Fast Chopper Group); F. A. Kahn[1] of the Pakistan Atomic Energy Commission (High Voltage Group); H. Muenzer[1] of the Institut für Radiumforschung und Kernphysik, Vienna, Austria (High Voltage Group); K. Nishimura[1] of the Japan Atomic Energy Research Institute, Tokoyo, Japan (High Voltage Group); V. A. Pethe[1] of the Atomic Energy Establishment, Bombay, India (Scintillation Spectrometry and Instrument Development Group); E. W. Schmid[1] of Florida State University, Tallahassee, Florida, and the University of Munich, Munich, Germany (High Voltage Group); and E. van der Spuy[1] of the South African Atomic Energy Board, Pretoria, South Africa (Theoretical Physics Group).

Those completing assignments during this period included: T. Dazai[1] of the Tokyo Institute of Technology, Tokyo, Japan (High Voltage Group); J. U. Kjellman[1] of the Research Institute of National Defense, Stockholm, Sweden (High Voltage Group); and N. J. Pattenden[1] of the Atomic Energy Research Establishment, Harwell, England (Fast Chopper Group).

N. H. Lazar of the Scintillation Spectrometry and Instrument Development Group of the Physics Division is on an eight-month assignment at the Los Alamos Scientific Laboratory. Lazar has been on loan to the Thermonuclear Division of ORNL since 1958. While at Los Alamos, he will be engaged in the study of the production and containment of plasmas as applicable to the Thermonuclear Program of the Laboratory.

K. L. Vander Sluis of the Spectroscopy Research Group is on a one-year assignment at the Massachusetts Institute of Technology, where his work pertains to the study of spectroscopy of the rare earths.

R. L. Macklin of the Nuclear Measurements for Reactor Design Group is on a one-year assignment at the Atomic Energy Research Establishment in Harwell, England. This assignment is a

---

[1]Temporary assignment.

continuation of the profitable liaison in physics between AERE and ORNL which was initiated in 1959.

T. A. Welton and R. L. Becker of the Theoretical Physics Group, and C. D. Moak of the High Voltage Group, have returned to ORNL following, respectively, one-year assignments at the Lawrence Radiation Laboratory in Berkeley, Princeton University, and the Atomic Energy Research Establishment in Harwell, England.

ADVISORY COMMITTEE

Research programs in the Physics Division and the Electronuclear Research Division are reviewed by a joint Advisory Committee at their Annual Information Meeting. Advisory Committee members at the time of the April 12–14, 1960, meeting were as follows:

Prof. H. Feshbach	Massachusetts Institute of Technology Cambridge, Massachusetts
Prof. W. A. Fowler	California Institute of Technology Pasadena, California
Dr. M. Goldhaber	Brookhaven National Laboratory Upton, Long Island, New York
Prof. M. S. Livingston	Cambridge Electron Accelerator Cambridge, Massachusetts
Prof. J. R. Richardson	University of California Los Angeles, California
Dean J. H. Van Vleck	Harvard University Cambridge, Massachusetts
Prof. J. A. Wheeler	Princeton University Princeton, New Jersey

---

ACTIVITIES RELATED TO EDUCATIONAL INSTITUTIONS

Research Participants

R. L. Gamble of the Georgia Institute of Technology has completed a one-year Research Participant assignment (sponsored jointly by the Oak Ridge National Laboratory, the Oak Ridge Institute of Nuclear Studies, and the Georgia Institute of Technology) with the Neutron Diffraction Group of the Division.

Under the cooperative ORINS-ORNL Research Participation Program during the summer months of 1960, the following investigators were engaged in research: R. L. Carovillano (Assistant Professor, Boston College) and W. T. Pinkston (Assistant Professor, Vanderbilt University), Theoretical Physics Group; F. Gabbard (Assistant Professor, University of Kentucky), High Voltage Group; W. T. Joyner (Assistant Professor, Hampden-Sydney College), Scintillation Spectrometry Group; E. S. Snyder (Associate Professor, Ursinus College), Nuclear Measurements for Reactor Design Group; J. O. Thomson (Assistant Professor, University of Tennessee), Low Temperature Group; W. G. Trawick (Associate Professor, Louisiana Polytechnic Institute), Spectroscopy Research Group; and F. C. Whitmore (Assistant Professor, A and M College of Texas), Neutron Diffraction Group.

Summer Visitors

Summer visitors with the Division in 1960 included: G. S. Acton, Jr. (Centenary College), J. Kronsbein (University of Florida), and F. S. Levin (University of Maryland), Theoretical Physics Group; W. M. Bugg (University of Tennessee) and S. S. Hertzbach (Johns Hopkins University), High Energy Research Group; and K. Wildermuth (Florida State University), High Voltage Group.

Student Trainee Program

The cooperative ORINS-ORNL Student Trainee Program (under the sponsorship of the U.S. Atomic Energy Commission) was set up primarily to give students from small southern colleges an opportunity to work in a full-time research laboratory during the summer months between their third and fourth years of college. During the summer of 1960, the following students were with the Division under this program: G. W. Brown (Union University), Low Temperature Group; D. E. Faulkner (Millsaps College) and P. Richard (Southwestern Louisiana Institute), High Voltage Group; W. J. Gavin (A and T College of North Carolina), Fast Chopper Time-of-Flight Group; J. P. King (Central State College), Theoretical Physics Group; L. J. Neihouse (University of Dallas), Nuclear Measurements for Reactor Design Group; and E. T. Ritter (Southwestern at Memphis), High Energy Research Group.

Co-op Students

The Co-op Program of the Oak Ridge National Laboratory is designed for promising students in engineering and science who have completed at least two quarters of undergraduate study. Students selected for the Co-op Program alternate between three months of work as technical assistants at the Laboratory and three months of school attendance. As a means for promoting the professional development of the students, as well as providing valuable technical assistants for scientific research in the Laboratory, this program has proved to be highly successful. Co-op students with the Division during the past Annual Report period have been assigned to the Theoretical Physics Group, the High Voltage Group, and the High Energy Research Group, and have included the following: W. A. Hartman, C. E. Hughey, A. F. Nickle, D. O. Patterson, and

M. C. Taylor of the University of Tennessee; J. F. Agnew and J. H. Williams of the Virginia Polytechnic Institute in Blacksburg, Virginia; and J. E. Thomas of the Virginia Polytechnic Institute in Norfolk, Virginia.

Thesis Research

Thirteen staff members of the Physics Division have served during the past year in an advisory or supervisory capacity for research conducted at ORNL by twelve Ph.D. candidates as listed below:

Staff Member(s)	Ph.D. Candidate	Field of Research
M. E. Rose	C. P. Bhalla[1] University of Tennessee	Pseudoscalar Interaction in Beta Decay
P. D. Miller and W. M. Good	J. L. Duggan[2] Louisiana State University	Some (He^3, n) Reactions in Light Nuclei
J. A. Harvey and H. W. Schmitt	A. K. Furr[2] Duke University	Neutron Capture by Activation Techniques
L. D. Roberts and J. W. T. Dabbs	S. H. Hanauer[1] University of Tennessee	Angular Distribution of Alpha Particles Emitted by Oriented Np^{237} Nuclei
W. M. Good and J. L. Fowler	R. W. Lamphere University of Tennessee	The Angular Distribution of Fission Fragments from the Fast-Neutron-Induced Fission of U^{234}
M. E. Rose	R. A. Mann[1,2] University of Alabama	The Depolarization of Negative Mu Mesons
T. A. Welton	J. H. Marable University of Tennessee	Nuclear Three-Body Problem
H. W. Schmitt, J. H. Neiler, and L. D. Roberts	W. F. Mruk University of Tennessee	Time-of-Flight and Magnetic Analysis of Fission Fragments
G. R. Satchler	S. K. Penny University of Tennessee	Theory of Nuclear Reactions
P. H. Stelson and F. K. McGowan	R. C. Ritter[2] University of Tennessee	Coulomb Excitation with Heavy Ions
L. D. Roberts and J. W. T. Dabbs	F. J. Walter University of Tennessee	Solid State Counters
T. A. Welton	C. D. Zerby[1] University of Tennessee	Electromagnetic Production of Pion Pairs

[1] Doctorate received in 1960.
[2] ORINS graduate Fellow.

Consultants Under Subcontract

University personnel currently serving as consultants to the Division are listed below. Numerous other consultants have, throughout the past year, presented seminar talks and are included in the list of speakers in the "Physics Seminars" section of this report.

L. C. Biedenharn, Jr.
Rice University

K. A. Brueckner
University of California
La Jolla, California

W. M. Bugg
University of Tennessee

H. A. Gersch
Georgia Institute of Technology

J. H. Goldstein
Emory University

E. Greuling
Duke University

J. M. Jauch
University of Geneva
Geneva, Switzerland

T. Lauritsen
California Institute of Technology

R. W. Lide
University of Tennessee

R. A. Mann
University of Alabama

J. B. Marion
University of Maryland
(Convair, San Diego, until fall of 1961)

H. W. Newson
Duke University

W. T. Pinkston
Vanderbilt University

N. F. Ramsey
Harvard University

R. H. Rohrer
Emory University

J. O. Thomson
University of Tennessee

K. Wildermuth
Florida State University

J. H. Wise
Washington and Lee University

Visiting Scientist Lecture Program in Physics

Five Division staff members participated in the Visiting Scientist Lecture Program in Physics (sponsored by the American Institute of Physics and the American Association of Physics Teachers) during the past year:

R. C. Block — Ashland College, Ashland, Ohio, March 4, 1960
"Interesting Problems in Science Today"

J. L. Fowler — Albion College, Albion, Michigan, March 14–15, 1960
"Nuclear Science: Foundation of Future Technology"
"The Neutron as a Tool for Science"

J. A. Harvey — Central State College, Wilberforce, Ohio, May 18–19, 1960
"Nuclear Physics and Atomic Energy"
"Neutron Spectroscopy"
"The Use of Computers in Nuclear Physics Research"

J. H. Neiler — Quincy College, Quincy, Illinois, March 14–15, 1960
"Science Careers at a National Laboratory"
"Some Recent Developments in Nuclear Particle Detection and Spectrometry"
"Nuclear Physics, A Tool for Studying the Universe"
"The National Laboratories, A Valuable Government Asset"

H. W. Schmitt — St. Cloud State College, St. Cloud, Minnesota, April 27–28, 1960
"Nuclear Physics: A Tool for Studying the Universe"

Traveling Lecture Program

The Traveling Lecture Program is conducted in cooperation with the Oak Ridge Institute of Nuclear Studies as a part of the AEC's program of disseminating scientific and technical information to universities, particularly those in the South. Lectures delivered by ORNL personnel present unclassified information to university undergraduate and graduate students and members of the faculty. The lectures serve to stimulate interest in research in the university departments and also assist the teaching staff in expanding the scope of instruction offered under their regular curricula. Through such personal contacts, ORNL staff members are also able to observe departmental activities at the universities. Listed below are members of the Physics Division who participated in the Traveling Lecture Program during the academic year 1959–1960, presenting a total of 32 lectures. To date, seven members of the Division have presented 14 lectures under this program for the current academic year; a complete listing of these lecturers will appear in the next Annual Report.

J. H. Gibbons	Duke University, September 23, 1959 "Recent Studies in Neutron Capture Cross Sections"
W. M. Good	University of North Carolina, November 4, 1959 (Joint colloquium: University of North Carolina – Duke University – North Carolina State) "Millimicrosecond Pulsed Techniques in Neutron Physics"
J. A. Harvey	Baylor University, November 16, 1959 Louisiana State University, November 19, 1959 Rice Institute, November 18, 1959 "Low Energy Neutron Spectroscopy"
C. H. Johnson	Indiana University, November 11, 1959 University of Kentucky, November 9, 1959 University of Wisconsin, November 13, 1959 "The Study of Beta Decay Interaction by a He^6 Recoil Experiment"
P. D. Miller, Jr.	Baylor University, December 7, 1959 Abilene Christian College, December 9, 1959 Howard Payne College, December 8, 1959 "Neutron Cross Sections in the Kilovolt Region"
H. W. Morgan	Fisk University, January 14, 1960 "Problems Involved in the Structure of Solid Solutions"
R. L. Robinson	Vanderbilt University, May 5, 1960 "A 4π Beta-Ray Scintillation Spectrometer and the Beta Spectra of Tm^{171}, Ag^{111}, and Rb^{86}"
G. R. Satchler	University of Kentucky, February 24, 1960 "Direct Nuclear Reactions
P. A. Staats	Louisiana State University, February 15, 1960 Texas A and M College, February 18, 1960 Northwestern State College of Louisiana, February 17, 1960 Memphis State University, February 19, 1960 "Techniques of Experimental Infrared Spectroscopy"

P. H. Stelson	Virginia Polytechnic Institute, January 14, 1960 University of Houston, October 6, 1959 Rice Institute, October 7, 1959 University of Virginia, January 15, 1960 "Recent Coulomb Excitation Experiments"
M. K. Wilkinson	University of Cincinnati, March 31, 1960 "The Unique Role of Neutron Diffraction in Solid State Physics" University of Georgia, May 6, 1960 "Techniques and Applications of Neutron Diffraction" Michigan State University, March 1, 1960 "Recent Neutron Diffraction Investigations of Magnetic Phenomena in Solids" University of Illinois, March 2, 1960 "Recent Investigations of Magnetic Phenomena by Neutron Diffraction"
H. B. Willord	Florida State University, November 19, 1959 University of Kentucky, May 18, 1960 University of Florida, November 17, 1959 "Non-Conservation of Parity in Beta Decay" University of Florida, November 18, 1959 University of Maryland, January 22, 1960 "Magnetic Analysis of Nuclear Reaction Products" Ohio State University, May 19, 1960 "Production of Polarized Particle Beams"

PHYSICS SEMINARS

Weekly divisional seminars are normally held at the Laboratory each Friday afternoon; for topics of especial timeliness or interest, additional seminars are frequently scheduled. During the period covered by this report, J. A. Harvey served as seminar chairman until May 1960, at which time W. C. Koehler assumed the duties of chairman. Lectures scheduled by these chairmen included the following:

1960

February 12	Lawrence W. Weston, Duke University "Average Neutron Cross Sections in the Kev Region"
February 19	J. O. Thomson, University of Tennessee "Heat Flush and Mobility of Ions in Liquid Helium II"
February 26	E. C. Campbell, ORNL "High Resolution Nuclear Spectroscopy by Resonance Gamma Absorption"
March 4	J. Neufeld, ORNL "Coherent Acceleration: A Report on Conversation with B. I. Veksler on November 16, 1959"

March 11	R. A. Gibbons and J. H. Gibbons, ORNL "The Maya: America's First Astronomers"
March 18	R. C. Block, ORNL "Neutron Radiative Capture Measurements with the ORNL Fast Chopper"
March 28	Rudolf Fleischmann, University of Erlangen "The Possibility of Making Polarized Protons"
April 1	J. A. Harvey, ORNL "Low Energy Neutron Experiments and Recent Mössbauer-Type Experiments in Europe"
April 19	H. S. Bowsher, Ohio State University "The Evidence for Direct Nuclear Interactions at Low Energies"
April 22	H. Schopper, Johannes Gutenberg University "Measurement of the Circular Polarization of Gamma Rays"
May 6	K. Alder, Swiss Federal Institute of Technology "Multiple Coulomb Excitation with Heavy Ions"
May 9	K. Brueckner, University of California, La Jolla "Nuclear Forces and Nuclear Structure"
May 10	"The Finite Nucleus"
May 11	"The Giant-Dipole Resonance in Nuclei"
May 20	G. T. Trammell, ORNL "Some Aspects of the Mössbauer Effect"
May 27	R. L. Mössbauer, California Institute of Technology "Nuclear Resonant Absorption of Recoil-Free Gamma Rays in Solids"
May 31	H. H. Staub, University of Zurich "Pair Production by Gamma-Rays and Protons"
June 3	L. Motz, Columbia University "Thermonuclear Reactions and the Evolution of Stars"
June 10	E. Inönü, ORNL "Application of Group Theory to Multiple Scattering Problems"
June 17	R. J. Blin-Stoyle, Massachusetts Institute of Technology "Parity Non-Conservation in Low Energy Nuclear Physics"
June 20	C. P. Bhalla, ORNL and the University of Tennessee "Pseudoscalar Interaction in Nuclear Beta Decay"
June 24	H. S. Jarrett, E. I. du Pont de Nemours and Co., Inc. "Evidence for an Antiferromagnetic-Ferromagnetic Transition in Cr-Modified Mn_2Sb"
June 29	R. Pauli, AB Atomenergi, Stockholm "Neutron Physics and Reactor Physics in Sweden"
June 30	R. B. Murray, ORNL "Response of Inorganic Scintillators to Various Charged Particles"
July 7	J. Sheridan, University of Birmingham, England "Recent Microwave Studies of the Structure of Simple Molecules"
July 8	G. C. Morrison, University of Chicago "Nuclear Reaction Products from the Lithium Bombardment of Li^6 and Li^7 Targets"

July 15	John Kronsbein, University of Florida "Comments on the Three Einstein Effects"
July 20, 22, 27, 29	Karl Wildermuth, Florida State University "Applications of the Cluster Model to Nuclear Physics"
August 2	Taro Tamura, Tokyo University of Education "Vibrational States in Even-Even Nuclei"
August 5	Lionel J. Bellamy, Ministry of Supply, England "Proton Transfer in Hydrogen Bonds"
August 8	R. A. Mann, ORNL and the University of Alabama "Depolarization of Negative Mu-Mesons"
August 12	J. U. Kjellman, Research Institute of National Defense, Stockholm "Time of Flight Measurements of the Reaction $Be^9(\alpha,n)C^{12}$"
August 17	A. Zucker, ORNL "Nuclear Physics and Nuclear Physicists in the USSR"
August 19	B. Elbek, University of California "Coulomb Excitation of Vibrational Levels with Heavy Ions"
August 26	David Finkelstein, Stevens Institute of Technology "The Megatron"
August 31	"The Chalice Experiment"
September 2	"Topological Relativity"
September 7	"Quantum Theory of Isotopic Spin"
September 6	Zeev Frankel, Weizmann Institute "Monte Carlo Calculations of High Energy Nuclear Reactions"
September 9	L. Waldmann, Max Planck Institute "Diffusion Theory of Particles with Spin"
September 13	J. K. Bienlein, Physikalisches Institut, Erlangen "Internal Bremsstrahlung in Beta Decay"
September 7, 9, 12, 14, 16, 19, 21	J. M. Jauch, University of Geneva "Meson Physics and Dispersion Relations"
September 29, 30	John Clark, Princeton University "The Theory of Many Boson Systems"
September 29, 30	John Nuttall, Princeton University "Theoretical Calculations on $(p, 2p)$ Reactions" "Survey of Recent Developments in Dispersion Relations"
October 7	F. W. K. Firk, Atomic Energy Research Establishment, Harwell, England "Experiments with the Harwell Electron Accelerator"
October 14	D. Maeder, CERN, Switzerland "Some Aspects of Nuclear Physics Research at CERN"
October 21	"Experimental Facilities at CERN"
October 28	"Approaches to the Fast Evaluation of Bubble Chamber Tracks"
November 4	Gilbert Perlow, Argonne National Laboratory "Experiments with Fe^{57}"
November 11	J. W. Cable, ORNL "Neutron Diffraction Studies of Rare Earth Metals"

November 18	T. Dazai, Tokyo Institute of Technology "An Analysis of the $F^{19}(d,p)F^{20}$ Reaction"
December 5	Kei Yosido, University of Tokyo "Theory of Rare Earth Metals"
December 9	Gunther Clausnitzer, University of Minnesota "A Source of Polarized Protons for the Minnesota Linac"
December 12	A. Overhouser, Ford Motor Company Scientific Laboratory "Instabilities of a Fermi Gas"
1961	
January 6	R. L. Becker, ORNL "Bound Pairs in Brueckner Theory"
January 13	R. J. Elliott, Oxford University "Excitons"
January 20	J. E. Sherwood, ORNL "A Source of Polarized Deuterons"
January 27	R. V. Neidigh and I. Alexeff, ORNL "Curious Oscillation Modes in a Vacuum Arc"

The following Special Theoretical Physics Seminar Series was arranged during the summer of 1960 by G. T. Trammell:

June 28	B. Bertotti, Princeton University "Experiments on Gravitation"
July 5	R. L. Carovillano, Boston College "Aspects of the Two-Nucleon Problem"
July 12	S. Yoshikawa, Japan Atomic Energy Research Institute "Recent Developments in the Theory of Plasma Oscillations"
July 19	K. Wildermuth, Florida State University "The Structure of Excited Levels in Light Nuclei"
July 26	J. Kronsbein, University of Florida "Report on V. Fock's New Book on Relativity"
August 2, 9	B. Kursunoglu, University of Miami "Relativity and Quantum Theory"

Informal Working Seminars on the Mössbauer Effect and Related Questions, arranged by E. C. Campbell, included the following:

August 16	G. T. Trammell, ORNL "Coherent Effects of Mössbauer Radiation"
September 8	H. H. F. Wegener, ORNL "Mössbauer Effect with Ni^{61}"
September 22	H. Schweinler, ORNL "Some Solid State Aspects of the Mössbauer Effect"
November 3	Gilbert Perlow, Argonne National Laboratory "The Mössbauer Effect"

INTERNAL DISTRIBUTION

1. C. E. Center
2. Biology Library
3. Health Physics Library
4-6. Central Research Library
7. Reactor Division Library
8-37. Laboratory Records Department
38. Laboratory Records, ORNL R.C.
39. A. M. Weinberg
40. J. P. Murray (K-25)
41. R. G. Jordan (Y-12)
42. J. A. Swartout
43. E. H. Taylor
44. E. D. Shipley
45-46. J. L. Fowler
47. M. L. Nelson
48. A. H. Snell
49. A. Hollaender
50. K. Z. Morgan
51. F. L. Culler
52. M. T. Kelley
53. D. Phillips
54. E. O. Wollan
55. H. E. Seagren
56. A. S. Householder
57. L. D. Roberts
58. R. B. Briggs
59. R. N. Lyon
60. W. C. Koehler
61. E. P. Blizard
62. M. E. Rose
63. G. E. Boyd
64. W. H. Sullivan
65. R. W. Stoughton
66. C. E. Winters
67. W. H. Jordan
68. E. C. Campbell
69. D. S. Billington
70. M. A. Bredig
71. R. S. Livingston
72. C. P. Keim
73. F. C. Maienschein
74. F. E. Obenshain, Jr.
75. R. C. Block
76. C. D. Susano
77. C. J. Borkowski
78. M. J. Skinner
79. M. K. Wilkinson
80. P. D. Miller
81. J. W. Cable
82. P. M. Reyling
83. G. deSaussure
84. W. M. Good
85. G. C. Williams
86. F. K. McGowan
87. R. W. Johnson
88. J. R. McNally, Jr.
89. J. L. Gabbard
90. R. A. Charpie
91. G. G. Slaughter
92. Eugene Guth
93. R. W. Peelle
94. P. R. Bell
95. G. G. Kelley
96. C. C. Harris
97. H. G. MacPherson
98. P. H. Stelson
99. J. E. Sherwood
100. W. Zobel
101. R. B. Murray
102. H. B. Willard
103. J. Schenck
104. J. H. Neiler
105. J. A. Harvey
106. C. F. Barnett
107. N. H. Lazar
108. J. W. T. Dabbs
109. A. Simon
110. J. H. Gibbons
111. J. J. Pinajian
112. S. Bernstein
113. F. Pleasonton
114. C. A. Preskitt
115. H. R. Child
116. C. G. Gardner
117. C. J. McHargue
118. J. A. Lane
119. C. S. Harrill
120. A. J. Miller
121. S. C. Lind
122. K. L. Vander Sluis
123. R. L. Robinson
124. G. R. Satchler
125. H. W. Morgan
126. H. W. Schmitt
127. P. M. Griffin
128. A. Zucker

129. R. W. Lamphere
130. S. J. Ovenshine
131. C. D. Goodman
132. E. P. Wigner (consultant)
133. J. H. Van Vleck (consultant)
134. M. S. Livingston (consultant)
135. J. R. Richardson (consultant)
136. M. Goldhaber (consultant)
137. W. A. Fowler (consultant)
138. J. A. Wheeler (consultant)
139. H. Feshbach (consultant)
140. ORNL – Y-12 Technical Library, Document Reference Section

EXTERNAL DISTRIBUTION

141-242. Given external distribution
243-870. Given distribution as shown in TID-4500 (16th ed.) under Physics category (75 copies – OTS)